

American University in Cairo

## AUC Knowledge Fountain

---

Theses and Dissertations

Student Research

---

2-1-2012

### Fabrication and characterization of carbon nanotube-reinforced polypropylene matrix composites

Hanady Hussein

Follow this and additional works at: <https://fount.aucegypt.edu/etds>

---

#### Recommended Citation

##### APA Citation

Hussein, H. (2012). *Fabrication and characterization of carbon nanotube-reinforced polypropylene matrix composites* [Master's Thesis, the American University in Cairo]. AUC Knowledge Fountain.

<https://fount.aucegypt.edu/etds/1270>

##### MLA Citation

Hussein, Hanady. *Fabrication and characterization of carbon nanotube-reinforced polypropylene matrix composites*. 2012. American University in Cairo, Master's Thesis. *AUC Knowledge Fountain*.

<https://fount.aucegypt.edu/etds/1270>

This Master's Thesis is brought to you for free and open access by the Student Research at AUC Knowledge Fountain. It has been accepted for inclusion in Theses and Dissertations by an authorized administrator of AUC Knowledge Fountain. For more information, please contact [thesisadmin@aucegypt.edu](mailto:thesisadmin@aucegypt.edu).

## Abstract

Carbon nanotube reinforced polymer composites have recently been the focus of numerous research efforts. With regards to mechanical behavior, the enhancements reported are much lower than the theoretical predictions. One of the main challenges being tackled is achieving a uniform dispersion. Solvent mixing has been used extensively. Concerns, however, arose that unevaporated solvents could negatively affect the mechanical properties. In this thesis, solvent and dry mixing for dispersing MWNT powders within the polymer prior to fabrication by melt processing are compared. Various weight fractions of CNT are added and the effect on the mechanical, crystallization and flow properties of the resulting composites is investigated. In both cases, enhancements in yield strength compared to the neat polymer were observed. It was found that dry mixing produced composites with the highest yield strength at 0.5 wt % CNT, whereas solvent mixing produced a similar enhancement at CNT contents of 1 wt %. It is believed that this difference is primarily dependent on the dispersion of CNTs within the polymer matrix. On the other hand, ductility was much higher for solvent mixed samples compared to dry mixed ones. FESEM analysis showed the presence of clusters in large wt % CNT samples produced by dry mixing. All samples produced by solvent mixing were found to contain homogeneously distributed CNTs. In most cases, CNT pull-out was found to be the dominant failure mechanism and may explain the limited enhancement observed. Further mechanical characterization was done using nanoindentation. The hardness and indentation modulus were calculated and they appear to concur with the tension test results. The crystallinity of the polypropylene matrix was also investigated before and after the addition of the CNTs. It was found that adding the lowest CNT wt% led to an increase in the crystallization temperature.

A gradual increase in the crystallization temperature occurred with the addition of higher CNT loadings. This indicated that the CNTs acted as nucleating agents for the polypropylene crystals. In the plastics industry the flow properties of the polymer is very important. Melt flow index measurements were used in this study to analyze this property. A decreasing trend in the melt flow index i.e. increasing viscosity was found for the solvent- mixed samples which have superior dispersion expected to contribute to decreasing the viscosity of the molten polymer. However, the effect of the addition of the CNTs overcame this and resulted in the increase of the viscosity. This occurrence could be due to the dispersion process of solvent mixing preceding the shear mixing stage. Another indication for the poor dispersion of CNT in the dry-mixed samples was that the decrease in the melt flow index of the produced samples is very limited if not negligible.

## Acknowledgments

I am deeply grateful to all those who have helped me in any way to finally be able to complete my thesis.

Firstly, I would like to thank my mentor and supervisor Dr. Hanadi Salem for her constant support and guidance throughout my master study. She was always there for me whenever I needed her help or advice in my personal and professional life. I really don't know what I would have done without her. She has taught me a lot throughout my undergraduate and graduate studies. She also helped me acquire new skills in research and presentation and report writing.

Secondly, I would like to thank my supervisor Dr. Amal Essawi for always providing me with useful information and bearing with me throughout this research. She was always available when needed and tried to facilitate any problems we confronted. I would like to thank her again for being there for me in the last part of my thesis writing and submission. She is the reason why I was able to finish my work and meet my deadlines.

Thirdly, I am very grateful to my co-advisor Dr. Adham Ramadan who was a real asset to this research and helped me a lot with the samples' fabrication. He always gave me good advice and positive criticism to enhance the quality of my work.

I would really like to show my appreciation to all the doctors who were involved in this research and were very patient with me so I was able to complete my work

I am really indebted to the mechanical engineering department at the American University in Cairo for financially support my study and always supporting me when in need.

I am thankful to the Yousef Jameel Science and Technology Research Center (YJSTRC), at the American University in Cairo for its financial support, and for providing the state of the art equipment used in this research. Also, special thanks to all my colleagues at the YJSTRC who tremendously helped me in my experimental work. I would like to thank in specific Eng. Ahmed Abdel Gawad for the nanoindentation tests, Eng Rami Wasfi for FESEM imaging and Eng Ehab Salama for DSC tests. I would also like to acknowledge the efforts of Ms Hager Amin in the Department of Chemistry for her assistance in the preparation of the solvent-mixed samples. I am grateful for all the technical assistance I have received from Mr Hussein Abdel Razek, Mr Zakria Taha and Mr Essam Aziz. They have been always ready to help in any ways they can.

A special thank you to all my friends here at the American University in Cairo: Irene, Nesma, Shada, Salwa, Rania, and Abdel Gawad for always encouraging me to finish what I have started.

Saving the best for last I will always be indebted to my loving and supporting family especially my mother and grandmother. I am also very grateful to my husband for supporting my decision in continuing my higher education and his continuous support and patience with me. I hope to make them all proud one day.

## **Dedication**

I would like to dedicate this work to my beloved mother who is constantly pushing me to be better. Without her continuous support and believe in me I would have never been the person I am today.

## List of Abbreviations

| Item     | Description                                   |
|----------|-----------------------------------------------|
| AFM      | Atomic Field Microscopy                       |
| Arc-MWNT | Arc discharge produced Multi walled nanotubes |
| ASTM     | American Society for Testing and Materials    |
| CB       | Carbon Black                                  |
| CNT      | Carbon nanotubes                              |
| CVD      | Chemical vapor deposition                     |
| DMTA     | Dynamic mechanical thermal analysis           |
| DSC      | Differential Scanning Calorimetry             |
| EXO      | Exotherm                                      |
| FESEM    | Field Emission Scanning Electron Microscopy   |
| MFI      | Melt Flow Index                               |
| MFR      | Melt Flow Rate                                |
| MWNT     | Multi Wall Nanotubes                          |
| PC       | Polycarbonate                                 |
| PE       | Polyethylene                                  |
| PP/CNT   | Polypropylene-Carbon Nanotube Composite       |
| PS       | Polystyrene                                   |
| PVA      | Polyvinylchloride                             |
| PVK      | Polyvinylcarbazole                            |
| SEM      | Scanning Electron Microscopy                  |
| SWNT     | Single Wall Carbon Nanotube                   |
| TEM      | Transmission Electron Microscopy              |

## Table of Contents

|                                                          |           |
|----------------------------------------------------------|-----------|
| ABSTRACT.....                                            | I         |
| ACKNOWLEDGMENTS .....                                    | III       |
| DEDICATION.....                                          | V         |
| LIST OF ABBREVIATIONS .....                              | VI        |
| LIST OF FIGURES .....                                    | IX        |
| LIST OF TABLES .....                                     | XIII      |
| <b>1. CHAPTER 1: INTRODUCTION AND OBJECTIVES .....</b>   | <b>1</b>  |
| 1.1 INTRODUCTION.....                                    | 1         |
| 1.2 OBJECTIVES.....                                      | 4         |
| <b>2. CHAPTER 2: BACKGROUND INFORMATION .....</b>        | <b>5</b>  |
| 2.1 CARBON NANOTUBES.....                                | 5         |
| 2.1.1 <i>Synthesis techniques for CNTs</i> .....         | 10        |
| 2.1.2 <i>Functionalization techniques for CNTs</i> ..... | 13        |
| 2.1.3 <i>Dispersion techniques for CNTs</i> .....        | 15        |
| 2.2 POLYPROPYLENE.....                                   | 18        |
| 2.2.1 <i>Advantages and disadvantages of PP</i> .....    | 19        |
| 2.2.2 <i>Mechanical properties of PP</i> .....           | 20        |
| 2.3 CNT/ POLYMER COMPOSITE PROCESSING:.....              | 22        |
| 2.3.1 <i>Solution Mixing Technique</i> .....             | 22        |
| 2.3.2 <i>Bulk mixing Technique</i> .....                 | 23        |
| 2.3.3 <i>Melt Mixing technique</i> .....                 | 24        |
| 2.3.4 <i>In situ Polymerization Technique</i> .....      | 25        |
| <b>3. CHAPTER 3: LITERATURE REVIEW .....</b>             | <b>26</b> |
| 3.1 MECHANICAL PROPERTIES.....                           | 26        |
| 3.2 DIFFERENTIAL SCANNING CALORIMETRY: .....             | 42        |
| <b>4. CHAPTER 4: EXPERIMENTAL PROCEDURES.....</b>        | <b>48</b> |
| 4.1 MATERIALS USED: .....                                | 48        |
| 4.2 COMPOSITE FABRICATION TECHNIQUES:.....               | 49        |
| 4.2.1 <i>Solvent Mixing Technique:</i> .....             | 49        |
| 4.2.2 <i>Dry Mixing Technique:</i> .....                 | 50        |
| 4.2.3 <i>Shear Mixing through Melt Processing</i> .....  | 51        |
| 4.3 MATERIAL CHARACTERIZATION: .....                     | 53        |
| 4.3.1 <i>Melt Flow index testing:</i> .....              | 53        |
| 4.3.2 <i>Tensile Testing:</i> .....                      | 54        |



|                                                              |           |
|--------------------------------------------------------------|-----------|
| 4.3.3 Nanoindentation Investigation: .....                   | 55        |
| 4.3.4 Scanning Electron Microscopy Investigation: .....      | 58        |
| 4.3.5 Differential Scanning Calorimetry: .....               | 58        |
| <b>5. CHAPTER 5: RESULTS AND DISCUSSION.....</b>             | <b>59</b> |
| 5.1 MELT FLOW INDEX.....                                     | 59        |
| 5.2 MECHANICAL TESTING: .....                                | 62        |
| 5.2.1 Tensile Testing.....                                   | 62        |
| 5.2.2 Nanoindentation:.....                                  | 66        |
| 5.3 FIELD-EMISSION SCANNING ELECTRON MICROSCOPY (FESEM)..... | 69        |
| 5.4 DIFFERENTIAL SCANNING CALORIMETRY: .....                 | 74        |
| <b>6. CHAPTER 6: CONCLUSION .....</b>                        | <b>78</b> |
| <b>CHAPTER7: FUTURE WORK .....</b>                           | <b>80</b> |
| <b>REFERENCES.....</b>                                       | <b>81</b> |
| <b>APPENDIX I .....</b>                                      | <b>85</b> |
| TENSION TEST RESULTS FOR ALL DRY MIXED SAMPLES .....         | 85        |
| TENSION TEST RESULTS FOR ALL SOLVENT MIXED SAMPLES.....      | 89        |
| <b>APPENDIX II.....</b>                                      | <b>93</b> |
| DSC TEST RESULTS FOR ALL DRY MIXED SAMPLES.....              | 93        |
| DSC TEST RESULTS FOR ALL SOLVENT MIXED SAMPLES .....         | 99        |

## List of Figures

|                                                                                                                                                                                                                                                                                                              |    |
|--------------------------------------------------------------------------------------------------------------------------------------------------------------------------------------------------------------------------------------------------------------------------------------------------------------|----|
| Figure 2.1 Different Allotropes of Carbon .....                                                                                                                                                                                                                                                              | 5  |
| Figure 2.2 Different structures of defect-free and opened carbon nanotubes: a) Concentric multi-walled carbon nanotubes (MWNT). b) “Metallic” armchair single-walled carbon nanotubes (SWNT). c) Helical chiral semiconducting SWNT. d) Zigzag SWNT. e) SWNT bundle (b) zigzag tubes (d) achiral tubes ..... | 6  |
| Figure 2.3 Schematic diagram showing how a graphene sheet is rolled up to form a nanotube ...                                                                                                                                                                                                                | 7  |
| Figure 2.4 The atomic structure of (a) an armchair and (b) a zig-zag nanotube .....                                                                                                                                                                                                                          | 7  |
| Figure 2.5 Schematic diagram of Arc Discharge Technique .....                                                                                                                                                                                                                                                | 11 |
| Figure 2.6 Schematic diagram of the Laser Ablation Technique .....                                                                                                                                                                                                                                           | 11 |
| Figure 2.7 Schematic diagram of Chemical Vapour Deposition Technique .....                                                                                                                                                                                                                                   | 13 |
| Figure 2.8 Different functionalization techniques: a) Noncovalent exohedral functionalization with polymers. b) Defect-group functionalization. c) Noncovalent exohedral functionalization. d) Sidewall functionalization. e) Endohedral functionalization .....                                             | 14 |
| Figure 2.9 Schematic Diagram of a calendaring machine .....                                                                                                                                                                                                                                                  | 17 |
| Figure 2.10 Propylene monomer .....                                                                                                                                                                                                                                                                          | 18 |
| Figure 2.11 Types of Polypropylene .....                                                                                                                                                                                                                                                                     | 19 |
| Figure 2.12 Typical Stress/Strain Curve for PP .....                                                                                                                                                                                                                                                         | 21 |
| Figure 3.1 1) Stress–strain curves of (a) pure PP and (b) PP/0.3 wt% MWNT nanocomposite at 18 °C for various strain rates 2) Stress–strain curves of pure PP and PP/0.5 wt% MWNT nanocomposite at a strain rate of $6.67 \times 10^{-5} \text{ s}^{-1}$ for various temperatures .....                       | 30 |
| Figure 3.2 SEM fractographs of (a) PP and (b) PP/0.5 wt% MWNT nanocomposite .....                                                                                                                                                                                                                            | 31 |

|                                                                                                                                                                                                                                                                            |    |
|----------------------------------------------------------------------------------------------------------------------------------------------------------------------------------------------------------------------------------------------------------------------------|----|
| Figure 3.3 Variation of (a) Young's modulus and (b) yield strength as a function of the SWNT content in the composite .....                                                                                                                                                | 33 |
| Figure 3.4 Tensile strength (a), notched Izod impact strength (b), tensile modulus (c), and flexural modulus (d) .....                                                                                                                                                     | 35 |
| Figure 3.5 Stress-strain Curves of PP/MWNT nanocomposites .....                                                                                                                                                                                                            | 37 |
| Figure 3.6 Transmission electron microscopic pictures of 2 wt. % PP/MWNT nanocomposites. (a) Regions of dispersed nanotubes in PP matrix, (b) regions of nanotubes agglomerations in PP matrix and (c) low magnification TEM picture showing the nanotube dispersion ..... | 38 |
| Figure 3.7 SEM image of 3 wt.% PP/MWNT nanocomposites showing a masterbatch clusters in PP matrix .....                                                                                                                                                                    | 39 |
| Figure 3.8 Flexural properties of PP and PP/MWNT nanocomposites .....                                                                                                                                                                                                      | 39 |
| Figure 3.9 Charpy impact properties of PP and PP/MWNT nanocomposites .....                                                                                                                                                                                                 | 40 |
| Figure 3.10 Stress-strain curves of PP and PP composite fibers .....                                                                                                                                                                                                       | 42 |
| Figure 3.11 Non-isothermal crystallization curves of PP and PP-SWNT Composites .....                                                                                                                                                                                       | 43 |
| Figure 3.12 Spherulitic structure of a) neat PP and 5wt % PP/SWNT .....                                                                                                                                                                                                    | 44 |
| Figure 3.13 DSC curves of neat PP and PP/SWNT composites at 10°/min rate .....                                                                                                                                                                                             | 45 |
| Figure 3.14 Micrographs of PP crystallization (a) PP at 132 °C, (b) PP/SWNT (0.25%) at 146 °C and (c) PP/SWNT (0.5%) at 146°C .....                                                                                                                                        | 46 |
| Figure 3.15 DSC curves of neat PP and PP/MWNT composites .....                                                                                                                                                                                                             | 47 |
| Figure 4.1 SEM image of the MWNT used in this research .....                                                                                                                                                                                                               | 48 |
| Figure 4.2 Solvent mixing Technique .....                                                                                                                                                                                                                                  | 50 |
| Figure 4.3 Dry mixing Technique .....                                                                                                                                                                                                                                      | 51 |
| Figure 4.4 Extrusion Apparatus .....                                                                                                                                                                                                                                       | 52 |

|                                                                                                                                                                                                                                                                                                                                                                                                                                                                                                                                 |    |
|---------------------------------------------------------------------------------------------------------------------------------------------------------------------------------------------------------------------------------------------------------------------------------------------------------------------------------------------------------------------------------------------------------------------------------------------------------------------------------------------------------------------------------|----|
| Figure 4.5 Schematic diagram of single screw extruder.....                                                                                                                                                                                                                                                                                                                                                                                                                                                                      | 53 |
| Figure 4.6 Melt Flow Index Apparatus.....                                                                                                                                                                                                                                                                                                                                                                                                                                                                                       | 54 |
| Figure 4.7 Tension Test Fixture.....                                                                                                                                                                                                                                                                                                                                                                                                                                                                                            | 55 |
| Figure 5.1 Melt flow indices results .....                                                                                                                                                                                                                                                                                                                                                                                                                                                                                      | 59 |
| Figure 5.2 Effect of MWNT content on melt flow index of three types PP/MWNT composites.<br>.....                                                                                                                                                                                                                                                                                                                                                                                                                                | 61 |
| Figure 5.3 Example of Stress Strain curves for 1 % CNT using dry and solvent mixing technique<br>.....                                                                                                                                                                                                                                                                                                                                                                                                                          | 62 |
| Figure 5.4 Load vs. displacement curve for a representative 1 wt% PP/CNT dry-mixed sample.<br>(b) Load vs. displacement curve for a representative 1 wt% PP/CNT solvent-mixed sample .....                                                                                                                                                                                                                                                                                                                                      | 68 |
| Figure 5.5 (a) 0.5 wt% dry mixed sample showing dispersed CNTs as well as a small cluster. (b)<br>1 wt% dry mixed sample showing dispersed CNTs as well as a small cluster. (c) Regions with<br>uniformly dispersed CNTs as well as a large cluster in the 5 wt% CNT dry-mixed sample. (d) 0.5<br>wt% solvent mixed sample showing dispersed CNTs. Dark spots are also seen. (e) The fracture<br>surface of the solvent-mixed 1 wt% CNT sample. (f) Uniformly dispersed CNTs in the 5 wt%<br>CNT solvent-mixed sample [38]..... | 71 |
| Figure 5.6 Clear presence of porosity in 1% CNT solvent-mixed sample .....                                                                                                                                                                                                                                                                                                                                                                                                                                                      | 72 |
| Figure 5.7 PP/CNT solvent-mixed sample, showing CNTs sticking out of the matrix .....                                                                                                                                                                                                                                                                                                                                                                                                                                           | 73 |
| Figure 5.8 SEM image of PP/-SWNT composite where nanotube pull out is obvious (cryogenic<br>fracture surface) .....                                                                                                                                                                                                                                                                                                                                                                                                             | 73 |
| Figure 5.9 Crystallization Temperature vs. CNT % .....                                                                                                                                                                                                                                                                                                                                                                                                                                                                          | 76 |
| Figure 5.10 Non-isothermal crystallization curves of PP and PP/MWNT composites (dry mixed<br>samples) .....                                                                                                                                                                                                                                                                                                                                                                                                                     | 77 |

Figure 5.11 Non-isothermal crystallization curves of PP and PP/MWNT composites (solvent mixed samples) ..... 77

## List of Tables

|                                                                                                                                                                   |    |
|-------------------------------------------------------------------------------------------------------------------------------------------------------------------|----|
| Table 2.1 Physical properties of different carbon materials .....                                                                                                 | 9  |
| Table 2.2 Comparison of unmodified PP with other Polymers .....                                                                                                   | 21 |
| Table 3.1 Mechanical properties of PP and PP/MWNT nanocomposites at 10mm/min and 18°C<br>.....                                                                    | 29 |
| Table 3.2 Mechanical properties of PP nanocomposites .....                                                                                                        | 34 |
| Table 3.3 Tensile properties of PP and PP/MWNT nanocomposites .....                                                                                               | 37 |
| Table 5.1 Melt flow indices results.....                                                                                                                          | 59 |
| Table 5.2 Tensile testing Results .....                                                                                                                           | 63 |
| Table 5.3 Average values of yield strength and flow strain for different extrudates normalized to<br>the respective values of the control samples.....            | 64 |
| Table 5.4 Nanoindentation Results.....                                                                                                                            | 67 |
| Table 5.5 Average values of the hardness and indentation modulus for the different<br>extrudates normalized to the respective values of the control samples. .... | 69 |
| Table 5.6 Peak crystallization and onset temperatures .....                                                                                                       | 75 |

# Chapter 1: Introduction and Objectives

## 1.1 Introduction

Nanotechnology is one of the most important areas of research and development. The spectrum of nanotechnology includes material science, biotechnology, electronics, and other sectors in industry. The definition of nanotechnology is the investigation and design of materials or devices on the atomic or molecular level [1]. Nanotechnology is not new to polymer science; nanoscale studies were conducted but were not referred to as nanotechnology until recently. Some of these studies were phase separated polymer blends, which often reached nanoscale phase dimensions; interfacial phenomena in blends and composites which also involved nanoscale dimensions. Furthermore, studies including nanocomposites with carbon black as reinforcement in elastomers and even naturally occurring fiber that have nanoscale dimensions are being investigated for decades now [2]. Adding nanoscale fillers to polymers shows good potential for improving the polymers' mechanical properties, thermal stability, fire retardancy and other areas. There are several types of polymer nanocomposites depending on the nanofillers such as layered silicates, carbon nanotubes, carbon nanofibers and nanoaluminum oxides and others [3]. Different polymer matrices are also used for nanocomposite fabrication: thermoplastic based, thermoset based and elastomer based nanocomposites.

Since the discovery of carbon nanotubes (CNTs) by Ijima in 1991 they have attracted attention of researchers for being superior candidates to act as reinforcement in advanced composites. The reason for the superiority of CNTs is that they possess excellent physical and chemical properties. They have high aspect ratios, high mechanical strength, and high electrical and thermal conductivity. Comparing conventional composites with CNT reinforced ones is that the

latter will be much easier to mold and the Polymer matrix retains most of its mechanical properties such as elasticity, strength and modulus [4]. The reason behind this could be that adding only small CNT loadings to the matrix can affect its overall performance and enhance its mechanical, electrical and rheological properties, without hindering the processability of the polymer. CNT/Polymer composites pave the way for the synthesis of new materials with a wide range of applications. CNTs tensile strength can reach 45 GPa in comparison to steel with only 2 GPa [5]. Their elastic modulus is about 1TPa. Depending on their synthesis technique carbon nanotubes can be single walled (single tubule of 1 nm) or multi walled (2-50 tubules concentrically positioned of 20-50 nm). Another important advantage for using CNTs as filler is that they enhance the properties of the composites with significantly lower filler concentrations due to their high aspect ratios. For Conventional fillers such as carbon black a minimum of 20 wt% is required to show any reinforcement. However, adding these high amounts of concentrations of conventional fillers can negatively impact the light weight, mechanical toughness and other properties [6]. CNT aspect ratio varies from (1000-10,000) [7].

The main challenge in CNT/Polymer composites is the homogenous dispersion of CNT in the Polymer matrix. This is due to the van der Waal interactions between nanotubes. The CNT tends to agglomerate during the synthesis of the composite [8, 9, 10].

There are several ways for CNT/Polymer composites fabrication. The most common techniques are solvent mixing, melt processing and in situ polymerization. The first technique is the most common one for the preparation of CNT/Polymer composites. In some cases the nanotubes are first dispersed in a solvent then the polymer is added to the solution. In other cases the polymer is first dissolved in a solvent then the CNTs are mixed in the polymer solution. The final solution is then energetically mixed. After the mixing step the solvent is then evaporated leaving a



composite. The second technique does not require any solvents that may cause polymer degradation or contamination. The polymer is melted to produce a viscous liquid then the nanotubes are added to the melt and mixed using shear forces. One of the main short comings of this technique is that it can cause polymer degradation due to the increased viscosity of the polymer with the addition of CNTs. To overcome the increased viscosity higher shear rates are needed which can result in the degradation [11]. The third technique is in situ polymerization where CNT are mechanically dispersed in an un-polymerized solution containing the polymer monomer then the nanotubes are locked into the polymer matrix by polymerization. Polymerization is used for thermoplastics [12]. This study will focus mainly on CNT/Polymer composites and in specific Polypropylene/MWNT composites. It will also focus on the processing techniques and how it is related to the dispersion of the MWNT in PP, the mechanical, crystallization and flow properties. Two alternative techniques are evaluated: the first involves solvent mixing followed by extrusion and the second one is solvent-free (or dry mixing) also followed by extrusion. As dispersion is also directly affected by the viscosity of the polymer melt, melt flow index testing was also conducted to assess the effect of adding the CNT and using different mixing techniques. Mechanical properties were investigated. Differential scanning calorimetry was also conducted to investigate the crystallization of polypropylene with different CNT weight percentages and mixing methods. `

## 1.2 Objectives

- Fabricating Carbon Nanotube-Reinforced Polymer Matrix Composites using solvent mixing and dry mixing techniques with different CNT content (0 wt%,0.5 wt%,1 wt% and 5 wt% MWNT)
- Studying the effect of processing techniques on the dispersion of CNT within PP/CNT composite
- Investigating the processing and mechanical properties of the composite
- Investigating the crystallization behavior of polypropylene with the addition of different CNT wt %

## Chapter 2: Background Information

### 2.1 Carbon Nanotubes

Carbon nanotubes (CNT) are an allotrope of carbon and they consist of long cylinders of rolled up seamless graphene sheets. Figure 2.1 shows the different allotropes for carbon.

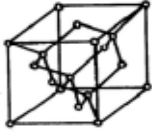
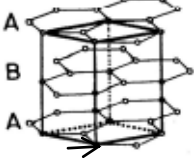
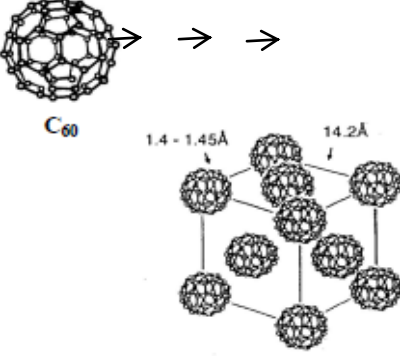
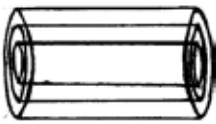
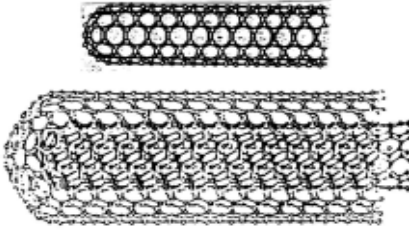
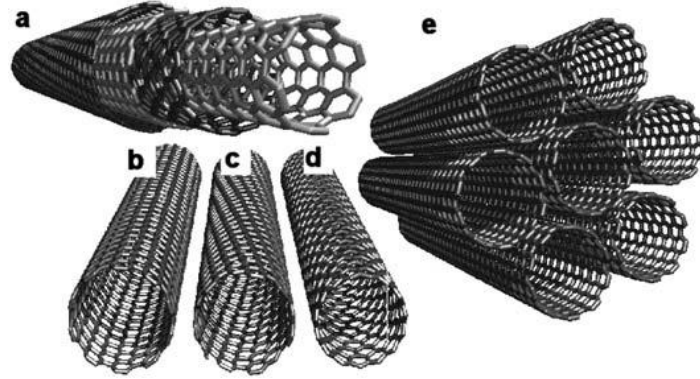
|                                                                                                                                |                                                                                           |                                                                                                |
|--------------------------------------------------------------------------------------------------------------------------------|-------------------------------------------------------------------------------------------|------------------------------------------------------------------------------------------------|
| <p>Diamond<br/>(a)</p>                                                                                                         |          | <p>Cubic (f.c.c.)<br/><math>a = 3.566 \text{ \AA}</math></p>                                   |
| <p>Graphite<br/>(b)</p>                                                                                                        |          | <p>Hexagonal<br/><math>a = 2.463 \text{ \AA}</math><br/><math>c = 6.714 \text{ \AA}</math></p> |
| <p>Fullerene<br/>(c)</p>                                                                                                       |        | <p>Cubic (f.c.c.)<br/><math>a = 14.17 \text{ \AA}</math></p>                                   |
| <p>Carbon Nanotubes<br/>(CNTs)<br/>(d)</p>  |       | <p>Single-Walled<br/>CNT<br/>Multi-Walled<br/>CNT</p>                                          |
| <p>Carbon nanofoams</p>                                                                                                        | <p>Carbon clusters with an average<br/>diameter <math>\sim 6\text{-}9\text{nm}</math></p> |                                                                                                |

Figure .2.1 Different Allotropes of Carbon [13]



**Figure 2.2** Different structures of defect-free and opened carbon nanotubes: a) Concentric multi-walled carbon nanotubes (MWNT). b) “Metallic” armchair single-walled carbon nanotubes (SWNT). c) Helical chiral semiconducting SWNT. d) Zigzag SWNT. e) SWNT bundle (b) zigzag tubes (d) achiral tubes [14]

There are two types of CNT: single-wall carbon nanotubes (SWNT) and multi-wall carbon nanotubes (MWNT). (see Figure (2.2)) SWNT is a single graphene sheet rolled up into a cylinder. MWNT are several cylinders nested in each other and placed coaxially around a hollow center. The interlayer separation is around 0.34nm. There are several ways to roll the graphene sheets into tubes this is described by the tube chirality [15]. The chirality can be defined by the chiral vector  $C_h$ , and the chiral angle  $\theta$ . The governing equation that determines the tube chirality is  $\vec{C}_h = n\vec{a}_1 + m\vec{a}_2$ . The integers (n, m) are the number of steps along the vectors ( $a_1$  and  $a_2$ ) as shown in figure 2.3.

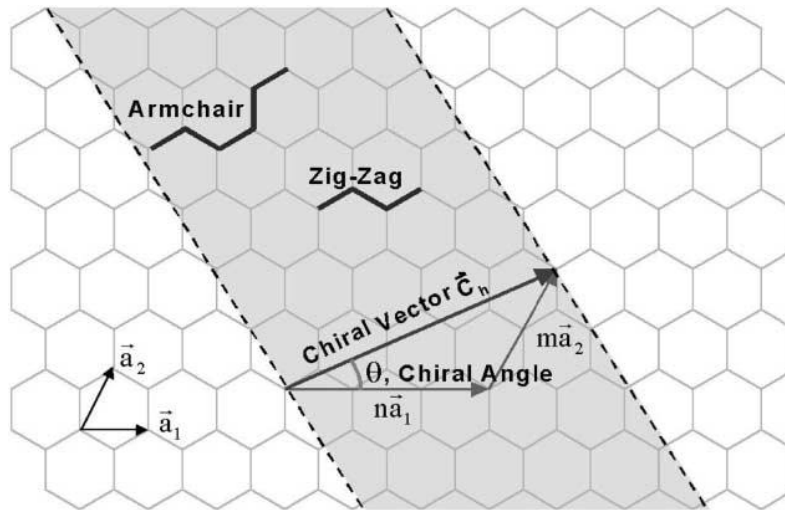


Figure 2.3 Schematic diagram showing how a graphene sheet is rolled up to form a nanotube [15]

A CNT can be rolled up to form a zig-zag structure where  $\theta=0^\circ$  or armchair structure where  $\theta=30^\circ$  and chiral structure where  $n \neq m \neq 0$  [15, 14]. Figure (2.4) shows a better illustration for the atomic structure of an armchair and a zig-zag nanotube.

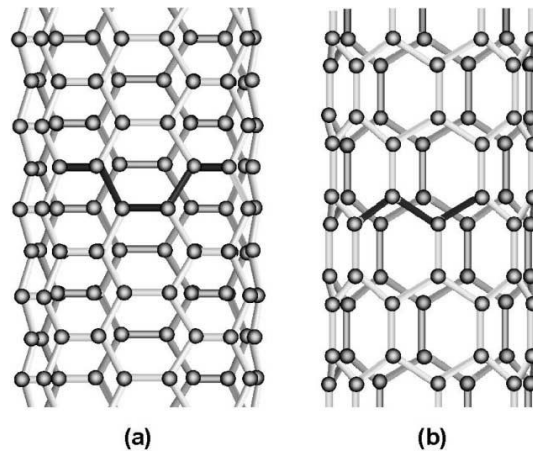


Figure 2.4 The atomic structure of (a) an armchair and (b) a zig-zag nanotube [14]

There is no agreement on the exact mechanical properties of CNTs. However, their mechanical properties surpass any materials. The Young's modulus according to theoretical and experimental results can reach up to 1.2 TPa and tensile strength of 50-200 GPa. The first actual mechanical measurements were made on MWNT fabricated by the arc-discharge method. Treacy et al. used the Transmission Electron Microscope (TEM) to measure the amplitude of intrinsic thermal vibrations. This technique was used to measure the moduli of a number of tubes, which varied from 0.41-4.15 TPa. Three years later Poncheral induced electromechanical resonant vibrations, which lead him to calculate moduli varying from 0.7-1.3 TPa. In 1997 the first direct measurement was made by Wong et al. The atomic force microscope (AFM) was used to measure the stiffness constant of arc discharge MWNTs fixed at one end. The Young's modulus measured from this technique was 1.28 TPa. The first strength measurement was also obtained, which was the average bending strength of 14 GPa. Salvetat et al. also used AFM to measure the average modulus (810 GPa) of a bent arc-MWNT pinned at the end. In 2000 Yu et al. were able to measure the stress-strain on individual arc-MWNTs inside an electron microscope. For a range of tubes the modulus values were 0.27-0.95 TPa and maximum strain was up to 12% and with strengths in the range of 11-63 GPa. Mechanical measurement on SWNT took longer because their handling is much more difficult. The SWNT have great flexibility and high surface energy, therefore they tend to cluster into large bouquets. These bundles exhibit inferior properties than the isolated SWNT. However, the first measurement on SWNT was carried out by Salvetat el al. using their AFM method. Their results yielded a tensile modulus of ~1 TPa for small diameter SWNT bundles. The mechanical properties of the larger diameter bundle were very much affected by the shear slippage of the individual nanotubes within the bundle. Yu et al. also continued their studies to include the measurement of tensile properties of SWNT bundles using

their same technique they have used with MWNT. The moduli ranged from 0.32-1.47 TPa and strengths between 10-52 GPa and maximum strain at 5.3%. The relatively high values of modulus and strength were measured on high quality SWNT and arc discharge MWNT. However, MWNTs synthesized via chemical vapor deposition (CVD) method are expected to exhibit notable reduced values. This is due to the presence of defects in the nanotubes produced by this method. Therefore, their thermal, electronic and mechanical properties deviate significantly from the expected pristine nanotube. However, the CVD produced MWNT are very significant because this technique produce very large quantizes of CNTs relatively cheaply. This could be very useful if nanotubes are ever to be used at the industrial scale. The first measurements on CVD-MWNT were conducted by Salvetat et al. [11] using their AFM technique as mentioned earlier. The Young's modulus values were between 12 and 50 GPa. Xie et al. measured stress-strain on bundles of CVD-MWNT. The moduls measured was 0.45 TPa and tensile strength around 4 GPa. The large variations in modulus for the CVD-MWNT compared to the arc-MWNT propose that the modulus is very sensitive to defect concentration and type [11].

| Property                                            | C material                                        |                                     |                        |                                  |                                  |
|-----------------------------------------------------|---------------------------------------------------|-------------------------------------|------------------------|----------------------------------|----------------------------------|
|                                                     | Graphite                                          | Diamond                             | Fullerene              | SWCNT                            | MWCNT                            |
| Specific gravity (g/cm <sup>3</sup> )               | 1.9-2.3                                           | 3.5                                 | 1.7                    | 0.8                              | 1.8                              |
| Electrical conductivity (S/cm)                      | 4000 <sup>p</sup> , 3.3 <sup>c</sup>              | 10 <sup>-2</sup> -10 <sup>-15</sup> | 10 <sup>-5</sup>       | 10 <sup>2</sup> -10 <sup>6</sup> | 10 <sup>3</sup> -10 <sup>5</sup> |
| Electron mobility (cm <sup>2</sup> /V s)            | 2.0 × 10 <sup>4</sup>                             | 1800                                | 0.5-6                  | ~10 <sup>5</sup>                 | 10 <sup>4</sup> -10 <sup>5</sup> |
| Thermal conductivity (W/(m K))                      | 298 <sup>p</sup> , 2.2 <sup>c</sup>               | 900-2320                            | 0.4                    | 6000                             | 2000                             |
| Coefficient of thermal expansion (K <sup>-1</sup> ) | -1 × 10 <sup>-6p</sup><br>2.9 × 10 <sup>-5c</sup> | (1~3) × 10 <sup>-6</sup>            | 6.2 × 10 <sup>-5</sup> | Negligible                       | Negligible                       |
| Thermal stability in air (°C)                       | 450-650                                           | <600                                | ~600                   | >600                             | >600                             |

p: in-plane; c: c-axis.

**Table 2.1 Physical properties of different carbon materials [17]**

Table (2.1) shows the physical properties of SWNT and MWNT and other carbon allotropes. It is obvious that CNTs have superior thermal and electrical properties than the rest of the carbon materials [17]. These properties make CNTs ideal candidates for reinforcement in polymer matrix composites.

### **2.1.1 Synthesis techniques for CNTs**

CNTs can be synthesized using 3 techniques: arc discharge, laser ablation and Chemical vapor deposition (CVD). All the mentioned techniques do not produce only the one type of CNTs but a mixture of several chiralities, diameters and lengths and also some impurities are also produced [14]. These impurities could be catalyst residue, amorphous carbon or other types of fullerenes [16]. Therefore the purification process of CNTs is an important step before starting the fabrication of CNT/Polymer composites.

The arc discharge technique involves two high purity graphite rods an anode and cathode. The electrodes are positioned in an inert gas atmosphere usually helium. The gap between the electrodes is always maintained by the repositioning of the anode. A voltage is applied until a stable arc is reached. The material of the anode is being consumed and deposited on the cathode. During this process a catalyst is also present. The depositions on the cathode consist of a fused material and a soft fibrous core containing the nanotubes. Figure (2.5) shows a schematic diagram of the arc discharge technique [16].



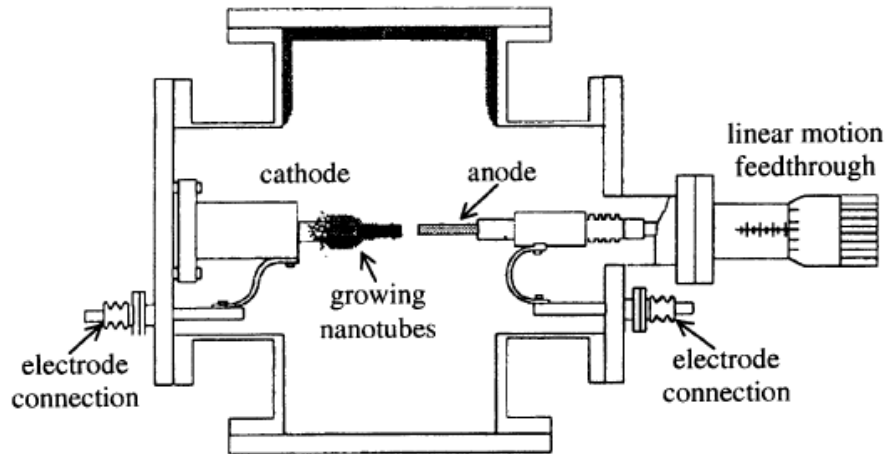


Figure 2.5 Schematic diagram of Arc Discharge Technique [16]

Laser ablation on the other was originally used to produce fullerenes, and it has been enhanced to also produce SWNTs. A laser hits a graphite target and vaporizes it. This procedure occurs under inert gas atmosphere and elevated temperature that reaches 1200°C. The vaporized graphite then hits a water-cooled substrate where it is then collected. To produce SWNT the graphite target was first doped with cobalt and nickel catalyst. Figure (2.6) shows the laser ablation technique.

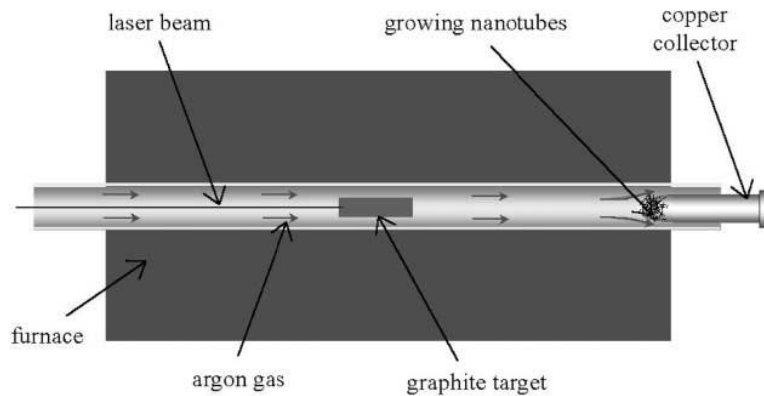


Figure 2.6 Schematic diagram of the Laser Ablation Technique [16]

Both techniques mentioned above are highly dependent on the carbon source either the anode or the carbon target. This results in a limited volume of CNT production. As mentioned before

other by-products and impurities are also produced this then requires a purification stage in order to separate the CNTs from the rest.

The third technique of CNT production is the chemical vapour deposition (CVD) method. This method depends on a continuous flow of a carbon-containing gas. It will produce CNTs as long as the carbon-containing gas is flowing. The final purity of the nanotubes produced is much higher which cuts down the proceeding purification stage [16]. The Arc discharge and laser ablation techniques require very high temperatures ( $>2500^{\circ}\text{C}$ ), on the other hand CVD only requires medium heat ranging from  $970\text{-}1750^{\circ}\text{C}$  [13]. The earlier production of CNTs via CVD produced “spaghetti like” and defective CNTs. However, the process has immensely improved and high quality multi-walled carbon nanotubes (MWNTs) and single-walled carbon nanotubes can be deposited directly on a substrate. The produced CNTs can be used directly without any purification. The main concept behind the CVD process is that the nanotubes grow onto substrate by decomposing a hydrocarbon gas in the presence of a metallic catalyst. There are several types of CVD: thermal CVD, plasma enhanced CVD and catalytic pyrolysis of hydrocarbon.

The thermal CVD reactor consists of a quartz ( $\text{SiO}_2$ ) tube surrounded by a furnace. The substrate material could be made of Si or alumina among others. The carbon-containing gas used usually in the thermal CVD is either acetylene ( $\text{C}_2\text{H}_2$ ) or ethylene ( $\text{C}_2\text{H}_4$ ) gas. The catalyst is Fe, Ni or Co nanoparticles. The temperature range of the process is ( $500\text{-}900^{\circ}\text{C}$ ). At these elevated temperatures the carbon dissolves in the catalyst particles until it reaches saturation. The CNTs then start growing on the substrate. The type, diameter and length and purity of the CNTs depend greatly on the hydrocarbon source, the catalyst’s material and size, the temperature and the reaction time. The second type of CVD is the plasma-enhanced chemical vapor deposition (PECVD). The PECVD is used to produce vertically aligned CNTs or selectively positioned

ones. With the presence of the plasma (highly energetic electrons) the substrate temperature can be lower than in the thermal CVD process. The final CVD method is the catalytic pyrolysis of hydrocarbon. This method is used for the mass production of CNTs. The main advantage of this method is that it produces CNT bundles at relatively low cost and the CNTs do not require any purification afterwards. The catalytic nanoparticles are introduced as a suspension with the carbon-containing gas into the CVD reactor. As long as the previous constituents are flowing into the reactor the production of CNTs occurs. A syringe pump and atomizer is added to a double furnace in order to continually feed the reactor. Figure (2.7) shows a schematic diagram of a catalytic pyrolysis CVD device.

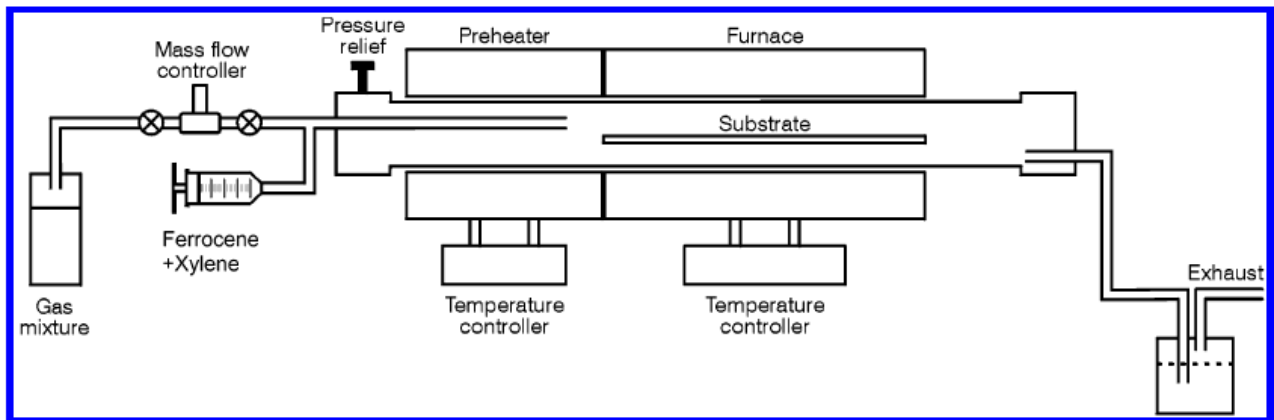
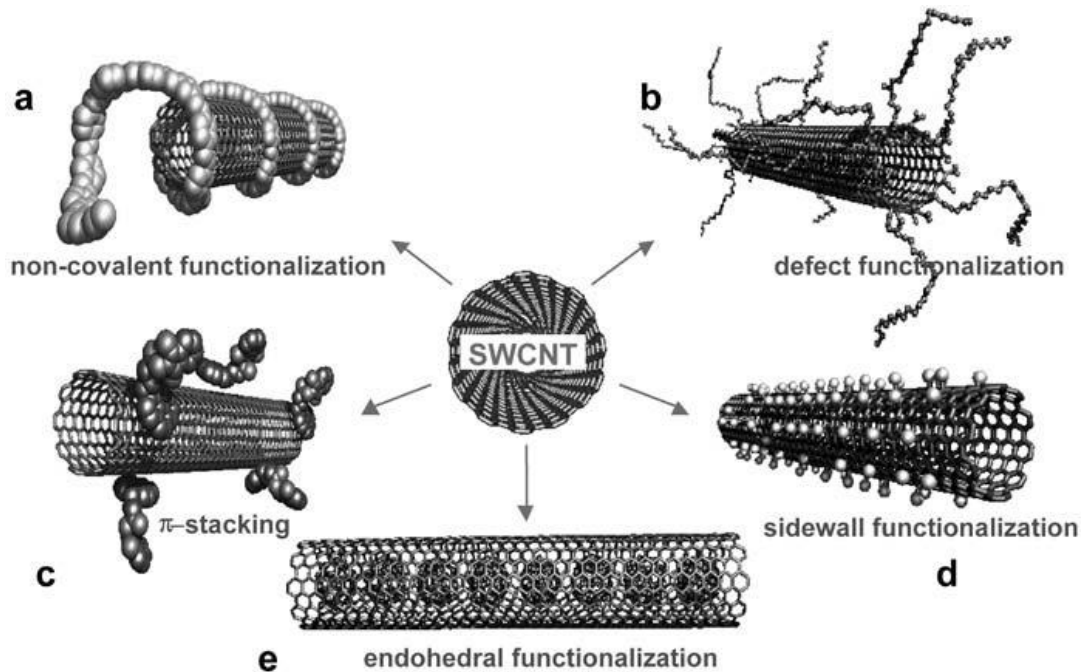


Figure 2.7 Schematic diagram of Chemical Vapour Deposition Technique [18]

### 2.1.2 Functionalization techniques for CNTs

The high aspect ratio and the relatively strong van der Waal forces between the nanotubes tend to produce clusters of CNT especially in SWNT. As mentioned before in the introduction section the dispersions of the CNT in the polymer matrix affects the properties of the composite tremendously. Therefore the entanglement of the nanotubes is an obstacle that should be overcome in order to produce well dispersed CNT in the Polymer composites. CNTs are difficult

to disperse in water or in any organic media and they resist wetting [14]. This is due to the aromatic nature of the carbon bonds. Therefore the CNTs can only bond with the matrix through van der Waal forces, which is not sufficient to ensure efficient load transfer through the CNT/matrix interface [17]. Therefore in order to overcome this obstacle, these chemical functional groups are attached either along or inside the nanotubes to enhance the solubility and processability of the CNTs. The chemical bonds can be used to improve the interaction between the CNT and the matrix. This chemical process is called the functionalization of carbon nanotubes. Figure (2.8) shows different functionalization scenarios for CNTs.



**Figure 2.8** Different functionalization techniques: a) Noncovalent exohedral functionalization with polymers. b) Defect-group functionalization. c) Noncovalent exohedral functionalization. d) Sidewall functionalization. e) Endohedral functionalization [14]

The functionalization process can be divided into two categories: chemical and physical functionalization. Chemical functionalization is the covalent bonding of functional groups on the carbon nanotube structure. These bonding can occur at the open-ends of the tubes or in the sidewalls. Another method of covalent functionalization is defect functionalization. The

functional groups attach themselves either at the open-ends or at defect sites in the sidewalls. The second type of functionalization is the physical one. This type can also be called non-covalent functionalization. The suspended presence of CNT in a polymer can allow the wrapping of the polymer around the CNTs to form a supermolecule. The bonding between the CNT and polymer depend on the van der Waal forces and  $\pi$ - $\pi$  stacking between both constituents. Another non-covalent method is the surfactant adsorption. The surfactant is physically adsorbed to the CNT which results in the decrease of the surface tension of the CNT and reduces the formation of clusters. The third physical method is the endohedral one where the guest atom or molecules is placed inside the hollow cavity of the CNTs. The placement occurs through the capillary effect and it is usually localized at defect sites at the end and the sidewalls of the CNT [17]. However, this thesis did not include any functionalization for the MWNTs used. This could be a beneficial recommendation for future research in this area.

### **2.1.3 Dispersion techniques for CNTs**

There are other ways to disperse the CNTs in the polymer matrix which do not include any type of functionalization. These dispersion techniques are considered to be mechanical distribution of the CNTs in the polymer matrix. These techniques involve: ultrasonication, calendaring, ball milling, stirring and extrusion. Ultrasonication method is usually attained by using an ultrasonic bath or an ultrasonic probe. Using ultrasound waves CNTs are dispersed in a low viscosity liquid for example: water, acetone and ethanol. If CNTs were to be dispersed in a polymer, it has to be first dissolved or diluted before this procedure is possible. The concept of this technique is that the ultrasonic waves produced help “peel off” the nanoparticles agglomeration or clusters thus separating them from each other.

The second mechanical dispersion technique of CNTs is the calendaring process. This process consists of a three roll mill. The mixing of viscous materials depends on the shear force created between the rollers. The calendaring machine consists of three adjacent cylindrical rollers. Each roller rotates with a different velocity. The first and third rollers are called the feeding and the apron roller respectively. These rollers rotate in the same direction, while the centre one rotates in the other direction. The material is fed into the hopper, which is located right above the feeding and the centre rollers. The material is still not mixed together. The material is attached to the bottom of the centre roller, and then it is transferred to the second gap. In this gap the material is dispersed to the degree of fineness needed. The milling cycle of the material can be repeated several times to enhance the dispersion. The calendaring process has been employed before in previous efforts to disperse CNTs in a polymer matrix. A high shear force at a low residence time can disentangle the CNTs without allowing breakage of the individual nanotubes. Nevertheless there are several concerns while using this technique in dispersing CNTs. Firstly, the minimum gap between the rollers can reach about (1-5 $\mu\text{m}$ ) which more or less in the range of the nanotubes' length but much larger than their diameters. This can result in disentanglement of only the bigger clusters of CNTs. Secondly; the material fed into the hopper should only be in viscous state when mixed with CNTs. This means that this method cannot be employed to thermoplastic matrices such as polyethylene, polystyrene and polypropylene. Figure (2.9) shows a schematic diagram of a calendaring machine.

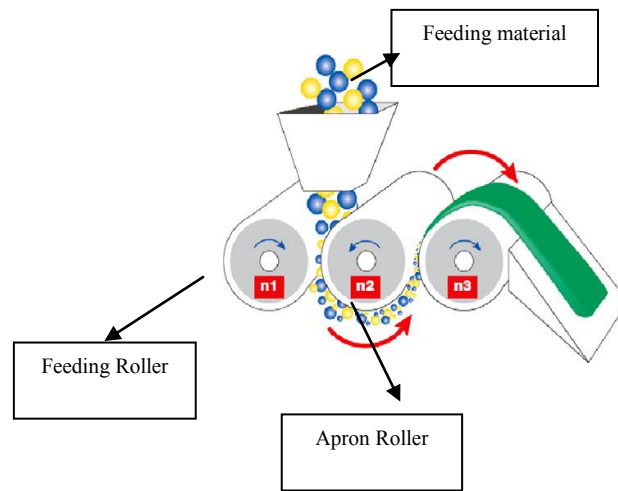


Figure 2.9 Schematic Diagram of a calendaring machine [17]

Another dispersion method is ball milling. Ball milling is mainly based on the refinement of the particle size of powders. Due to the localized high pressure generated from the collision of the balls during milling; the powders particle size is refined. Furthermore, ball milling of CNTs has been employed before with the presence of chemicals. This method increased the dispersion of the CNTs in the chemical and also some functional groups were attached to the CNT surface. This is a chemo-mechanical way of functionalizing the nanotubes. During milling the CNT length can be compromised but this can be controlled by regulating the milling time and the addition of chemicals. In addition to the above mentioned dispersion technique stir and extrusion is also another method to evenly distribute the CNTs in the matrix. Stir includes mixing particles in a liquid medium; this includes mixing CNTs in a polymer matrix. The propeller's size, shape and speed affect very much the homogeneity of the dispersion. In severely clustered CNTs the use of shear forces is essential to attain a finer dispersion. Therefore a shear mixer, which can reach up to 10,000 rpm, is utilized to achieve this goal. Extrusion is used to mix CNT with solid polymers. Both the CNTs and the polymer are fed into the hopper of the extruder. Shear forces are created as a result of the speed of the extruder's twin screw. These forces allow for the

dispersion of the CNTs in the polymer melt. This method is very useful in producing CNT/polymer composites with high CNT loadings [17].

## 2.2 Polypropylene

Polypropylene is the matrix in the CNT/Polymer composite that will be fabricated and investigated in this study. This section will discuss some background information about polypropylene (PP) and its physical and mechanical properties. Polypropylene was produced in 1954 by G. Natta who followed the work of K. Ziegler [19]. PP is a macromolecule that consists of 10,000 to 20,000 monomer units of propylene. There are several types of Polypropylene. This depends on the steric arrangement of the methyl group attached to the carbon atoms backbone. If methyl groups are all arranged on the same side of the chain this is referred to as isotactic PP (used in this research). If the methyl group is attached to the polymer backbone in an alternating matter then this is called syndiotactic PP. The random orientation of the methyl group to the backbone is called atactic PP. Figure (2.11) shows the different types of PP [19].

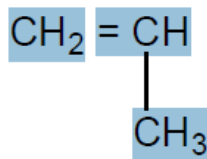


Figure 2.10 Propylene monomer [19]



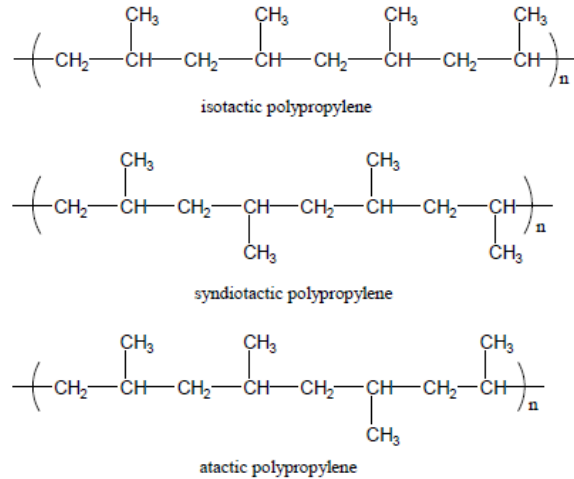


Figure 2.11 Types of Polypropylene [19]

### 2.2.1 Advantages and disadvantages of PP

PP is present in a lot of our daily life experience. Some household products are made from it, such as buckets, bottles, toys, and luggage. Parts of domestic appliances are also produced from PP for example: Dishwasher and washing machine and refrigerator parts ...etc. It is also a part of the automobile industry as well; several parts are manufactured from PP such as Radiator expansion tanks, brake fluid reservoirs fittings, steering wheel covers, bumpers spoilers, battery cases and tool boxes. Polypropylene fulfils some critical requirements for the above mentioned products. As an example, car bumper require high impact strength at low temperatures, excellent weathering and high rigidity. Some kitchen appliances require rigidity, surface gloss, transparency, and good heat ageing resistance. Luggage requires high impact strength and warpage [19]. PP is a very popular service plastic. It has a major advantage which allows it to be present in a lot of domestic appliances, packaging and also furniture which are used in our daily life. The major advantages of PP are high stiffness at low density and resistance to relatively elevated temperature when not subjected to mechanical stresses. PP also has good fatigue, chemical and environmental stress cracking resistance [19]. One of the most important properties

in service polymers is its ease of processability by injection moulding and extrusion to facilitate the large scale industrial production of PP products. The major disadvantage of PP is that it has high mould shrinkage, high thermal expansion and low impact strength at sub-ambient temperature. Other disadvantages of PP are limited solvent and adhesive bonding, limited transparency and low wear properties. Regarding industrial manufacturing processes PP is difficult to blow mould or form under vacuum and elevated temperatures. Another important drawback of PP is that although it resists crack initiation once a crack is present in the matrix PP has a very low crack propagation resistance especially at lower temperatures [20]. Another important property to discuss is PPs crystallinity. The polymeric chains of PP are ordered in a linear manner and they are able to be packed in an ordered crystal structure. However due to the length of the chains there is a possibility of chain entanglement and other imperfections such as branching, which compromises the ordered crystal structure. Therefore PP is considered a semi-crystalline polymer [19].

### **2.2.2 Mechanical properties of PP**

According to Devesh Tripathi [19] the tensile force of the sample increases with increasing elongation until the yield point is reached. Figure (2.12) shows a schematic diagram of a typical tensile test for PP. The force decreases with further increase in elongation. This occurs at the necking of the sample. The necking propagates all through the length of the sample. At that point a further increase in force is observed until elongation at break is reached. This is due to a partial orientation of the macromolecules of the polymer which results in the increase of the tensile strength of the sample. This behaviour is also present in other ductile polymers. Table (2.2) lists some of the mechanical properties of PP

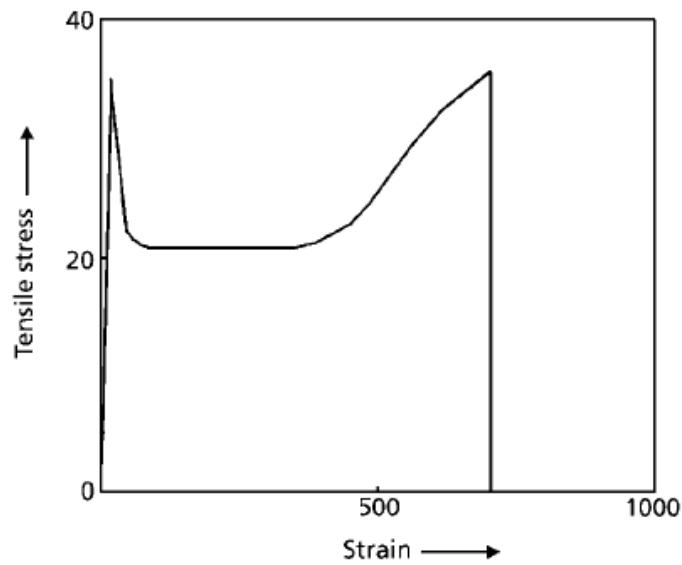


Figure 2.12 Typical Stress/Strain Curve for PP [19]

| Property                                | PP    | LDPE | HDPE | HIPS | PVC   | ABS   |
|-----------------------------------------|-------|------|------|------|-------|-------|
| Flexural modulus (GPa)                  | 1.5   | 0.3  | 1.3  | 2.1  | 3.0   | 2.7   |
| Tensile strength (MPa)                  | 33    | 10   | 32   | 42   | 51    | 47    |
| Specific density                        | 0.905 | 0.92 | 0.96 | 1.08 | 1.4   | 1.05  |
| Specific modulus (GPa)                  | 1.66  | 0.33 | 1.35 | 1.94 | 2.14  | 2.57  |
| HDT at 0.45 MPa. (°C)                   | 105   | 50   | 75   | 85   | 70    | 98    |
| Maximum continuous use temperature (°C) | 100   | 50   | 55   | 50   | 50    | 70    |
| Surface hardness                        | RR90  | SD48 | SD68 | RM30 | RR110 | RR100 |
| Cost (£/tonne)                          | 660   | 730  | 660  | 875  | 905   | 1550  |
| Modulus per unit cost (MPa/£)           | 2.27  | 0.41 | 1.97 | 2.4  | 3.31  | 1.74  |

ABS = acrylonitrile butadiene styrene  
HIPS = high impact polystyrene  
RR = Rockwell R

RM = Rockwell M  
SD = Shore Durometer

Table 2.2 Comparison of unmodified PP with other Polymers [19]

## **2.3 CNT/ Polymer Composite Processing:**

The most significant factors that affect the composite properties are the exfoliation of the CNT clusters, homogenous dispersion, alignment and interfacial bonding between the reinforcement and the matrix [11]. CNTs cluster due to attractive Van der Waal forces. In order to maximize the reinforcement of the CNTs in the polymer matrix one should reduce the agglomeration of the CNTs and enhance its dispersion. The main processing techniques of CNT /Polymer composites include solution mixing, melt mixing, bulk mixing and in situ polymerization and chemical modification processes.

### **Preprocessing of CNT:**

In order to be able to process CNT/Polymer composites on a macroscopic scale CNTs need to be preprocessed to ensure optimum properties' enhancements in the composites.

- 1- Purification to eradicate non-nanotube components that emerge from the CNT fabrication techniques such as amorphous carbon, fullerenes...etc.
- 2- Detanglement of CNTs for better dispersion of individual nanotubes in the composites.
- 3- Chemical functionalization of CNTs to enhance the interfacial bonding between the reinforcement and the matrix [21]

### **2.3.1 Solution Mixing Technique**

The most common technique for processing CNT-Polymer composite is to dissolve the polymer in a suitable solvent and mix the CNTs in the solution. The solvent is then evaporated to form the composite. The most important advantage of this technique is that the stirring of the CNTs in the

dissolved polymer facilitates the dispersion of the CNTs in the composite and reduces its clustering [11]. The good dispersion of the CNT in the polymer matrix enhances the interfacial interaction between the constituents of the composite.

There are several steps to produce the composite using solution mixing:

- 1- Dispersion of the CNT in a solvent or polymer solution using energetic agitation
- 2- Mixture of CNT and Polymer in solution using energetic agitation
- 3- Controlled evaporation of the solvent leaving a composite [11]

It was mentioned above that agitation of the CNT Polymer solution is an important step the processing technique. Agitation can be done using magnetic stirrer, shear mixing, reflux and commonly ultrasonication (mild or high power) [22].

There are also some concerns regarding the solution mixing process. Using high power ultrasonication can shorten the CNTs length which can affect the aspect ratio as a result the composites' properties. Furthermore, during slow solvent evaporation the CNT incline to agglomerate and inhomogeneous dispersion can occur. However, this can be decreased by placing the nanotube/polymer suspension on a rotating substrate (spin casting) or dropping it on a hot substrate (drop casting) [15].

### **2.3.2 Bulk mixing Technique**

Bulk mixing technique is another alternative to produce CNT/Polymer composites [22, 15]. This entails the incorporation of milling as a mechanical procedure to generate high stresses, due to the colliding action of grinding that can create chemical reactions and structural changes in the materials [22, 15]. Pan milling is considered to be a mechanochemical process because the polymer can be grafted on the nanotube which can help with the dispersion and improve the

interfacial bonding [15]. Hesheng Xia et al. [4] used pan milling to produce PP/CNT composite powder then melted the powder using twin roll masticator to obtain the PP/CNT composite. However as a drawback from milling the CNT used was shortened after each milling cycle until it was reduced from a few micrometers to 0.4-0.5 $\mu$ m.

### **2.3.3 Melt Mixing technique**

Melt mixing entails combining the polymer melt with CNT using intense shear forces [22]. This technique is widely used with thermoplastic polymers. The advantages of this method are its speed and simplicity and compatibility with the industrial processes. This technique is also very favorable because the fabrication of the CNT/polymer composite is free of solvents and any other contamination factors which can be present in the solution mixing or in situ polymerization techniques [21].

Bulk samples can be produced using several techniques such as compression molding, injection molding or extrusion. However the most important factor in the melt blending technique is to optimize the processing conditions. The addition of CNT to the polymer melt changes the melt properties of the polymer such as its viscosity, which can result into polymer degradation under the high shear stresses that accompanies this process. As an example for polymer degradation due to increased viscosity Potschke et al. [11] blended masterbatches of CVD-MWNT in Polycarbonate (PC) with pure PC in a microcompounder at 260°. The samples were then extruded through a circular die. However some polymer degradation occurred due to the increased viscosity of the polymer with the addition of CNT. To overcome the increased viscosity higher shear rates were needed which resulted in the degradation [11].

An important concern to be taken into consideration is that the melt blending technique is less effective in dispersing the CNT in the polymer matrix than the solution mixing method. This is due to the high viscosities of the composites at higher CNT loadings. Therefore it is advised to use the melt blending technique at lower concentrations of CNT [15].

### **2.3.4 In situ Polymerization Technique**

This technique includes the dispersion of the nanotubes in the monomer followed by the polymerization of the monomers. Through a series of condensation reactions covalent bonds are formed between the nanotubes and the polymer matrix. The most commonly used polymers that use this technique for composite fabrication are epoxies. The nanotubes are first dispersed in the resin subsequently curing of the resin with the hardener. It is worth mentioning that as the polymerization process continues the viscosity increases which can hinder the in situ polymerization reactions [15]. Due to the small size of the monomers' molecules the resulting composite has homogeneously dispersed reinforcements. This technique produces even better homogeneity than the solution mixing one [22]. Another advantage to this technique is that higher loadings of CNT can be used because this process grafts the Polymer macromolecules onto the nanotubes' walls. This procedure could also be implemented for the preparation of insoluble and thermally unstable polymers [11].

## Chapter 3: Literature Review

### 3.1 Mechanical properties

The area of CNT/polymer composites is heavily researched with hundreds of papers published each year. Therefore, this literature review will focus on studies of relevance to this current research, namely the melt processing and solution mixing of PP/CNT composites. It will also include the effect of the CNT content on the mechanical properties and the crystallization and flow behavior.

In this section, mechanical properties of solution and melt processed composites will be presented and discussed. The first study using CNTs in solution-based composites for reinforcement was by Shaffer and Windle [23] in 1999. They determined the tensile elastic modulus and damping properties of the composite films using a dynamic mechanical thermal analyzer (DMTA) as a function of nanotube loading and temperature. The composite used in this study was CVD-MWNT-PVA films with nanotube weight fractions that reach up to 60%. Very little reinforcement was observed; the storage modulus for the polymer doubled from 6 GPa to 12 GPa with the addition of 60 wt% MWNT. The presence of the nanotubes stiffens the material, particularly at elevated temperature, and in some cases delayed the beginning of thermal degradation [11, 23].

Further research was conducted by Qian et al. [24] where CVD-MWNT-PS was fabricated and the tensile properties of the composite were investigated. An increase in modulus at 1 wt% from 1.2 GPa to 1.62 GPa and 1.69 GPa for composite filled with short (15  $\mu\text{m}$ ) and long (50  $\mu\text{m}$ ) CNTs respectively was observed. The tensile strength also increased from 12.8 MPa to 16 MPa for both types of CNT. As part of Qian et al. research, they also investigated the failure mode of the CNT within the matrix. It was found that the CNTs either fractured or pulled out of the matrix.



This was due to poor interfacial bonding and the existence of weak spots that facilitated pull-out. It was clear that the weakest location that affects the mechanical properties of the CNTs is associated with structural defects [11, 24].

Safadi et al. [25] also investigated the tensile properties of composites made from CVD-MWNT and PS. The PS was first dissolved in Toluene same as Qian et al. [24]. An increase in modulus from 1.53 GPa for the polymer to 3.4 GPa for 2.5 vol% CNT was observed. The tensile strength also increased from 19.5 MPa to 30.6 MPa for the same CNT loading. In concurrence with Qian's research CNT fracture and pull out were present in Safadi's work.

In 2002 PVA polymer was used again as a matrix by Cadek [11] to investigate the mechanical properties of the CNT/Polymer composite using nanohardness testing. However, the reinforcement used was arc discharge MWNT. The composites were spun cast films with PVA and PVK (polyvinylcarbazole) used as matrices. As increase in modulus from 7 GPa to 12.6 GPa at 0.6 vol% in PVA and 2 GPa to 5.6 GPa at 4.8 vol% in PVK were observed [11].

In 2004 Cadek et al. [11] addressed the question of which type of CNT will be more effective as a reinforcement. They fabricated a PVA matrix filled with different types of CNT ranging from: SWNT, DWNT, CVD-MWNT and arc-MWNT. They found that for all the CNT types except for SWNT, the Young's Modulus of the composite scales directly with the total interfacial surface area in the matrix (the film in this case). As for SWNT composite the reinforcement was much lower due to the slippage of SWNT in bundles. This research showed that the optimum candidate for reinforcement would be CVD- MWNT.

Another area to highlight due to its relevance to this research is the previous efforts regarding the mechanical properties of melt processed composites. One of the early studies on the mechanical

properties of CNT reinforced polymer processed by melt compounding was conducted by Jin et al. [26]. The composite used in this study was Poly(methyl methacrylate) reinforced with arc-discharge MWNT. The samples were first mixed using a mixing molder then compressed under heat and pressure to produce the required composites. An increase in modulus from 0.7 GPa to 1.63 GPa at 17% CNT was observed. In 2002 2 similar studies researched the effect of adding CVD-MWNT on PS on the mechanical properties of the composite. An increase in modulus from 2GPa to 2.6GPa and 4.5GPa at 5wt% and 25 vol% respectively was obvious. In both cases the fracture surface of the composites showed signs of CNT pull out. However, in one case the pulled out CNT was covered with polymer which is an indication of very strong interfacial bonding between the reinforcement and the matrix [11].

In 2004 significant improvement in the mechanical properties of CNT reinforced polymer composite was reported. Meincke et al. [27] fabricated CVD-MWNT in polyamide-6. At 12.5 wt% CNT the modulus almost doubled from 2.6 GPa to 4.2 GPa [11]. The polymer composite was extruded using a twinscrew extruder

Zhang [11] and colleagues fabricated CVD-MWNT in polyamide-6 and they observed an increase in modulus from 0.4 GPa to 1.24 GPa at 2 wt% CNT which corresponds to a tripling in the value of the modulus. An increase in the yield strength from 18 to 47 MPa was also reported.

With regards to the use of PP as a matrix efforts were carried out in order to investigate the mechanical properties of CNTs when added as reinforcement to a polypropylene matrix. Different processing and fabrication techniques were used to produce the composite as well as different CNT loadings. Bao et al. [28] investigated the mechanical behavior of PP/CNT under varied loading rate and temperature. PP nanocomposites filled with 0.1, 0.3, 0.5 and 1.0 wt%

MWNT were mixed in a twin screw Barbender Plaiticorder at 60 rpm. Virgin PP was also processed in a similar manner as a reference sample. The extrudates were pelletized. The melt mixing step was repeated to ensure homogenous blending. The pellets produced were then injection molded into dog-bone samples. The samples were then tested under tensile loading with various strain rates (0.05-500 mm/min) and under different temperatures ranging from 18°C-80°C. Table (3.1) below shows the mechanical properties of the pure polymer and the PP/MWNT at different CNT wt%. The addition of small amounts of MWNT to PP improved the yield strength and Young's Modulus. The stiffness of PP increased dramatically after 0.3 wt% MWNT by ~31%. The yield strength reached its maximum at 0.3% then started to decrease gradually as the MWNT% increased. After further analysis of the yield strength at different strain rates and different temperatures it was clear that the PP/MWNT composites are strain rate and temperature sensitive materials. The reinforcing effect of MWNT in PP is more prominent at higher temperatures [28].

| Specimens       | Yield strength (MPa) | Young's modulus (MPa) |
|-----------------|----------------------|-----------------------|
| Pure PP         | 30.71 ± 0.18         | 1570 ± 24             |
| PP/0.1 wt% MWNT | 34.89 ± 0.39         | 1743 ± 65             |
| PP/0.3 wt% MWNT | 35.98 ± 0.27         | 2107 ± 72             |
| PP/0.5 wt% MWNT | 35.88 ± 0.39         | 2070 ± 66             |
| PP/1.0 wt% MWNT | 35.65 ± 0.41         | 2056 ± 83             |

**Table 3.1 Mechanical properties of PP and PP/MWNT nanocomposites at 10mm/min and 18°C [28]**

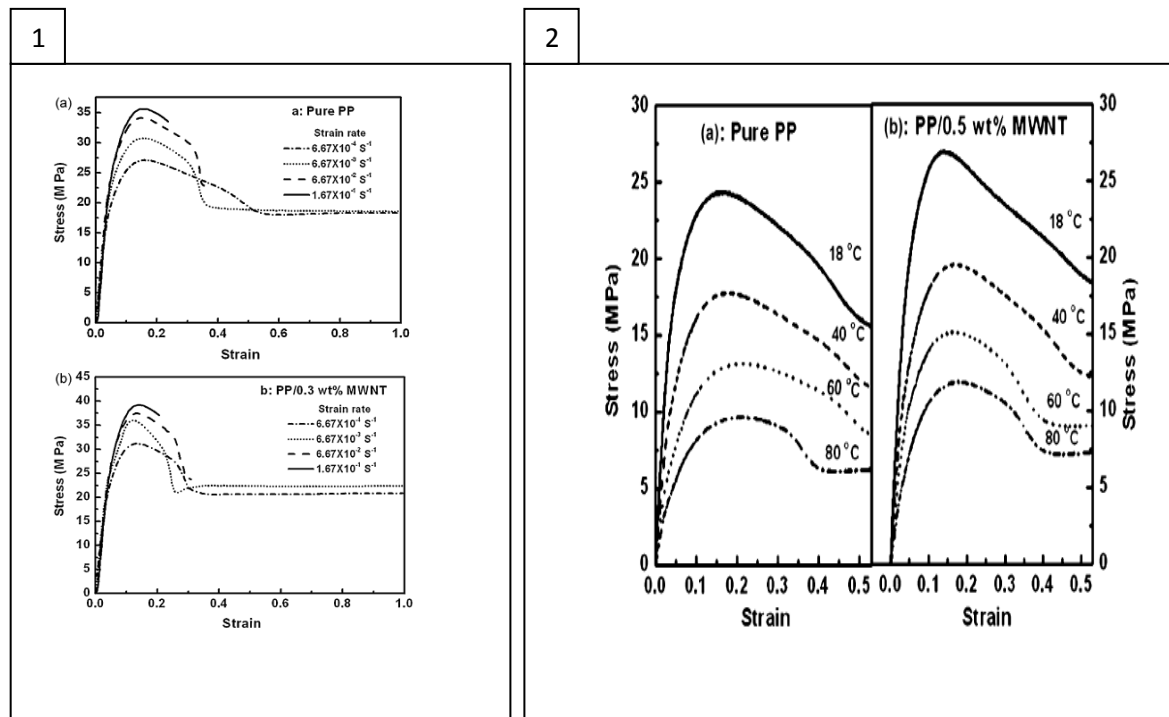


**Figure 3.1** 1) Stress–strain curves of (a) pure PP and (b) PP/0.3 wt% MWNT nanocomposite at 18 °C for various strain rates 2) Stress–strain curves of pure PP and PP/0.5 wt% MWNT nanocomposite at a strain rate of  $6.67 \times 10^{-5} \text{ s}^{-1}$  for various temperatures [28]

Figure (3.1) shows the effect of different strain rates at a constant temperature on the yield strength of the composite. The yield strength of the composite increases with increasing strain rate but the composite loses ductility. The second part of the figure shows the effect of increased temperature on the yield strength of the composite. The yield strength of the composite increases with the addition of 0.5 wt% MWNT at different temperatures compared to the neat polymer. However, with increasing temperature the strength decreases dramatically for the pure PP as well as PP/0.5wt% MWNT. Bao et al. [28] has also presented an SEM images for a PP and a 0.5wt% PP/MWNT sample. Figure (3.2) shows well dispersed nanotubes in the matrix. The

homogenous distribution of the nanotubes at this loading could be the reason for the increase in yield strength compared to the neat polymer [28].

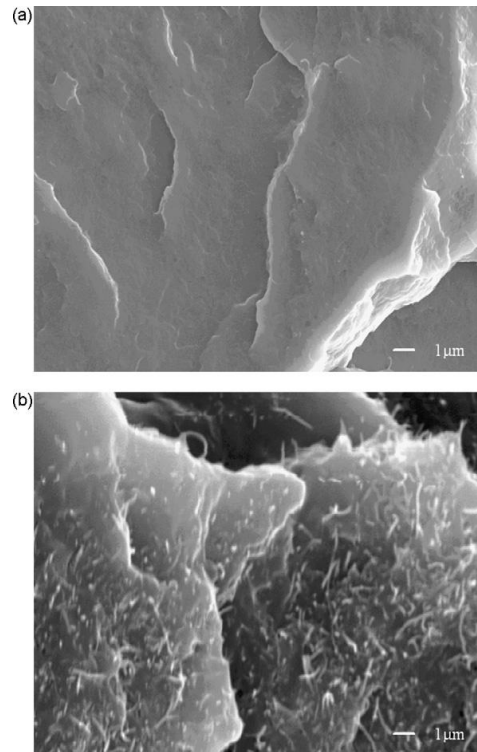


**Figure 3.2 SEM fractographs of (a) PP and (b) PP/0.5 wt% MWNT nanocomposite [28]**

In 2005 Lopez et al. [6] fabricated PP/SWNT composites using shear mixing and tested the thermal and mechanical properties of the composites. A commercially available isotactic polypropylene (iPP) and arc discharge SWNT were used in this work. The composites were prepared using a Haake Rheomix internal mixer, fitted with double high shear roller-type rotors. After melting the polymer 0.25%, 0.5%, 0.75%, and 1% of SWNT was added to it. The resulting mixture was then compression molded. Tensile testing was performed at room temperature according to ASTM D 638 M. In this study Lopez et al. compared the reinforcing effect of SWNT vs. Carbon Black (CB) to PP matrix. As the SWNT content increases in the polymer the

Young's modulus gradually increases until it reaches 0.75% SWNT when it starts to decrease. This is seen in Fig (3.3). The tensile modulus goes from 0.85 GPa for pristine PP to 1.19 GPa for 0.75% SWNT. However by increasing the SWNT to reach 1% the tensile modulus decreases to 1.1 GPa. Whereas using CB as filler, the tensile modulus increases with increasing filler content. Regarding the shape and the interfacial area of SWNT vs. CB the difference between them is not that considerable. The main factor for the dissimilar behavior in the tensile modulus could be related to the morphology described by the average aspect ratio. In order to exhibit similar interfacial area the tubelous SWNT bouquets and the isometric particles of carbon blacks may show a considerable difference in their aspect ratio. As the SWNT entangle together more easily at higher concentrations (1%) decreasing the interfacial bond between the filler and the matrix. This is when the clustering effectively reduces the aspect ratio (length/diameter) of the reinforcement. The maximum tensile strength was also affected by the clustering of the SWNT as the matrix showed its maximum strength at 0.5% SWNT where it reached 35.9 MPa then it started to decrease to 33.8 MPa at 1%SWNT [6].

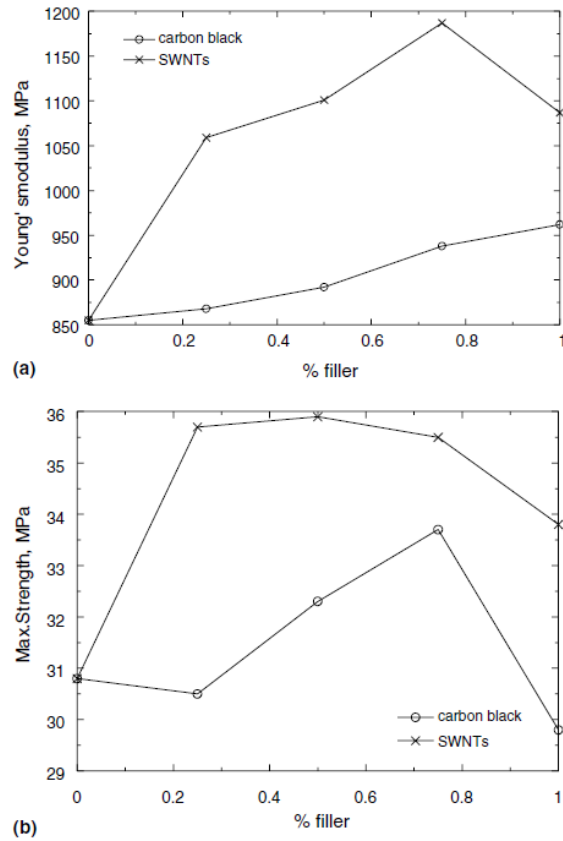


Figure 3.3 Variation of (a) Young's modulus and (b) yield strength as a function of the SWNT content in the composite [6]

Hemmati et al. [29] also investigated the mechanical properties of PP/MWNT composites fabricated using melt blending. The MWNT and PP pellets were placed in a Barbender internal mixer and then heated up. The MWNT percentages were 0%, 0.25%, 0.5%, 1%, 1.5%, 2%, 4% and 8%. After the melt mixing process the molten material was then compression molded into sheets using a hydraulic press. The final specimen size was cut for the prepared sheet. The tensile, flexural and impact testing was conducted on the PP and its composites according to the ASTM D638, ASTM D790 and ASTM D256 respectively. The tensile test sample had a 5 cm gage length and was pulled at 50mm/min crosshead speed. The flexural test's crosshead speed was 1.3 mm/min. The tensile, flexural and impact properties are presented in table (3.2). The

values in the brackets are for the percent increase or decrease of the properties. MWNT have high failure strain (10-30%) which allows the composite to bend and buckle under impact loading. During impact loading the damage zone magnifies the stress locally because of the cracking of the matrix. However, this is hindered from the MWNTs and its high failure strain mentioned earlier. Therefore the increase in impact strength was anticipated. In figure (3.4 a and b) the tensile and impact strength are plotted vs. MWNT content. In these figure it is clear that a maximum peak has occurred for tensile and impact strength. The maximum tensile strength was reached at 1.5% MWNT and the maximum impact strength was at 1% MWNT. In figure (3.4 c and d) tensile and flexural modulus are plotted vs. MWNT content. These figures show a continuous increase in both moduli from 648 MPa to 730MPa and from 1254MPa to 2304MPa, respectively, as the MWNT content increased from 0 to 8 wt%. At 8%MWNT the tensile modulus decreased slightly. According to the authors [29], tensile strength and modulus, flexural modulus and impact strength of the composites increased as long as the MWNT were uniformly distributed throughout the matrix. Once agglomerates started formation these properties were decreased [29].

| Sample | MWNT content (wt%) | Flexural Modulus (MPa) | Flexural Strength (MPa) | Tensile Modulus (MPa) | Tensile strength (MPa) | Notched Izod Impact strength (J/m) |
|--------|--------------------|------------------------|-------------------------|-----------------------|------------------------|------------------------------------|
| NC0    | 0                  | 1254                   | 399                     | 648                   | 28.3                   | 2.7                                |
| NC1    | 0.25               | 1300 (4)               | 408 (2.25)              | 669 (3.3)             | 31 (10)                | 3 (11)                             |
| NC2    | 0.5                | 1396 (11.3)            | 418 (4.8)               | 733 (13)              | 32.07 (13.1)           | 3.2 (18)                           |
| NC3    | 1                  | 1418 (13)              | 417 (4.5)               | 752 (16)              | 32.2 (13.7)            | 4.2 (56)                           |
| NC4    | 1.5                | 1497 (20)              | 435 (10)                | 766 (18)              | 34.62 (22)             | 4.1 (52)                           |
| NC5    | 2                  | 1547 (23)              | 554 (39)                | 781 (21)              | 33.12 (17)             | 3.3 (22)                           |
| NC6    | 4                  | 2241 (79)              | 617 (55)                | 811 (25)              | 31.1 (10)              | 2.5(-7)                            |
| NC7    | 8                  | 2304 (84)              | 629 (58)                | 730 (12.6)            | 28.15 (-0.5)           | 2.0(-25)                           |

Table 3.2 Mechanical properties of PP nanocomposites [29]



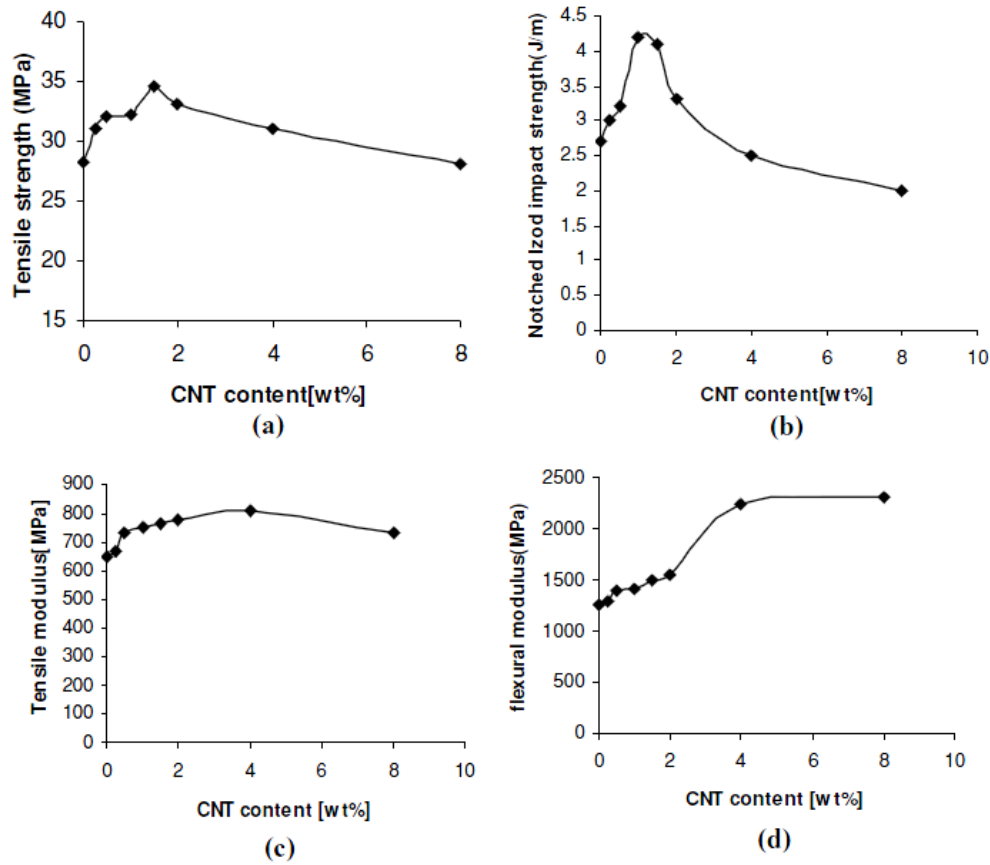


Figure 3.4 Tensile strength (a), notched Izod impact strength (b), tensile modulus (c), and flexural modulus (d) [29]

Prashatntha et al. [8] produced MWNTs reinforced polypropylene composite by mixing PP pellets with the commercial masterbatch “Plasticyl-2001” containing 20 wt. % of MWNT produced by extrusion process. The dilution was prepared by using a co-rotation twin screw extruder. The resulting composite was pelletized then compression molded into 4 mm thick plates for rheological experiments. For the mechanical investigation the pellets were injection molded into standard test specimens for tensile, impact and flexural tests. The final composites contained 1, 2, 3 and 5 wt% MWNT in the PP matrix. The neat polymer was also processed the same way as the composites and used as reference sample. The tension, impact and flexural tests were conducted according to the ISO 527, ISO 179 and ISO 178 respectively. The stress-strain

curves of the nanocomposites with respect to their nanotube content are shown in Figure (3.5). The tensile properties of the neat Polypropylene and the different nanocomposites are shown in Table (3.3). For the neat PP, the maximum elongation was observed at 620% and the strain hardening region appears at 400%. At 1 and 2 wt% CNT relative high ductility and necking were observed. However, the strain at fracture was low and the no strain hardening region was present. At higher loading of CNT (3 and 5 wt %) brittle behavior was present and fracture occurred after the yield point. The percentage increase of the Young's modulus is from 26.9%-40.2% and of yield stress is from 17%-30.3% with increasing CNT wt%. With increasing the MWNT content the nanotubes start forming interconnecting network. With the increase in the network density intense strain localization areas start forming which hinder the plastic deformation of the matrix. These strain localization areas cause matrix cracking. Therefore the reduction in ductility with high MWNT content could be due to the presence of nanotube aggregates which act as stress raisers [8]. The results of this study were found similar to the work done by Bao et al. [28] mentioned earlier in this section.

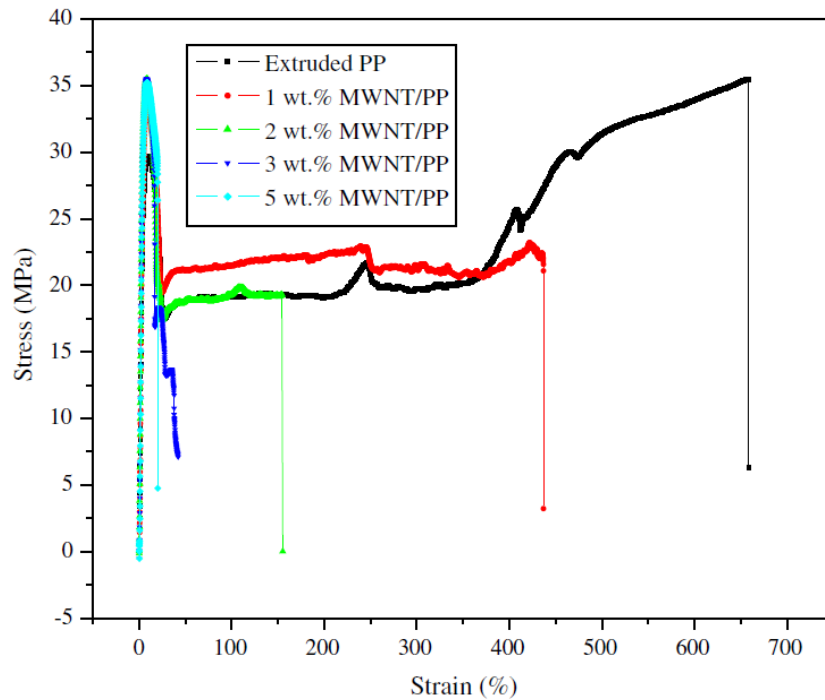


Figure 3.5 Stress-strain Curves of PP/MWNT nanocomposites [8]

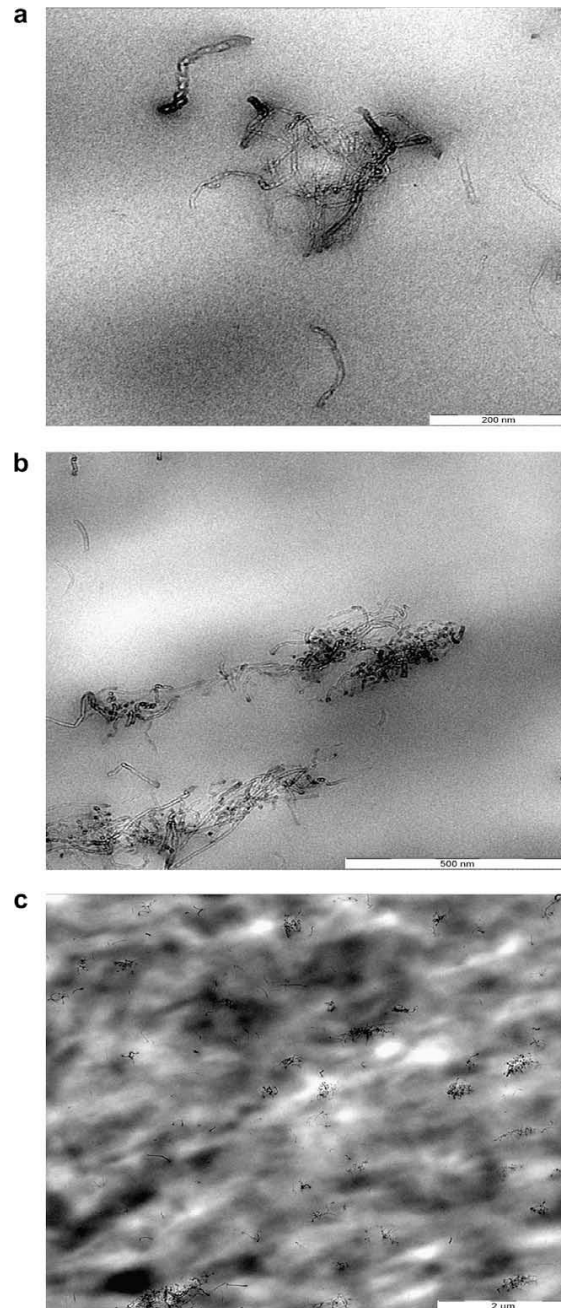
| Material        | Tensile properties |                    |                     |
|-----------------|--------------------|--------------------|---------------------|
|                 | Modulus (MPa)      | Yield stress (MPa) | Strain at break (%) |
| Neat PP         | 1280 ± 20          | 28.2 ± 0.5         | 620 ± 15            |
| 1 wt.% MWNT/PP  | 1625 ± 25          | 33.2 ± 0.6         | 436 ± 10            |
| 2 wt.% MWNT/PP  | 1728 ± 15          | 35.5 ± 0.5         | 154 ± 08            |
| 3 swt.% MWNT/PP | 1795 ± 20          | 36.8 ± 0.5         | 64 ± 05             |
| 5 wt.% MWNT/PP  | 2150 ± 25          | 35.25 ± 0.8        | 12 ± 02             |

Table 3.3 Tensile properties of PP and PP/MWNT nanocomposites [8]

Prashatntha's [8] TEM images confirmed the results of the tensile tests. They showed regions of individually dispersed nanotubes (figure 3.6 a) as well as aggregates of different sizes (figure 3.6 b) at 2wt% MWNT. Figure 3.6 c) shows the dispersion of MWNT at lower magnification [8].

Another observation is the SEM image of the 3wt% MWNT composite shows a masterbatch

clusters in the PP matrix (see figure (3.7)). With increasing MWNT wt% more clusters were formed which lead to the brittle behavior and decrease in yield strength at higher loadings of MWNTs.



**Figure 3.6** Transmission electron microscopic pictures of 2 wt. % PP/MWNT nanocomposites. (a) Regions of dispersed nanotubes in PP matrix, (b) regions of nanotubes agglomerations in PP matrix and (c) low magnification TEM picture showing the nanotube dispersion [8]

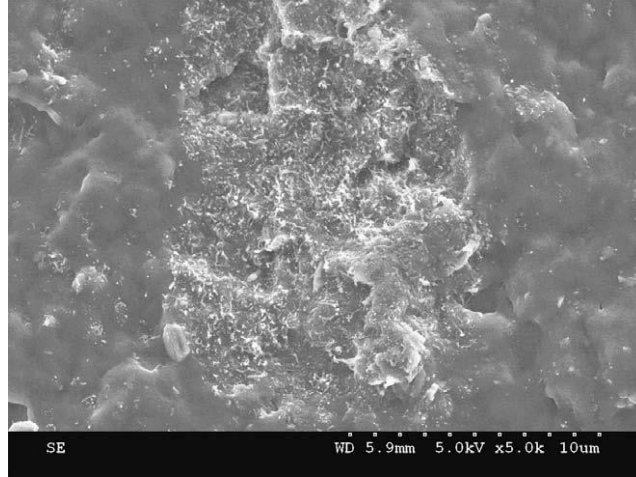


Figure 3.7 SEM image of 3 wt.% PP/MWNT nanocomposites showing a masterbatch clusters in PP matrix [8]

The flexural strength and modulus were also investigated in this study and both showed an increase with increasing MWNT content up to 2 wt%. At higher CNT loadings (3 and 5wt%) the flexural properties started to decrease due to the formation of CNT clusters, which caused filler-filler interaction and lower interfacial properties encouraging shear delamination. Figure (3.8) shows the flexural properties of neat PP and PP/MWNT nanocomposites.

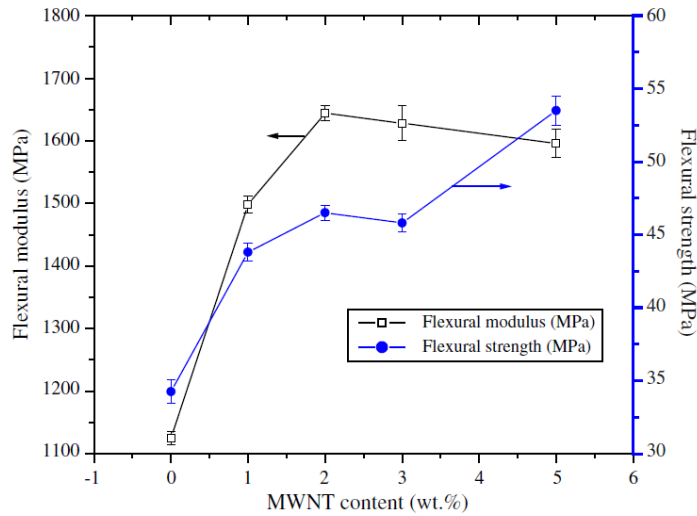


Figure 3.8 Flexural properties of PP and PP/MWNT nanocomposites [8]

Impact properties of the neat PP were also investigated and compared to that of the PP/MWNT nanocomposites. Impact strength for the un-notched samples decreased with increasing CNT loading. The decrease in strength was more pronounced at 3 and 5wt% because of the presence of nanotube clusters in the matrix. As for the notched specimens the impact strength of the samples showed a slight increase as the MWNT content increased. The 2 wt% sample had a 40 % increase in impact energy compared to the neat PP one. Notched impact behavior is governed to a greater extent by factors that can affect the propagation of fracture starting at the stress concentration region at the notch tip. Therefore, the fiber pullout, fiber fracture and nanotube bridging effect are specifically visible in the notched samples. Figure (3.9) shows the Charpy impact properties of PP and PP/MWNT nanocomposites which compared notched and un-notched samples [8].

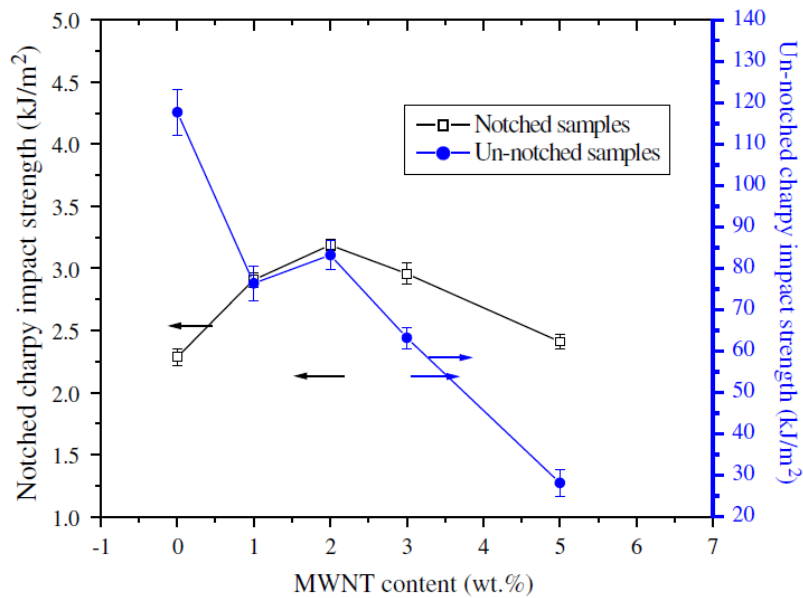


Figure 3.9 Charpy impact properties of PP and PP/MWNT nanocomposites [8]

Chang et al. [30] analyzed the mechanical properties of polypropylene fibers with different concentrations of SWNTs. The SWNTs were sonicated in decahydronaphthalene for an amount of time then the SWNT containing solution was heated. The PP granules were then added to the solution and dissolved by mechanical stirring. The viscous solution was then dried and broken into small pieces. Using an Instron capillary rehometer with a 1.6 mm die, the fibers were spun. The SWNT weight percentages were: 1, 2, 3, 4 and 5 wt%. Tensile testing was performed using a mini-tensile testing machine. The Young's modulus is very much dependant on the SWNT content. A strong increase was observed with the addition of 1wt% and a quite weak increase with the addition 5wt% SWNT. An obvious change in the slope of the stress-strain curves (Figure (3.10)) is very obvious. This could be due to nanotube slippage in the polymer matrix or another explanation could be the change of the PP crystallinity under stress. The isotactic PP has four different crystalline structures: monoclinic ( $\alpha$ ), hexagonal ( $\beta$ ), triclinic ( $\gamma$ ), and smectic or quenched polymorphs. The monoclinic PP can be obtained under regular industrial and laboratory processing techniques. The hexagonal  $\beta$ -form PP is obtained under certain thermal and shear stress. The mechanical properties of the composite can be reduced with increasing  $\beta$ -phase content. After further investigations, Chang et al. found that the  $\beta$ -crystal of PP is being formed when the fibers are being stretched uniaxially. Therefore, it was confirmed that the decrease in modulus and change in stress-strain slope was due to the formation of the  $\beta$ -crystal in the PP matrix [30].

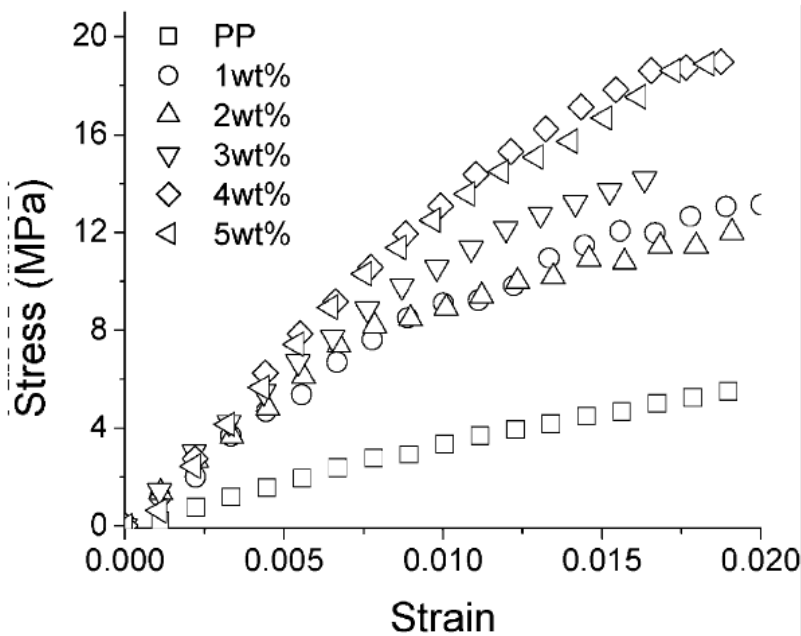


Figure 3.10 Stress-strain curves of PP and PP composite fibers [30]

### 3.2 Differential Scanning Calorimetry:

Since the crystalline structure has a great impact on most physical and mechanical properties of semicrystalline polymers, a comprehension of the crystallization process as well as the crystallization effects of using CNTs is very important [6,31]. The earlier studies on the effect of fillers on the crystallinity of a polypropylene matrix were done with carbon fibers. Carbon fibers, which are somewhat similar to carbon nanotubes can nucleate crystallinity in isotactic polypropylene [32]. Several studies after that investigated whether or not carbon nanotubes nucleate crystallization in polypropylene. Some of these studies will be mentioned shortly [6, 15, 28, 33, 34, 35].

Grady et al. [32] fabricated PP/SWNT composites via solution mixing technique. The solvent used in this study was decalin and the SWNT weight percentages were 0.6 and 1.8 wt%. The



nanotube were also functionalized to make them hydrophobic then allow them to be soluble in an organic solvent. Non-isothermal crystallization and dynamic mechanical thermal analysis were conducted. The isothermal testing revealed that the crystallization temperature- the temperature at which maximum crystallization exotherm occurs- increases with increasing CNT loading. This suggests that the nanotubes act as nucleating agents for crystallization. It was also clear that 0.6wt% SWNT was almost enough to provide sufficient surface area to allow crystal growth.

Valentini et al. [36] also investigated the effect of SWNTs on the crystallinity of polypropylene matrix. The composites tested were produced using the melt blending method. The SWNT loadings were: 5, 10, 15 and 20 wt%. Non-isothermal crystallization analysis was performed using Differential Scanning Calorimetry (DSC). Figure (3.11) shows crystallization curves of neat PP and PP/SWNT composites.

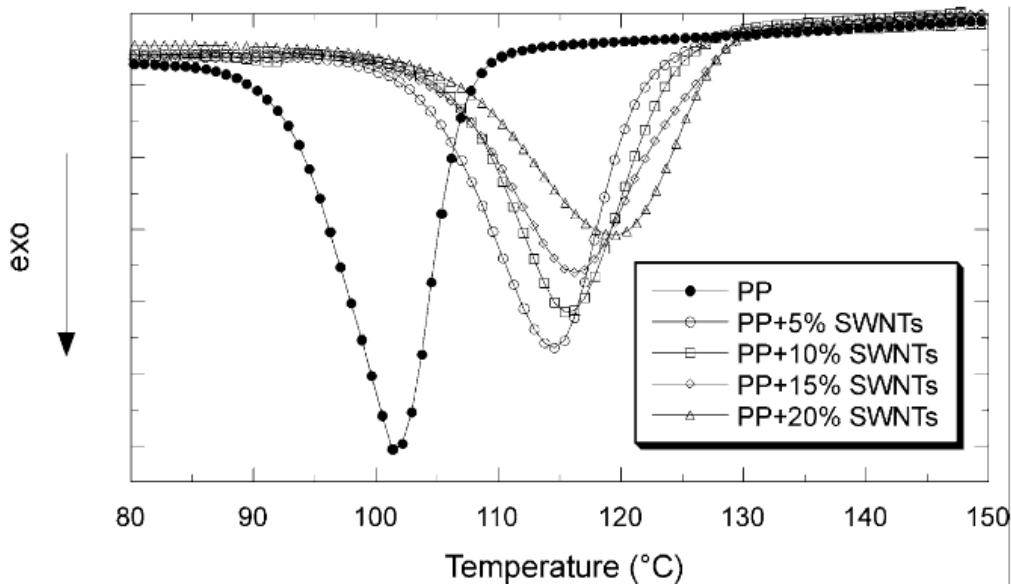


Figure 3.11 Non-isothermal crystallization curves of PP and PP-SWNT Composites [36]

It is clear from the curves that the addition of SWNT's in the polymer matrix increased the crystallization temperature  $T_c$ . A significant shift in  $T_c$  is obvious at the lowest reinforcement content (5wt %) with a slow but continuous increase with increasing SWNT content. As a result, it has been shown that the incorporation of SWNT speeds up the nucleation and crystal growth mechanism of PP. This phenomenon is clearer at lower SWNT concentrations. Figure (3.12) shows micrographs of the crystalline morphology of the neat PP and 5wt% SWNTs/PP after the crystallization process. At 0% SWNTs large grains are visible with an average diameter of 100 $\mu$ m. On the other hand at 5wt%PP/SWNT high quantity of smaller grains are seen with an average diameter of 10  $\mu$ m. These micrographs were taken using an optical polarizing microscope [36]. The addition of SWNTs to the matrix increased the nucleation sites, therefore reduced the grain size of the crystals. Valentini also reported that no major changes in the melting points were noticed [36].

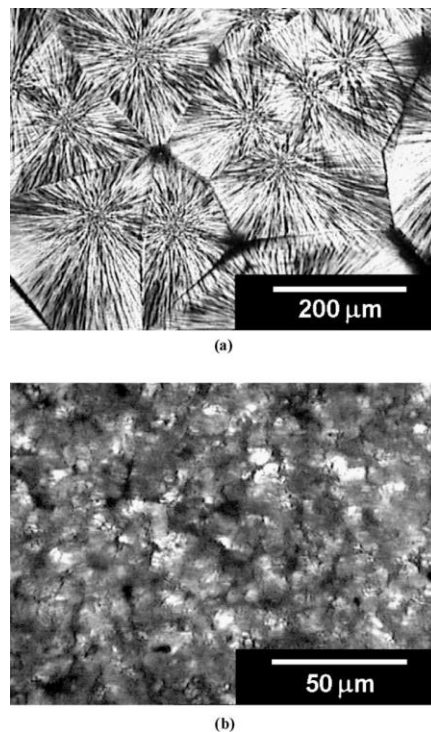


Figure 3.12 Spherulitic structure of a) neat PP and 5wt % PP/SWNT [36]

Leelapornpisit [31] also investigated the crystallization of the PP matrix with the addition of 0.25, 0.5, and 1 wt% SWNT. The PP powder was dry-blended with SWNTs and the resulting mixture was then extruded in a twin- screw mini-compounder. Non-isothermal DSC experimentation was conducted. At 0.25 wt% a significant increase in  $T_c$  was observed. The  $T_c$  continued to increase with increasing SWNT loading. It can be concluded that the SWNT acted as a nucleating agent and promoted crystal growth and creation of large number of smaller spherulites. From SEM images it was clear that the polymer composite had the same spherulitic structure as the neat PP but they had much more smaller spherulites. This also indicates that nanotubes acted as nuclei for the crystallization process. This is similar to the findings of Valentini [36] mentioned in the previous paragraph. Figure (3.13) shows the DSC curves of neat PP and PP/SWNT composites.

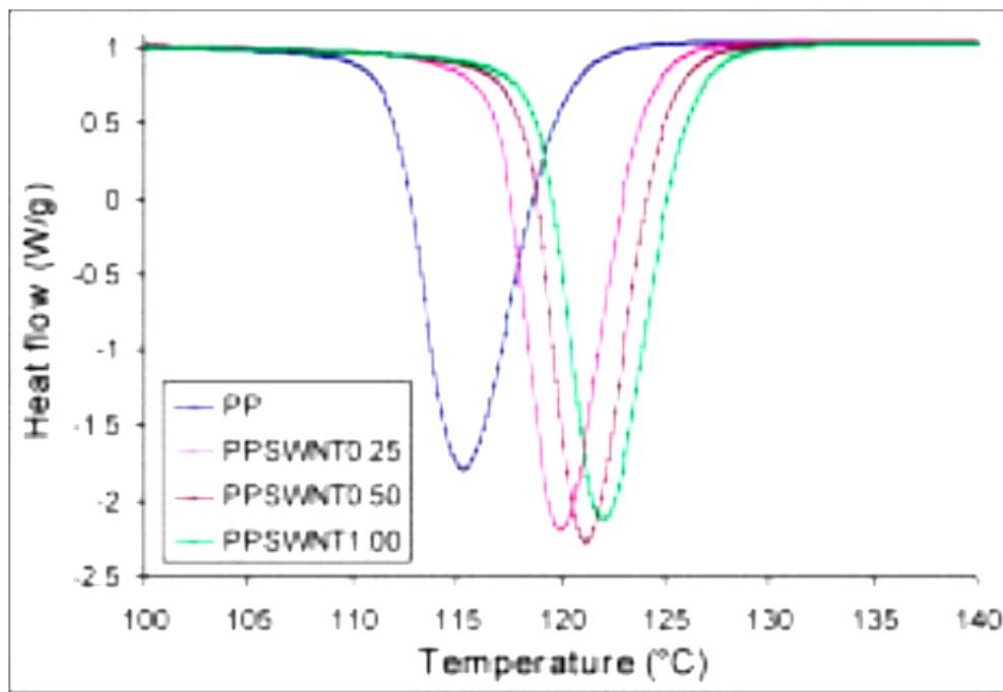
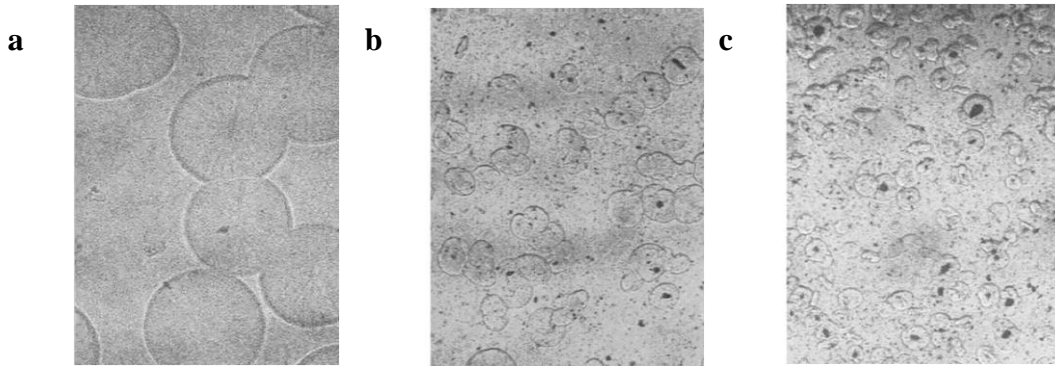


Figure 3.13 DSC curves of neat PP and PP/SWNT composites at 10°/min rate [31]

Similar results to that of Leelapornpisit [31] were also obtained by Razvi-Nouri et al. [35] when they investigated the crystallization of PP/SWNT composites with CNT loadings of 0.25, 0.5, 0.75, 1 and 2 wt % [35]. Figure (3.14) shows Razvi-Nouri spherulitic size change of the PP crystals by the addition of SWNTs.



**Figure 3.14** Micrographs of PP crystallization (a) PP at 132 °C, (b) PP/SWNT (0.25%) at 146 °C and (c) PP/SWNT (0.5%) at 146 °C [35]

All the previous studies used SWNT, with regards to MWNT which is the type used in the current research, similar investigations were also conducted.

Avil-Orta et al. [37] studied the effect of MWNT on the crystallization of the PP matrix. The composite was fabricated using the solution mixing technique and the CNT loading was 1 and 2 wt%. It was reported that the MWNT decreased the induction time and acted as a nucleating agent for the PP crystal growth. The result of MWNT being a nucleating agent is that it changed the morphology of the spherulitic structure of the PP into a fibrillar-like structure. Figure (3.15) shows the DSC curves of the neat polymer and the PP/MWNT composites. The DSC results are similar to the previous mentioned studies, with increasing CNT content the crystallization temperature increases. Avil-Orta [37] also reported the change in the crystallization onset temperature ( $T_o$ ), which is the temperature at the intercept of the tangents at the baseline and the

high-temperature side of the exotherm [35]. The increase in  $T_o$  indicates a decrease in the crystallization induction time. He observed an increase in  $T_o$  with increasing MWNT content. The  $T_o$  increased from 120.6°C for PP to 129.3°C and 132.5°C for composites containing 1% and 2% MWNTs respectively. This confirms the enhancement in nucleation since the time to form the critical nucleus has been decreased.

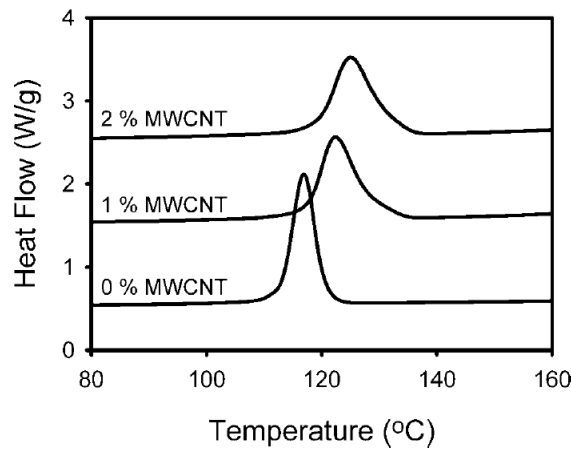


Figure 3.15 DSC curves of neat PP and PP/MWNT composites [37]

Limited work has been done regarding the comparison of the effects of the fabrication techniques on the composites mechanical, flow and crystallization properties. The majority of the papers published focused either on one processing technique and its affect on one or two properties. This current study compares the effect of the two fabrication techniques on more than one property which is the tensile, hardness, modulus, viscosity and crystallization property. A paper has been also published based on several parts of this study. The details of the paper are as follows: Esawi, Amal M. K. "Effect of Processing Technique on the Dispersion of Carbon Nanotubes within Polypropylene Carbon Nanotube-Composites and its Effect on their Mechanical Properties." *Polymer composites* 31.5 (2010): 772-80 [38].

## Chapter 4: Experimental Procedures

### 4.1 Materials used:

Polypropylene (isotactic polypropylene (iPP) from Crown Egypt for raw plastics) is an inexpensive commodity polymer therefore it was chosen to be the matrix in the fabrication of this nanocomposite. The size of the as received polymer pellets was 3.5 mm. The solvent for iPP is xylene (Sigma Aldrich, 99 % purity), which can be easily dissolved in it. The CNTs used are catalytic multi-wall carbon nanotubes (MWNT) (> 90 % purity, approximately 140 nm in average diameter and 3-4  $\mu\text{m}$  in length, MER Corporation). In order to minimize the dispersion energy this type of CNTs was chosen to avoid the excessive agglomeration accompanied with SWNT and smaller diameter MWNT. As received CNTs were used without any type of surface treatment (functionalization, grafting to method....etc). Figure (4.1) shows an SEM image of the CNTs, which appear to be straight due to their large diameters. It also shows the clustering of as received CNTs.

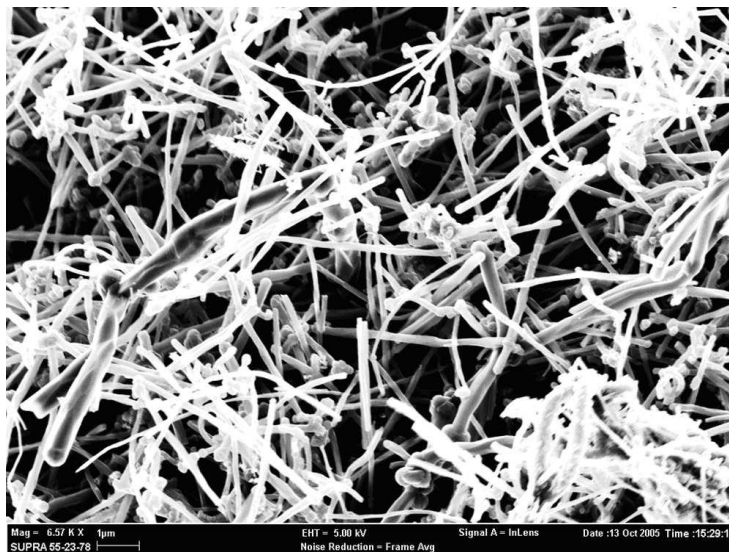


Figure 4.1 SEM image of the MWNT used in this research [38]

## 4.2 Composite Fabrication Techniques:

### 4.2.1 Solvent Mixing Technique:

Three loadings of CNT were added in order to obtain composite samples of 0.5%, 1%, and 5% CNT wt% in polypropylene. As reference 0% PP/CNT was also fabricated. The 0% samples also were subjected to the same mixing and processing techniques. The main challenge in the fabrication of this composite is the uniform dispersion of the CNT throughout the PP matrix. Therefore, two mixing techniques were used for detangling the CNT clusters present. The first technique (solvent mixing technique) entails dissolving the PP pellets in xylene (Sigma Aldrich, 99 % purity) at 80°C with constant stirring to form a clear homogeneous liquid phase. CNTs were then added to the warm polymer solution. The stirring continues for another 2 minutes. The PP/CNT solution is then sonicated for 60 minutes at 80°C, using an ultrasonic bath (Guyson, UK). The sonication step is to improve the CNT dispersion in the PP solution. The mixture is then cooled down and allowed to solidify. The jelly-like composite still contains a considerable amount of solvent. The composite is left to dry at room temperature ranging from 24 to 26°C until it reaches constant weight. The final step before the extrusion of the composite is to crush it to powder. The mixture is crushed to a 1mm particle size (not less) in order to avoid the shortening and damaging of the CNTs. Virgin PP was also processed in the same way and used as a reference sample. Figure (4.2) shows the process of solvent mixing technique and extrusion of the composite.



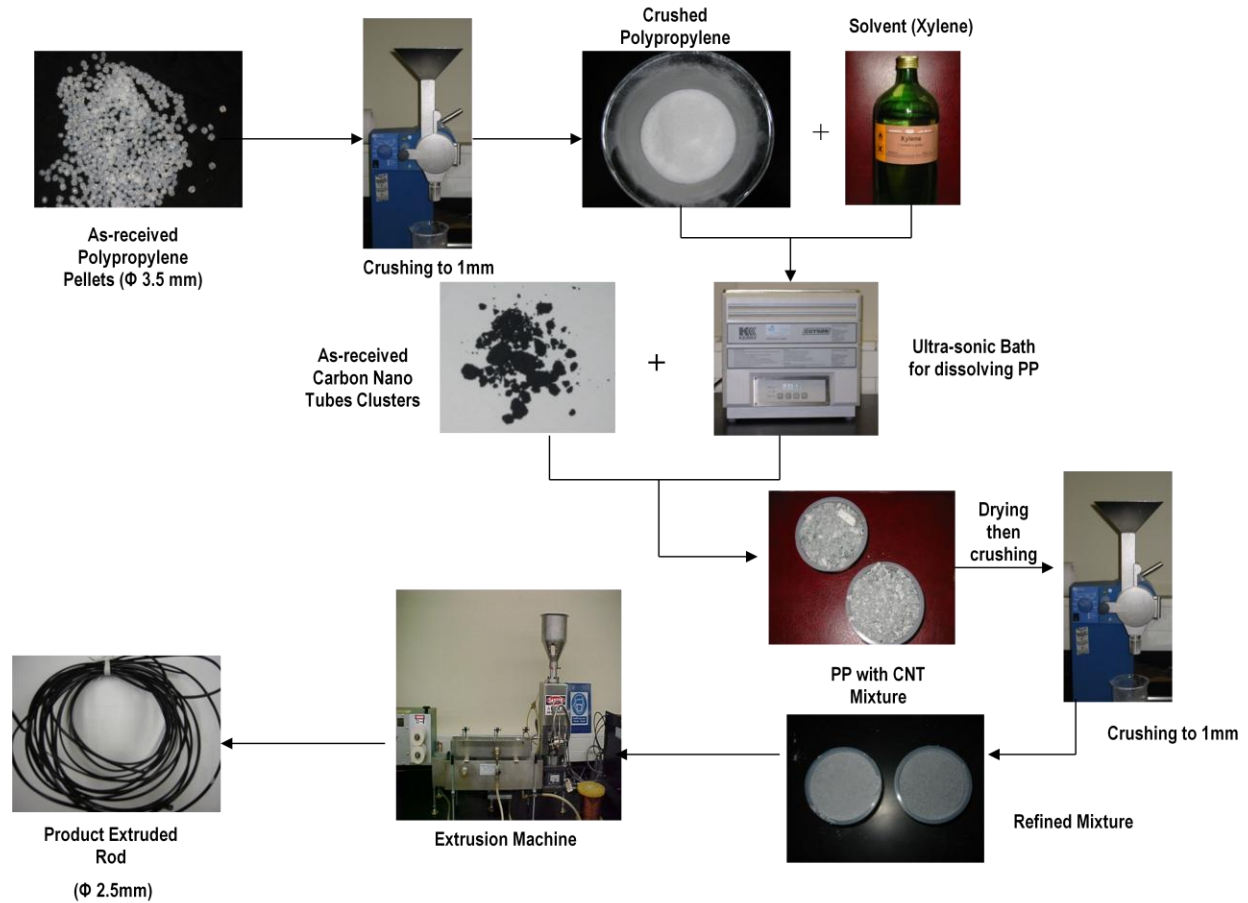


Figure 4.2 Solvent mixing Technique [38]

#### 4.2.2 Dry Mixing Technique:

The second technique used was the dry mixing one. The PP pellets were first crushed to 1mm size particle then mixed together with the different percentages of CNT in the turbula mixer (Turbula T2F, Switzerland) for 2 hours at 46 rpm. The resulting powder mixture was then extruded. Figure (4.3) shows the process of the dry mixing technique and extrusion of the composite. Virgin PP underwent the same processing steps and was used as a reference sample.



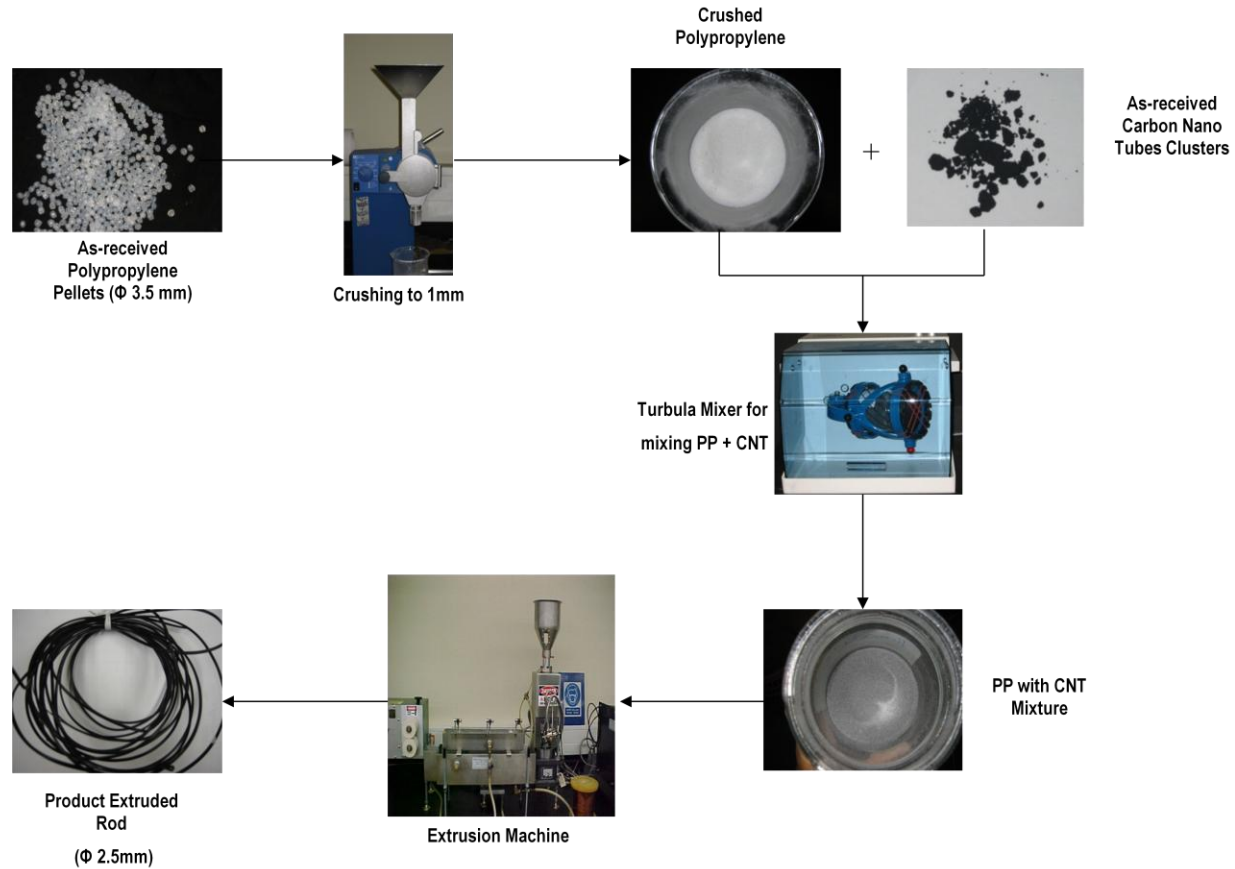


Figure 4.3 Dry mixing Technique [38]

### 4.2.3 Shear Mixing through Melt Processing

The main challenge in the fabrication of this composite is to ensure as much as possible homogenous dispersion of the CNT in the PP matrix. Therefore another stage of mixing is introduced. The mixing in this stage depends on the shear forces applied on the polymer composites during the extrusion process. After both mixing technique were completed (solvent and dry mixing) the Polymer/CNT mixture was introduced into the single-screw microtruder. The microtruder used was as Randcastle Extrusion Systems, Inc, USA. After passing through the three zones of the extruder which were: 177 °C, zone 2: 205 °C, zone 3: 232 °C. The composite

melt is extruded through a 3 mm circular die at 232 °C. The extrudate is pulled from the die with a roller speed of 5 rpm. The extrudate goes through a water bath for cooling.

Figure (4.4) shows the extrusion machine used for the Shear mixing step and producing the final product of the composite.

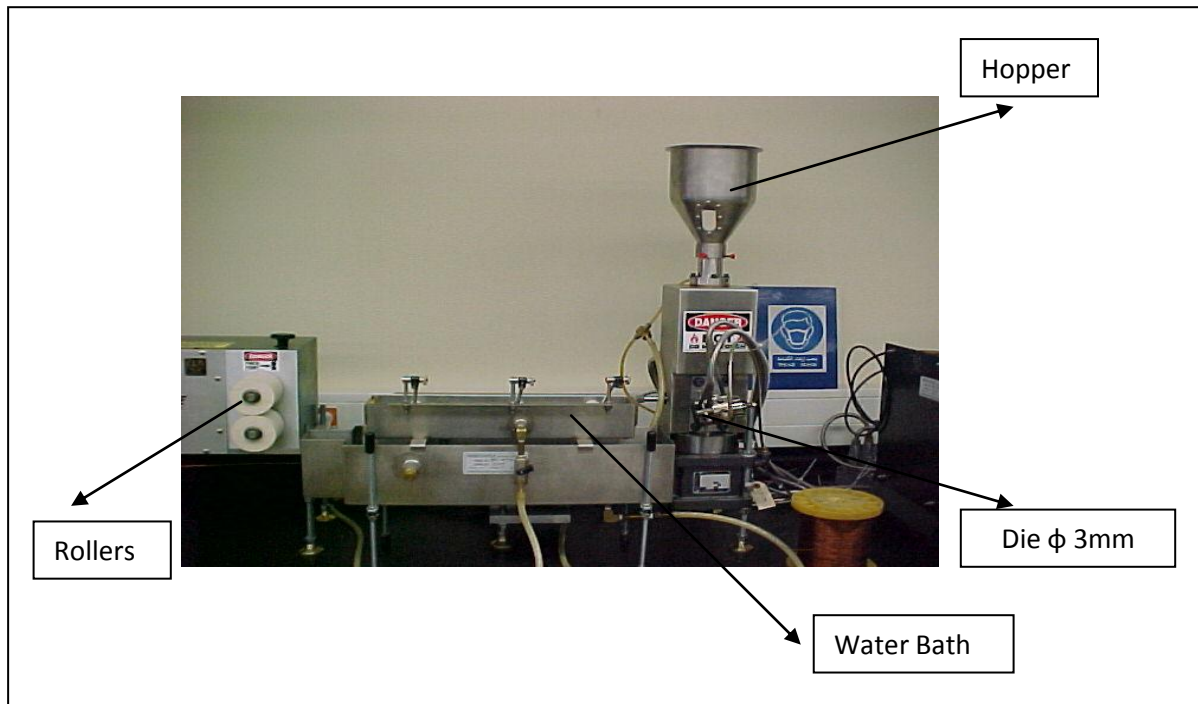


Figure 4.4 Extrusion Apparatus

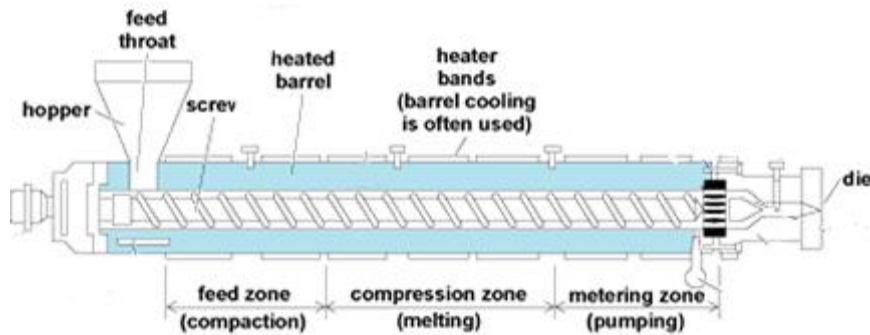


Figure 4.5 Schematic diagram of single screw extruder

[<http://www.accessscience.com/content.aspx?searchStr=single+screw+extruder+&id=526800#S2>] adapted from

### 4.3 Material Characterization:

#### 4.3.1 Melt Flow index testing:

In Polymer industry the most significant factor to consider is the flow property of the polymer. In order to assess the flow of the polymer viscosity measurements can be a good indication for this property. One of the factors that can affect the viscosity of the polymer is the addition of any filler to the polymer matrix. Therefore, an investigation for the viscosity of the PP/CNT composite was in order. The increase of the viscosity can also decrease the dispersion of the CNT in the matrix. Melt flow index (MFI) investigation was conducted to the composite as it is the inverse of melt viscosity. The MFI testing was measured according the ASTM standard D 1238-04c. The test conditions used were: temperature = 230°C and load = 2.16 kg. The extrudates were cut in to small pieces and were placed in the heated die, extruded and collected during a specified interval of 1 min. After the extrusion from the MFI apparatus the samples weights were recorded. Each sample condition was extruded 3 times for each mixing technique. In order to ensure flow rate consistency any bubble containing extrudate was discarded and some

material of the sample was purged before starting to time the procedure. Figure (4.6) shows the MFI apparatus.

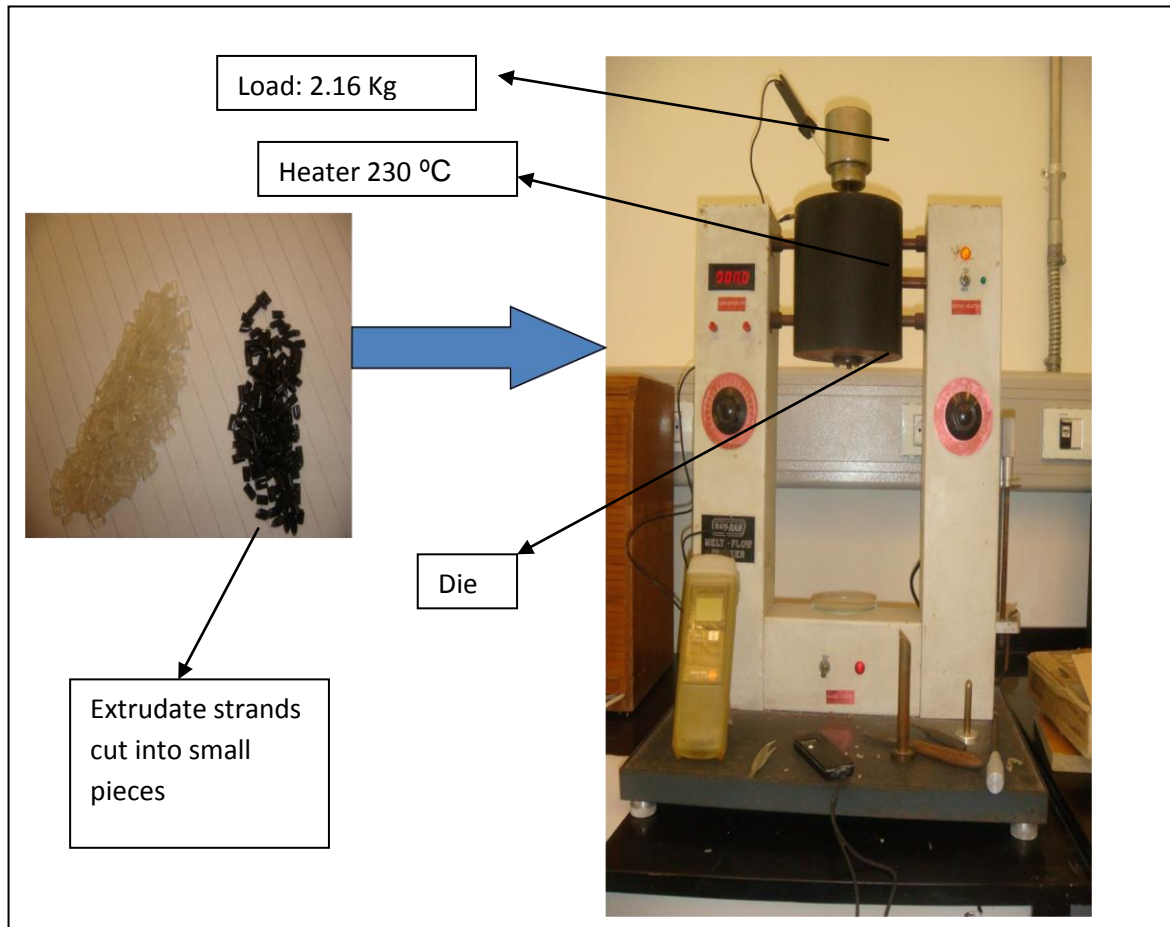


Figure 4.6 Melt Flow Index Apparatus

#### 4.3.2 Tensile Testing:

In order to investigate the mechanical properties of the composite and compare the two mixing techniques together tensile testing was conducted. The tension tests were performed on an INSTRON universal testing machine. The sample gage length was 50 mm. Three specimens per condition were tested and the average was then calculated. As mentioned earlier the final product was extrudate strands therefore a special fixture was designed and manufactured in order to perform the tensile test.

With this fixture no slippage was ensured. The strain rate for the test was 30 mm/min and the average diameter of the sample ranges from 1.5-2 mm. Figure (4.7) shows the tension test fixture.

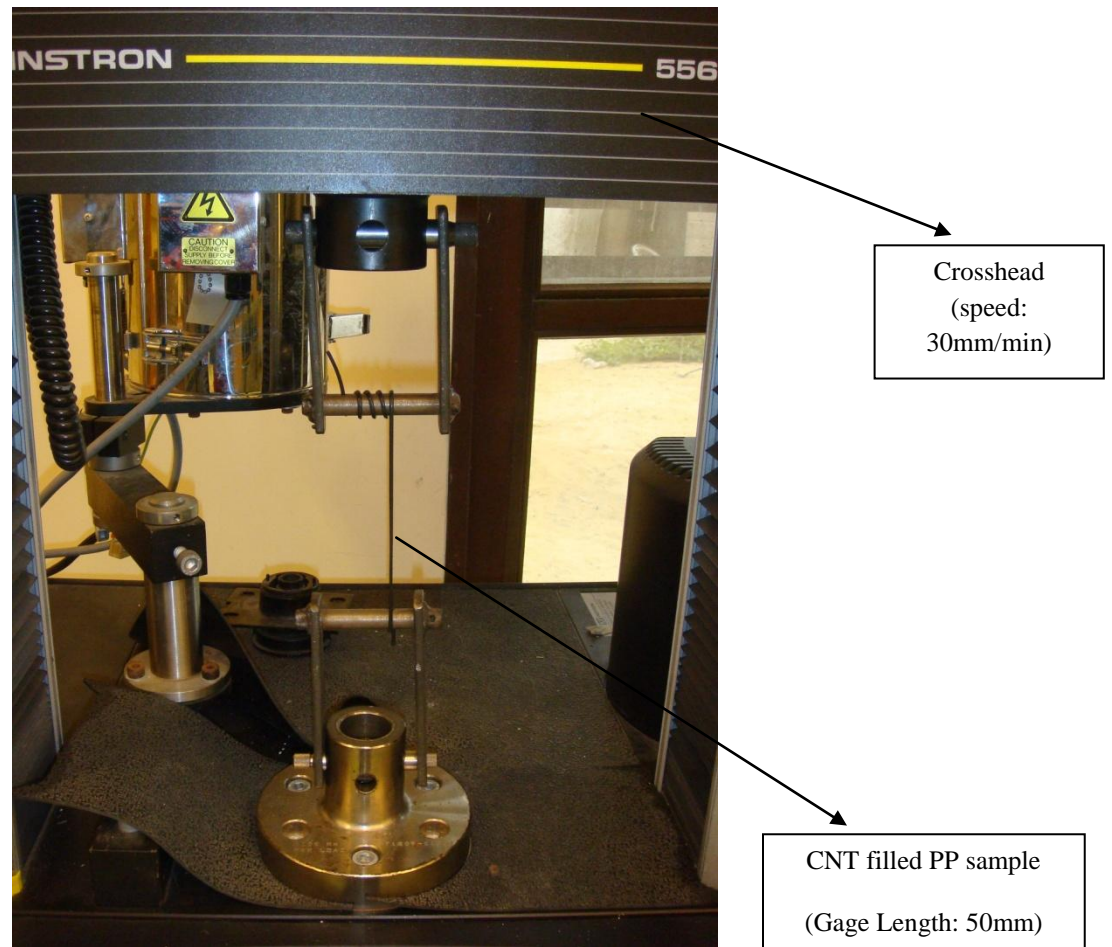


Figure 4.7 Tension Test Fixture

#### 4.3.3 Nanoindentation Investigation:

Nanoindentation characterization was done in order to determine the hardness and the indentation modulus of the samples. The testing was conducted using Nanoindenter XP, MTS systems Co., Oak Ridge, TN, USA. Samples were cut along the longitudinal direction, mounted

and ground to level and expose the core of the extrudates. This step was vital for the solvent mixing samples in order to determine if any solvent was entrapped in the core of the extrudate. Shear mixing due to extrusion has the maximum effect at the surface of the samples which can result in poorer distribution of the CNT in the center of samples. Therefore testing the samples after grinding would show the real behavior of the weakest zone of the polymer composite.

The testing conditions were as follows:

Arrays of 4x5 indentations were made under load-control conditions using a sharp Berkovich tip. The basic testing method was used with the loading rate = unloading rate = 2625.107  $\mu\text{N/s}$ , the dwell time = 30 s, the number of times to load = 5, the maximum load = 20  $\mu\text{N}$  and the spacing between indentations = 100  $\mu\text{m}$ . Calculations of hardness and modulus are based on the Oliver and Pharr method. [40]

Hardness (H) is calculated by dividing the indentation load ( $P_{\text{max}}$ ) by the projected area (A) at that load using equation (4.1)

$$H = \frac{P_{\text{max}}}{A} \quad (4.1)$$

The elastic modulus ( $E_r$ ) of the tested material can be obtained by equation (4.2)

$$E_r = \frac{\sqrt{\pi} S}{2\beta \sqrt{A}} \quad (4.2)$$

Where  $E_r$  is the reduced modulus,  $\beta$  is a parameter that depends on the geometry of the tip (1.034 for a Berkovich tip) and S is the contact stiffness.

For a Berkovich tip, the projected area can be related to the contact depth by equation (4.3)

Where  $h_c$  is the true contact depth.

$$A = 24.56h_c^2 \quad (4.3)$$

This relation represents the area function for a perfect Berkovich tip. Other terms are added from a curve fitting procedure to substitute for tip blunting and geometry changes.

The reduced elastic modulus can then be calculated by equation (4.4)

$$\frac{1}{E_r} = \frac{1-\nu^2}{E} + \frac{1-\nu_i^2}{E_i} \quad (4.4)$$

Where  $E_i$ ,  $\nu_i$  are the elastic modulus and Poisson's ratio for the indenter and  $E$ ,  $\nu$  are the elastic modulus and Poisson's ratio for the sample.

For a diamond indenter,  $E_i = 1140$  GPa, and  $\nu_i = 0.07$ . The value of  $\nu$  for the sample was set to 0.35 as estimated by for semicrystalline polymeric materials.[40]



#### **4.3.4 Scanning Electron Microscopy Investigation:**

During the tensile testing most of the samples showed high ductile behavior and the majority of the samples splitted into thin fiber which complicated the imaging process. The Field emission scanning electron microscope (FESEM, Leo Supra 55) was incapable of showing the fractured surfaces due to the thin deformed cross-section. Therefore investigating the dispersion of CNT in the matrix was not possible using the failed samples from the tension test. Another batch of samples was used for the imaging process. The samples were chilled using liquid nitrogen then subjected to tensile loading until failure. The fracture surfaces where then sputter-coated with gold to minimize charging of the samples during imaging. Then the samples were scanned using the FESEM.

#### **4.3.5 Differential Scanning Calorimetry:**

The effect of the addition of MWNT to the polypropylene matrix on the crystallization temperature was studied using a Perkin-Elmer differential scanning calorimeter (DSC).

The test was conducted under nitrogen atmosphere to avoid any oxidation of the samples. The samples were  $15 \pm 6$  mg and they were cut out of the composite extrudates into appropriate size in order to be encapsulated in the aluminum pans. The following procedure was used in non-isothermal conditions to determine the crystallization temperature of the different samples. The sample was heated from RT to  $200^{\circ}\text{C}$  at  $10^{\circ}/\text{min}$  rate, and held for 5 min to erase any previous thermal history. The sample was then cooled to  $50^{\circ}\text{C}$  at  $10^{\circ}/\text{min}$  rate, held for 5 min then heated again to  $200^{\circ}\text{C}$  at the same rate and held at  $200^{\circ}\text{C}$  for 3 min. The DSC test was conducted according to the ASTM standard D3418-08.



## Chapter 5: Results and Discussion

### 5.1 Melt Flow Index

In plastic industries the flow property of the polymer is very important. Melt flow index measurement is used to analyze this property [39]. As mentioned above in the material characterization section the MFI investigations were done according to the ASTM D 1238-04c for both dry-mixed and solvent-mixed samples with different CNT wt%. The average of three samples was taken to calculate the melt flow indices presented in Table (5.1).

|                  |                | CNT wt%         | 0%       | 0.5%       | 1%        | 5%         |
|------------------|----------------|-----------------|----------|------------|-----------|------------|
| Mixing technique | Dry Mixing     | Melt Flow index | 16±(0.0) | 13.7±(2.1) | 12±(1.0)  | 12.3±(1.5) |
|                  | Solvent Mixing | g/10 min        | 11±(1.7) | 12±(0.0)   | 9.7±(2.9) | 7.3±(0.6)  |

Table 5.1 Melt flow indices results

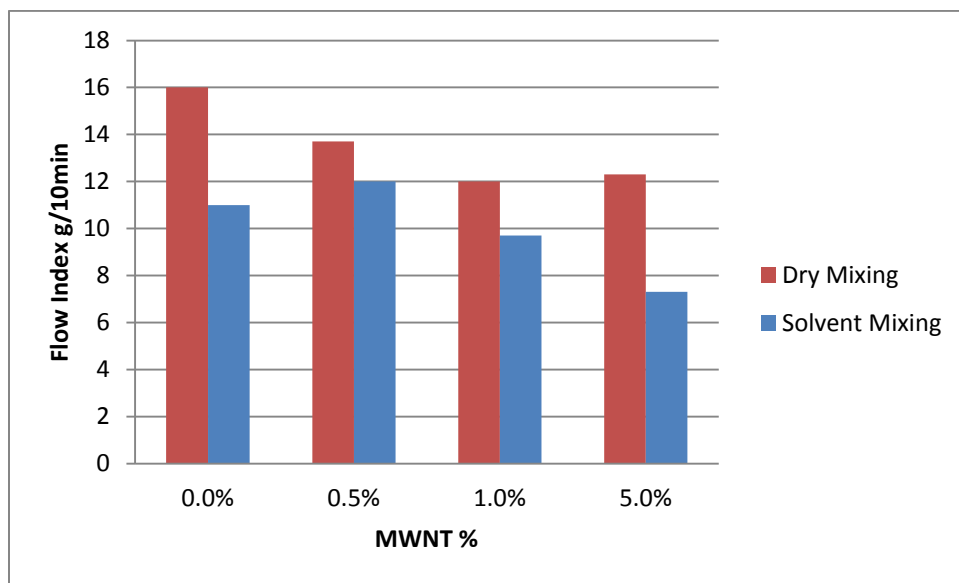


Figure 5.1 Melt flow indices results

It is obvious from Figure (5.1) above that the results for the solvent mixed samples compared to the dry mixed ones are lower; i.e. viscosity is higher. This could be an indication that the dry-mixed samples have inferior CNT dispersion than the solvent-mixed ones. Therefore their melt flow indices are higher than those of the solvent-mixed samples. Another indication for the poor dispersion of CNT in the dry-mixed samples is that the decrease in the melt flow index of the samples is very limited if not negligible, putting in mind the value of the errors between brackets. This means that the addition of the CNTs did not affect the viscosity of the matrix much because their effect was countered by their poor dispersion. Although higher viscosities, i.e. lower melt flow indices, limit the homogenous dispersion of CNT in the matrix, solvent- mixed samples show better dispersed CNTs even at high CNT loadings. A decreasing trend in the melt flow index is much obvious in the solvent- mixed samples. Even though the dispersion is better in the solvent-mixed samples, which means decreasing viscosities for the molten polymer, the effect of the addition of the CNTs overcame this and resulted in the increase of the viscosity. This occurrence could be due to the dispersion process, solvent mixing, preceding the shear mixing stage. This solvent mixing stage has a dominant effect in the improved dispersion compared to the single screw extrusion stage that follows. The dry mixing stage involving the turbula mixer did not play such a significant role in the dispersion compared to the solvent mixing one.

Chih Chun et al. investigated the rheological property of PP/MWNT composites with three different melt flow indices of PP matrix. The MWNT content was (0, 1, 2,3,5,7.5 and 10%). He reported that the MFI increased slightly at low CNT loading (1phr), this might indicate that the viscosity of the polymer decreased. Adding the 1 % of MWNT to the matrix provided a flow favoring orientation [39]. A similar trend was also observed in this research at 0.5% MWNT for the solvent-mixed samples. In Chih Chun study as the MWNT content increased

above the 1phr a gradual decrease in MFI was observed which indicates that the network formed from the MWNT deterred the molecular motion of the polymer chains [39]. In this study the MFI also continued to decrease gradually beyond 0.5% MWNT for the solvent-mixed samples. However, for the dry-mixed samples the MFI decreased significantly only at 0.5% MWNT then it remained fairly constant till 5%MWNT. This could be due to the poor dispersion of the MWNT in the polymer matrix as explained earlier in this section. The study of Chih Chun et al. also showed that the structure of polypropylene did not affect much the MFI of the composites as much as the addition of the MWNT affected it [39]. Figure (5.2) shows the MFI results of their study.

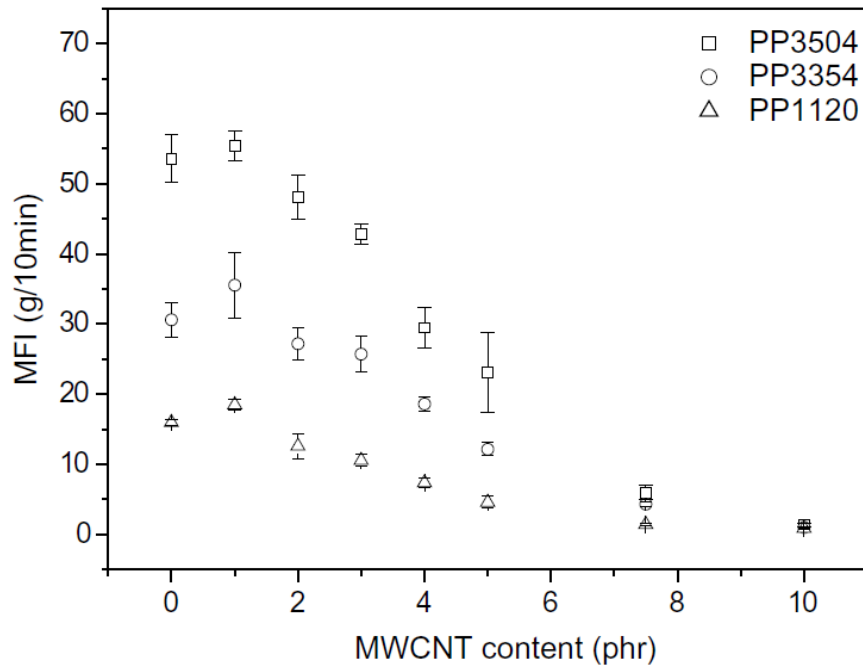


Figure 5.2 Effect of MWNT content on melt flow index of three types PP/MWNT composites. [39]

Lee et al. investigated the rheological property of polypropylene/MWNT composites prepared with MWNT masterbatch chips. The MWNT content was (0.5, 1, 2, 3.and 5 wt% The MFR of

PP/MWNT composite decreased from 24.0 to 7.5 as MWNT content increased from 0 to 5 wt% [41]. As mentioned before a similar trend was also observed in this study.

## 5.2 Mechanical testing:

### 5.2.1 Tensile Testing

Tensile testing was conducted in order to compare the yield strength and ductility of the samples produced by both techniques. The solvent-mixed samples exhibited very high strains. Figure (5.3) shows a representative stress-strain curve of 1% dry and 1% solvent sample in tensile loading. In some cases the elongated extrudates reached the end limit of the testing machine frame and did not fail. This made it not possible to record the ultimate strength of some samples. Therefore yield strength and flow strain, the region were the selected mechanical properties to compare both techniques in the tensile testing phase. The flow strain (postyielding strain) of the solvent-mixed samples was significantly higher than the dry-mixed ones.

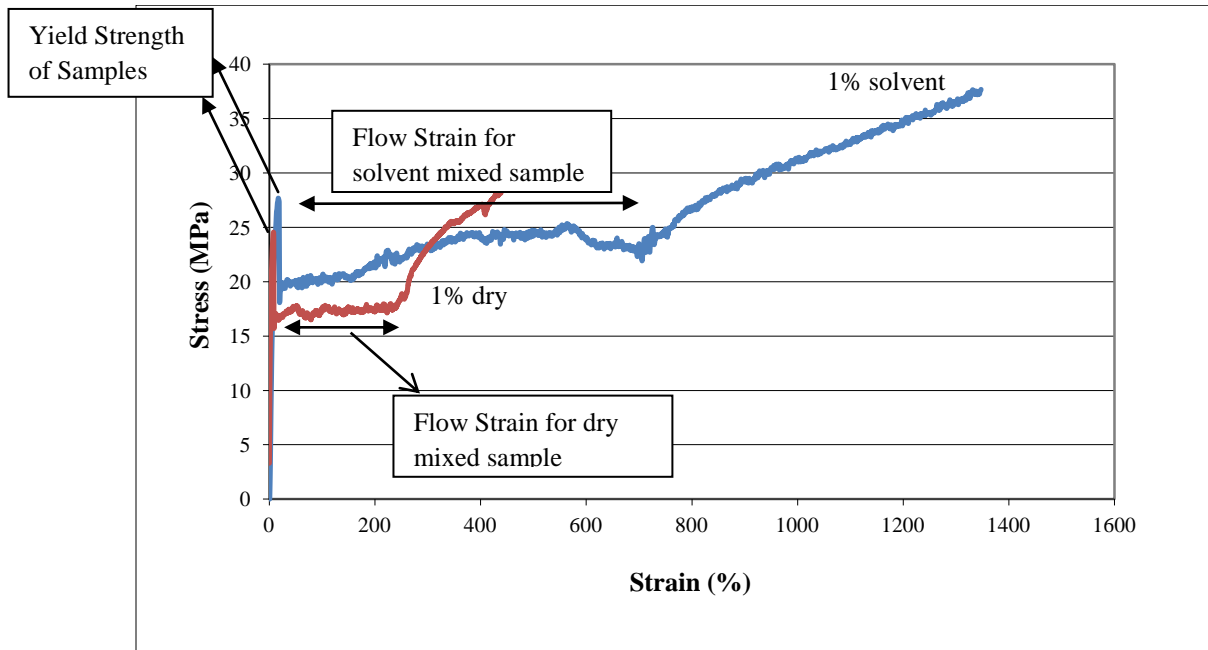


Figure 5.3 Example of Stress Strain curves for 1 % CNT using dry and solvent mixing technique [38]

| CNT wt %             |                             | 0%             | 0.5%           | 1%             | 5%             |
|----------------------|-----------------------------|----------------|----------------|----------------|----------------|
| <b>Dry-Mixed</b>     | <b>Yield strength (MPa)</b> | 17( $\pm$ 3)   | 25( $\pm$ 3)   | 21( $\pm$ 3)   | 18( $\pm$ 2)   |
|                      | <b>Flow Strain (%)</b>      | 183( $\pm$ 7)  | 172( $\pm$ 26) | 151( $\pm$ 54) | 139( $\pm$ 25) |
| <b>Solvent-Mixed</b> | <b>Yield strength (MPa)</b> | 13( $\pm$ 4)   | 14( $\pm$ 4)   | 25( $\pm$ 7)   | 16( $\pm$ 4)   |
|                      | <b>Flow Strain (%)</b>      | 512( $\pm$ 29) | 439( $\pm$ 21) | 419( $\pm$ 63) | 446( $\pm$ 53) |

**Table 5.2 Tensile testing Results**

It is obvious from table (5.2) that the yield strength of the control sample of the solvent-mixed samples is lower than that of the dry-mixed ones. This suggests that some polymer degradation due to the solvent addition has occurred. At 0.5wt % the yield strength of the dry-mixed samples is higher than the solvent-mixed ones. However, at 1wt% the yield strength of the solvent-mixed samples is higher than the dry-mixed ones. This indicates that the better dispersion of CNTs in the PP matrix of the solvent-mixed samples enhanced the mechanical properties of the samples despite of the suspected polymer degradation. For the 5wt% samples the yield strength of the dry-mixed samples was greater than the solvent-mixed ones but it was not a significant enhancement compared to the neat polymer samples. The enhancement reached was only 6%. In the solvent-mixed samples the enhancement of the mechanical properties of the 5 wt% was 20%. This is therefore attributed to the homogenous dispersion of the CNTs in the matrix. The FESEM images in Figure (5.5) show the distribution of the CNTs in the samples. Clusters of CNTs start appearing in the 1wt % samples and increase significantly in the 5wt% dry-mixed ones. On the other hand the solvent-mixed samples show uniformly dispersed CNTs throughout the different CNT loadings. This supports the mechanical testing observations. A continuing enhancement in

the yield strength of the solvent-mixed samples is observed until it reaches its maximum at 1wt% then deterioration occurred at 5 wt%. On the other hand the deterioration in the mechanical properties in the dry-mixed samples started at 1wt% and continued in the 5wt% samples. The maximum yield strength occurred at 0.5wt% for dry-mixed samples and at 1wt % for solvent mixed samples. Manchado et al. [6] also recorded an enhancement in strength up to 0.5wt% followed by a considerable drop. It is believed that the clustering of CNTs at higher loading is responsible for the decrease in strength as they acted as stress raisers and stress concentration points. Table (5.3) lists the average values of yield strength and flow strain for different extrudates normalized to the respective values of the control samples. It is obvious from the results that the strain was very much affected by the addition of the CNTs. The dry-mixed samples showed a continuous decrease in strain with the addition of CNTs till it reached a total of 24% decrease in strain in reference to the control sample. A similar trend was observed in the solvent-mixed samples but the decrease in strain was reduced at the 5 wt% samples. However, with respect to the reference sample the strain was still decreasing at 5 wt% till it reached a total of 13% decrease. According to Prashantha et al. with the continuous addition of MWNTs the strain at break continues also to decrease [8].

|                             | CNT wt%       | 0.5% | 1%   | 5%   |
|-----------------------------|---------------|------|------|------|
| <b>Yield strength (MPa)</b> | Dry mixed     | 1.47 | 1.24 | 1.06 |
|                             | Solvent mixed | 1.08 | 1.92 | 1.23 |
| <b>Flow strain (%)</b>      | Dry mixed     | 0.06 | 0.17 | 0.24 |
|                             | Solvent mixed | 0.14 | 0.18 | 0.13 |

**Table 5.3 Average values of yield strength and flow strain for different extrudates normalized to the respective values of the control samples**

Bao et al. investigated the mechanical properties of PP/MWNT composites processed using the melt-mixing technique. The yield strength of the samples reached its maximum at 0.3 wt% MWNT then started to decrease gradually as the MWNT content increased till 1 wt% MWNT [28]. This trend was also found in Hemmati et al. study when the tensile strength reached its maximum value at 1.5% MWNT. A decrease in strength was obvious for higher MWNT loadings. Tensile strength increased as long as the MWNT were uniformly distributed throughout the matrix. As soon as clusters began to form the mechanical properties started deteriorating [29]. These two studies could be related to the research at hand because they both showed an enhancement in mechanical properties until a specific MWNT content then the agglomerations formed at higher loadings acted as intense strain localization areas which negatively affected the mechanical properties of the samples. Further studies were conducted that showed a similar trend. Prashantha et al. also recorded an increase in yield strength at 3 wt% MWNT. With increasing the MWNT content the nanotubes started forming clusters, which act as stress raisers [8]. The samples in the above mentioned studies were all fabricated using the melt mixing method. Chang et al. fabricated their samples using the solvent mixing technique and also observed a similar trend in the mechanical properties. However, it was obvious that the maximum tensile stress occurred at 4wt% SWNT which is higher than all the other loadings presented in the previous studies, and the one at hand included [30]. This could be due to the better dispersion of SWNTs the solution mixing technique offers.

### 5.2.2 Nanoindentation:

Nanoindentation was conducted in order to be able to measure the hardness and indentation modulus of the samples. This will further assist in understanding the effect of the mixing techniques on the mechanical properties of the composites. Table (5.4) shows the hardness and indentation modulus results for the different samples at different CNT weight percentages. The dry-mixed samples show maximum hardness and indentation modulus at 0.5% CNT (10% enhancement in hardness, and 6.4% enhancement in indentation) as the solvent-mixed ones peaked at 1% CNT (42% enhancement in hardness, and 10% enhancement in indentation modulus). These results also coincide with the maximum values reached in yield strength; where the dry-mixed samples exhibited a 47% enhancement in yield strength at 0.5% CNT and the solvent-mixed samples a 92% enhancement in yield strength at 1% CNT. It is clear from figure (5.4) that the solvent mixed samples at 1wt% exhibited higher resistance to indentation (maximum displacement was 3.6 $\mu$ m compared with 4.5 $\mu$ m for the dry-mixed samples). This could be due to the better dispersion of the CNTs in the solvent-mixed samples' matrix, which resisted the indentation action. However, the results clearly show that the mechanical properties (yield strength, hardness, and indentation modulus) are lower in value for the control solvent-mixed sample relative to the control dry-mixed sample. This could be an indication for polymer degradation, a concern highlighted by other researchers [6]. However, in the current study no visual signs of polymer degradation were observed. An indication for matrix degradation is the decrease in molecular weight, which was not currently investigated due to unavailability of the equipment. All these results confirm that the enhancement in mechanical properties in the composites rely substantially on the uniform distribution of the CNTs in the polypropylene



matrix. Table (5.5) presents the average values of the hardness and indentation modulus for the different extrudates normalized to the respective values of the control samples.

| CNT wt %             |                                  | 0%                  | 0.5%                | 1%                  | 5%                  |
|----------------------|----------------------------------|---------------------|---------------------|---------------------|---------------------|
| <b>Dry-Mixed</b>     | <b>Hardness (GPa)</b>            | 0.060( $\pm$ 0.002) | 0.066( $\pm$ 0.002) | 0.046( $\pm$ 0.003) | 0.049( $\pm$ 0.030) |
|                      | <b>Indentation modulus (GPa)</b> | 1.72( $\pm$ 0.05)   | 1.83( $\pm$ 0.06)   | 1.23( $\pm$ 0.07)   | 1.35( $\pm$ 0.48)   |
| <b>Solvent-Mixed</b> | <b>Hardness (GPa)</b>            | 0.045( $\pm$ 0.007) | 0.052( $\pm$ 0.009) | 0.064( $\pm$ 0.007) | 0.040( $\pm$ 0.03)  |
|                      | <b>Indentation modulus (GPa)</b> | 1.50( $\pm$ 0.14)   | 1.44( $\pm$ 0.14)   | 1.65( $\pm$ 0.10)   | 1.22( $\pm$ 0.52)   |

**Table 5.4 Nanoindentation Results**

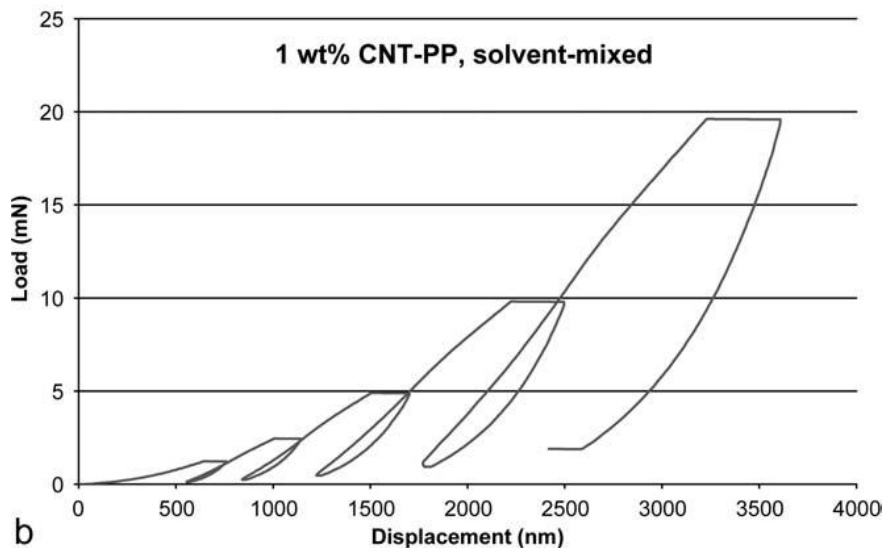
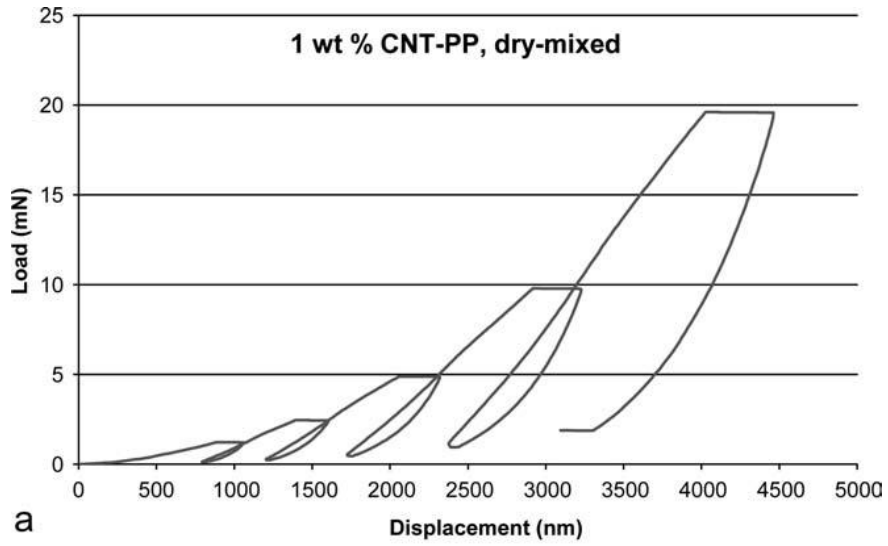


Figure 5.4 Load vs. displacement curve for a representative 1 wt% PP/CNT dry-mixed sample. (b) Load vs. displacement curve for a representative 1 wt% PP/CNT solvent-mixed sample [38]

|                                  | CNT wt%       | 0.5% | 1%   | 5%   |
|----------------------------------|---------------|------|------|------|
| <b>Hardness (GPa)</b>            | Dry mixed     | 1.10 | 0.77 | 0.82 |
|                                  | Solvent mixed | 1.16 | 1.42 | 0.89 |
| <b>Indentation modulus (GPa)</b> | Dry mixed     | 1.06 | 0.72 | 0.78 |
|                                  | Solvent mixed | 0.96 | 1.10 | 0.81 |

**Table 5.5 Average values of the hardness and indentation modulus for the different extrudates normalized to the respective values of the control samples.**

### **5.3 Field-Emission Scanning Electron Microscopy (FESEM)**

One of the main areas of focus of this study is the investigation of the effect of the two mixing techniques employed in the fabrication of the composite on the mechanical properties of the extrudates. Since, it is expected that the mechanical properties of the composite are very much affected by the homogenous dispersions of the CNTs in the polymer matrix. FESEM imaging was carried out to investigate the distribution of the CNTs in the matrix. Figures 5.5 (a-f) show cross-sectional fracture surface images of samples with different CNT loadings. Images (a-c) are the dry-mixed samples. It is obvious that at lower CNT wt% (0.5 and 1 %) good dispersion of the CNTs took place. In addition, small clusters (less than 2  $\mu\text{m}$ ) are present and also individually dispersed CNTs. The maximum tensile strength in the dry mixed samples occurred at 0.5% CNT. However the tensile strength was not affected by the presence of small clusters in the 0.5% dry-mixed samples. This could be due to the well dispersed CNTs at that specific loading, which might have cancelled out the stress concentration effect that could arise from the presence of

clusters. Another explanation is that these clusters did not at all act as stress concentrators. At 5% CNT larger clusters were obvious (larger than 20  $\mu\text{m}$ ) as shown in Figure 5.5 c). The tensile strength at 5% CNT dropped this could be explained by the presence of the CNT clusters. Figures 5.5 (d-f) show the cross-sectional images of the solvent- mixed samples at different CNT loading. It is visible that the solvent- mixed samples show a homogenous dispersion of CNTs with almost no clusters at all CNT wt fractions. The uniform distribution of CNT in the solvent-mixed samples also attributed to the large strain observed in these samples. On the other hand the dry-mixed samples did not exhibit such a behavior (Figure 5.3). This is due to the presence of clusters which acted as stress raisers.

Prashantha's [8] TEM images showed well dispersed MWNTs as well as clusters at lower nanotube loadings. At higher MWNT wt% more clusters are visible. (see figure (3.6)) These observations are similar to the ones being reported in the current study .Bao's SEM image also showed [28] well dispersed MWNTs at 0.5wt% which contributed to the increase of the yield strength compared to the neat PP.(see Fig(3.2))

Some porosity was present in the solvent-mixed samples which could be due to the xylene evaporation. The existence of porosity in the sample may have contributed to the overall decrease in strength compared to the dry-mixed samples. Figure (5.6) shows the presence of porosity, in a solvent-mixed sample, as mentioned earlier.

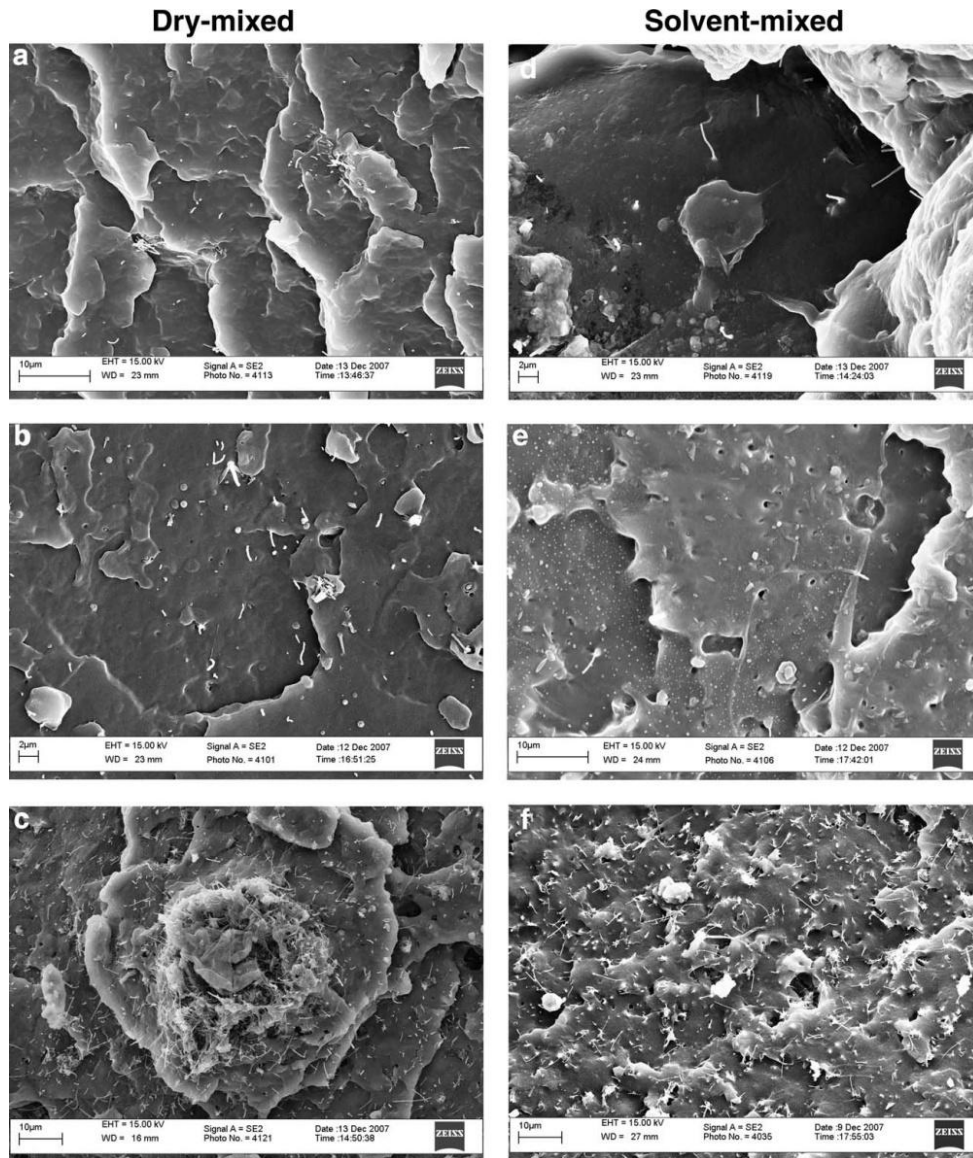


**Figure 5.5 (a) 0.5 wt% dry mixed sample showing dispersed CNTs as well as a small cluster. (b) 1 wt% dry mixed sample showing dispersed CNTs as well as a small cluster. (c) Regions with uniformly dispersed CNTs as well as a large cluster in the 5 wt% CNT dry-mixed sample. (d) 0.5 wt% solvent mixed sample showing dispersed CNTs. Dark spots are also seen. (e) The fracture surface of the solvent-mixed 1 wt% CNT sample. (f) Uniformly dispersed CNTs in the 5 wt% CNT solvent-mixed sample [38]**

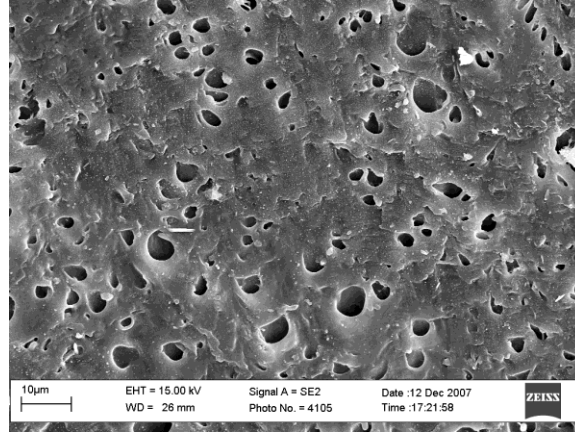


**Figure 5.6** Clear presence of porosity in 1%CNT solvent-mixed sample [38]

Another important parameter to consider is the interfacial bonding between the CNTs and the polymer matrix. This interfacial bonding plays a great role in the load transfer between the reinforcement and the matrix. FESEM images of the fracture surface of the samples showed CNT pull out and poor wetting (see Figure (5.7)). A poor interfacial bond could explain why the increase in the tensile strength of the samples was not that significant. In spite of the well distributed CNT in the solvent-mixed samples a decrease in tensile strength occurred at 5% CNT. This could be due to the poor interfacial bonding between the unfunctionalized CNTs and the polypropylene matrix.

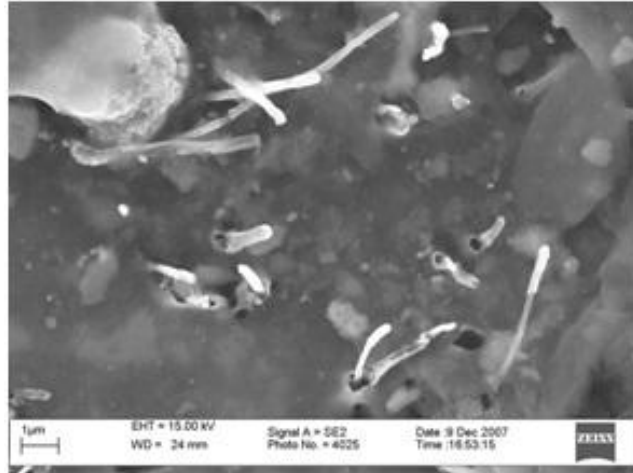


Figure 5.7 PP/CNT solvent-mixed sample, showing CNTs sticking out of the matrix [38]

Leelapornpisit [31] also presented a similar case of SWNT pull out from the PP matrix. The samples were processed using a dry-blending technique. Figure (5.8) shows a SEM image for his observation [31].

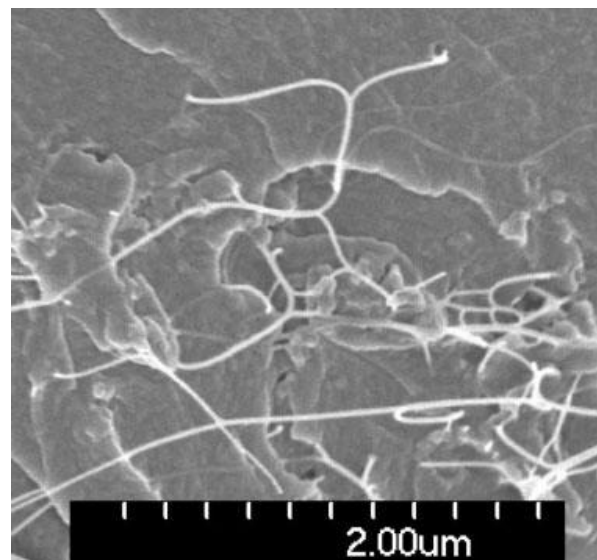


Figure 5.8 SEM image of PP/SWNT composite where nanotube pull out is obvious (cryogenic fracture surface) [31]



#### 5.4 Differential Scanning Calorimetry:

The effect of MWNTs on the crystallization of PP was investigated by using non-isothermal DSC experiments. The results show that the crystallization temperature ( $T_c$ ) shift about 10 and 6 °C for the dry mixed and the solvent mixed samples respectively to higher temperatures for nanocomposites containing 5wt % MWNTs compared to neat PP. As it is obvious from figure (5.9) that the crystallization temperatures of the solvent mixed samples are lower than those of the dry mixed samples. For both techniques, as the CNT content increase the crystallization temperature increases. This indicates that the CNTs dispersed in the matrix act as nucleating agents for PP. The results are in agreement with the research done by Valentini et al. [36] where the addition of SWNTs in the polymer matrix increased the crystallization temperature. A significant shift in the crystallization temperature occurred at the lowest reinforcement content (5wt %) with a slow but continuous increase with increasing SWNT content. This trend is very clear in Figure (5.10) and Figure (5.11). They are representative cooling curves of neat PP and PP/MWNT samples with different weight percentages. The curves of both techniques show a similar trend to Valentini's where a shift in the crystallization temperature occurs at the lowest MWNT wt% followed by a gradual increase with increasing carbon nanotubes content. Similar results to that of Valentini [36] were also obtained by Leelapornpisit [31] and Razvi-Nouri. [35]. All the previous studies used SWNT, with regards to MWNT which is the type used in the current research, similar investigations were also conducted. Avril-Orta et al. [37] studied the effect of MWNTs on the crystallization of the PP matrix and reported that also with increasing nanotube content the crystallization temperatures increases.

Another indication that shows that the MWNTs acted as nucleating agents is related to the crystallization onset temperature ( $T_o$ ). The increase in  $T_o$  indicates a decrease in the



crystallization induction time. A similar trend was observed in the current research when the overall crystallization onset temperature also decreased with increasing MWNT content. Table (5.6) shows the results for the peak crystallization and onset temperatures. Razavi-Nouri [35] and Bao [28] also reported similar results regarding the crystallization onset temperatures. Table (5.6) also lists the melting temperatures of the PP and PP/MWNT composite samples. It is obvious that no significant changes have occurred to the melting temperatures. This was also the case in Valentini et al. study [36].

| CNT % | Dry mixed |         |         | Solvent mixed |         |         |
|-------|-----------|---------|---------|---------------|---------|---------|
|       | Tc (°C)   | To (°C) | Tm (°C) | Tc (°C)       | To (°C) | Tm (°C) |
| 0%    | 110.93    | 117.03  | 165     | 109.495       | 114.3   | 158     |
| 0.5%  | 118.79    | 123.8   | 161     | 111.743       | 113.2   | 157     |
| 1%    | 116.547   | 121.5   | 161     | 112.01        | 116.8   | 159     |
| 5%    | 121.007   | 126.2   | 163     | 115.247       | 118.6   | 156     |

Table 5.6 Peak crystallization and onset temperatures

As mentioned before the solvent mixed sample show decreased crystallization temperatures than the dry mixed ones this could be due to the effect of solvent used in the fabrication stage of the composite.

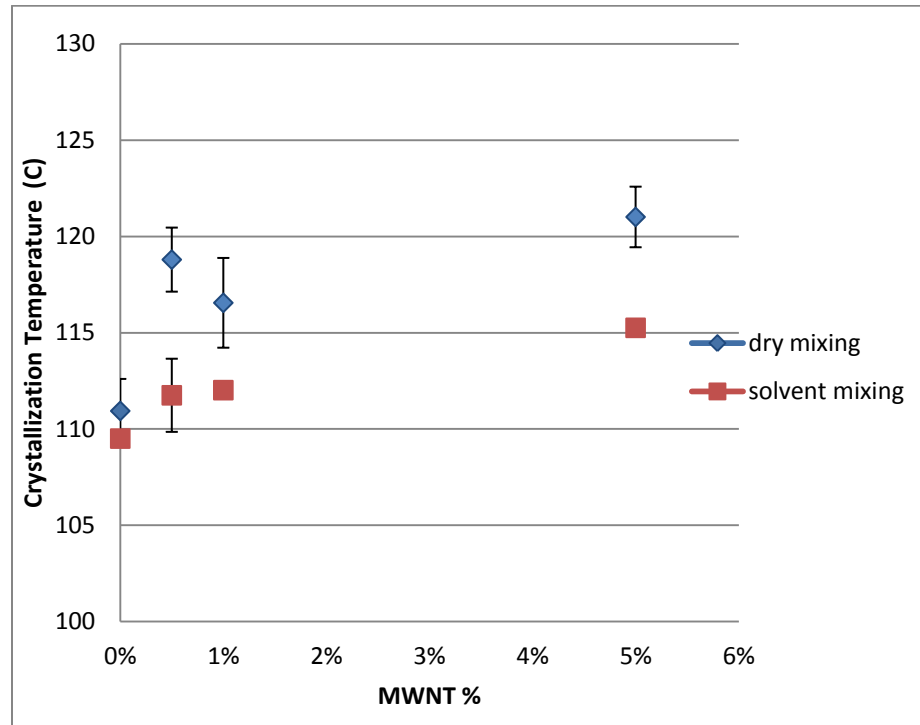


Figure 5.9 Crystallization Temperature vs. CNT %

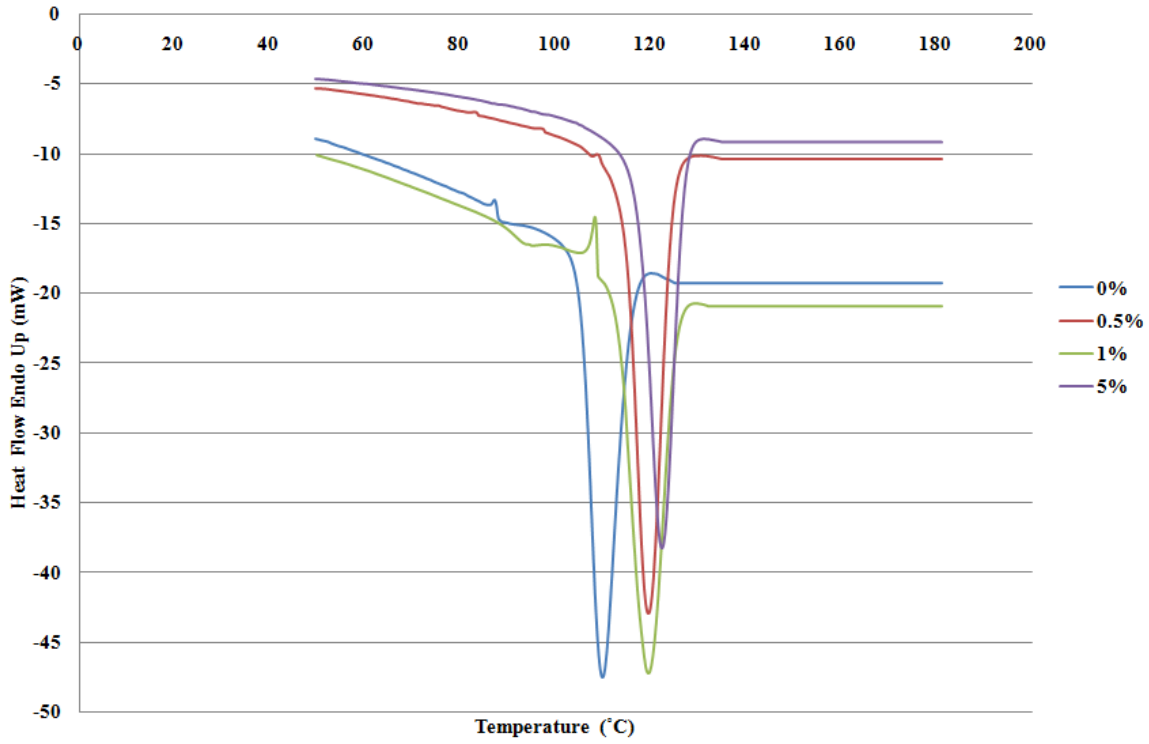


Figure 5.10 Non-isothermal crystallization curves of PP and PP/MWNT composites (dry mixed samples)

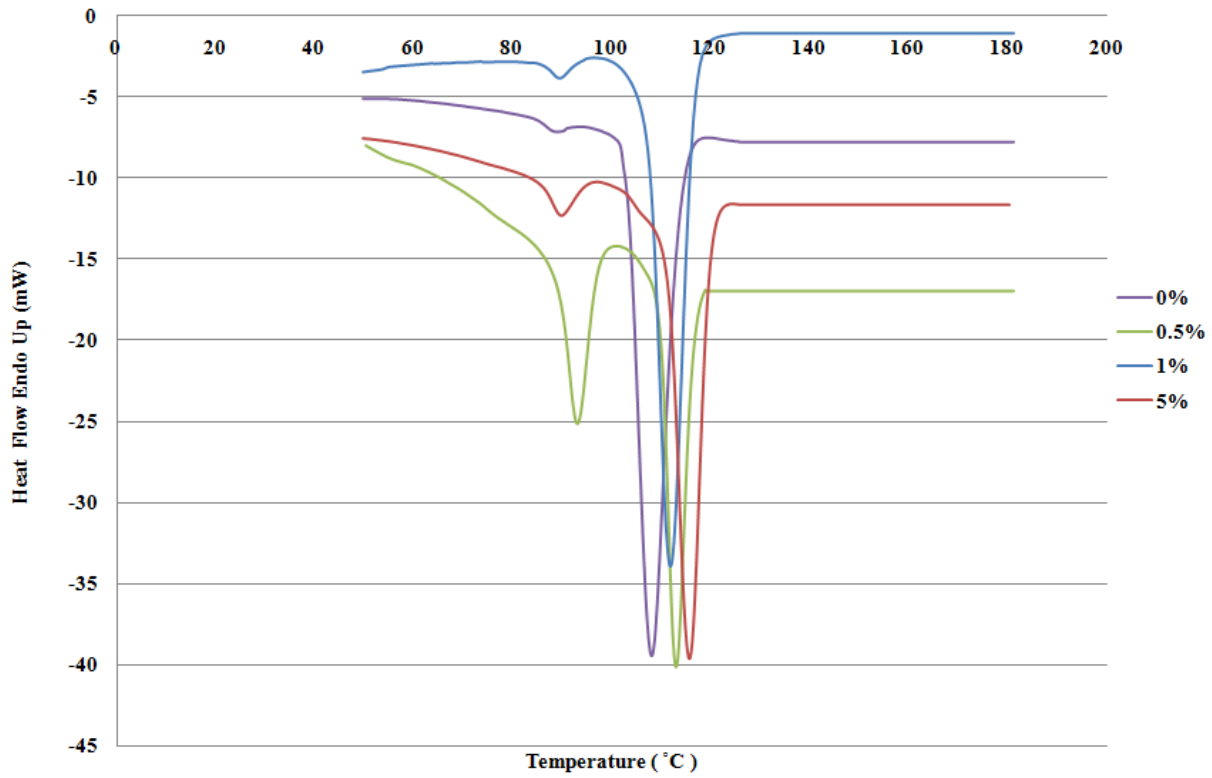


Figure 5.11 Non-isothermal crystallization curves of PP and PP/MWNT composites (solvent mixed samples)

## Chapter 6: Conclusion

In this work, PP/MWNT composites were prepared using two different mixing techniques: solvent mixing and “solvent-free” dry mixing, before further melt mixing by extrusion. Melt flow index was measured to determine the effect of the CNTs on the viscosity of the polymer. It was found that by adding different CNT loadings the viscosity of all the solvent mixed samples was increased. This was not the case for the dry mixed samples which showed negligible amount of change in its melt flow indices. In addition, the use of solvent-mixing for incorporating CNTs into the polymer resulted in more viscous melts which should have limited the degree of dispersion. However, better dispersion for solvent-mixed samples was observed. This might imply that, for our investigations, the contribution of shear mixing during extrusion to effective dispersion is more limited than the contribution of prior mixing by means of solvent sonication, which might be a consequence of the use of a single screw extruder. The effect of several CNT content on the mechanical properties of the CNT-PP composite was investigated. Enhancements in yield strength, hardness and Young’s modulus were observed for both the dry and the solvent-mixed samples. FESEM analysis showed uniform dispersion for solvent-mixed samples up to 5 wt%. This was not the case in the dry mixed samples where small clusters of CNT started appearing at lower CNT loadings. The mechanical properties of the samples are very much affected by the agglomeration of the CNTs in the PP matrix. Providing that the CNTs are uniformly dispersed throughout the matrix the mechanical properties of the samples were enhanced. Polymer degradation was suspected due to the inferior mechanical properties of the solvent mixed samples. However, another important factor to consider is that the FESEM images also showed porosity in some of the solvent mixed samples. This could be due to the evaporation of the solvent. The presence of porosity in the matrix could negatively affect the mechanical

properties of the solvent samples and result in premature failure. FESEM images also showed CNT pull-out which indicates poor interfacial bond between the CNT and the PP matrix. Therefore, enhancing the interfacial bonding between the composites' constituents might even increase the mechanical properties further. DSC testing was also conducted to investigate the crystallization behavior of the PP matrix with the addition of CNTs. It was found that for both techniques the addition of nanotubes increased the crystallization temperature of the composite which means that the CNTs acted as nucleating agents. The overall crystallization temperatures of the solvent mixed samples were lower than those of the dry mixed samples. This could be the effect of the solvent used in the fabrication process. Therefore optimizing the processing parameters to enhance dispersion of the CNTs, while minimizing polymer degradation, is also necessary.

## Chapter7: Future Work

1. Investigating in depth the affect of the solvent on the polymer matrix
2. Promoting wetting between the composite constituents to improve the interfacial bonds between them
3. Conducting comparative studies on other matrices apart from polypropylene.
4. Understanding the polymer structure of the matrix with the addition of CNTs using X-ray diffraction (XRD)

## References

- [1] Bhushan, 2003 Handbook of nanotechnology
- [2] Paul, D. R. "Polymer Nanotechnology: Nanocomposites." *Polymer (Guilford)* 49.15 (2008): 3187-204. Web.
- [3] Koo, Joseph. *Polymer Nanocomposites.*, 2006. Web.
- [4] Xia, Hesheng, et al. "Preparation of polypropylene/carbon Nanotube Composite Powder with a Solid-State Mechanochemical Pulverization Process." *Journal of Applied Polymer Science* 93.1 (2004): 378-86. Web.
- [5] Funck, Andreas. "Polypropylene Carbon Nanotube Composites by in Situ Polymerization." *Composites Science and Technology* 67.5 (2007): 906-15. Web.
- [6] Manchado, M. A. López. "Thermal and Mechanical Properties of Single-Walled Carbon nanotubes–polypropylene Composites Prepared by Melt Processing." *Carbon (New York)* 43.7 (2005): 1499-505. Web.
- [7] DESAI, A. "Mechanics of the Interface for Carbon Nanotube-Polymer Composites." *Thin-walled structures* 43.11 (2005): 1787-803. Web.
- [8] Prashantha, K. "Masterbatch-Based Multi-Walled Carbon Nanotube Filled Polypropylene Nanocomposites: Assessment of Rheological and Mechanical Properties." *Composites Science and Technology* 69.11 (2009): 1756-63. Web.
- [9] Zhao, Bo. "Mechanical Strength Improvement of Polypropylene Threads Modified by PVA/CNT Composite Coatings." *Materials Letters* 62.28 (2008): 4380-2. Web.
- [10] Pfaendner, Rudolf. "Nanocomposites: Industrial Opportunity Or Challenge?" *Polymer Degradation and Stability* 95.3 (2010): 369-73. Web.
- [11] Coleman, J. "Small but Strong: A Review of the Mechanical Properties of Carbon nanotube–polymer Composites." *Carbon (New York)* 44.9 (2006): 1624-52. Web.
- [12] Li Chen, Xiu-Jiang Pang, et al, "Fabrication and characterization of polycarbonate/carbon nanotubes composites." *Composites Part A* 37.9 (2006): 1485-1489. Web.
- [13] Awasthi, K. et al, "Synthesis of Carbon Nanotubes". <http://arxiv.org/ftp/cond-mat/papers/0505/0505526.pdf>
- [14] Hirsch, A. "Functionalization of Carbon Nanotubes." *Topics in current chemistry* 245 (2005): 193-237. Web.

- [15] Moniruzzaman, Mohammad. "Polymer Nanocomposites Containing Carbon Nanotubes." *Macromolecules* 39.16 (2006): 5194-205. WOS. Web.
- [16] Thostenson, Erik T. "Advances in the Science and Technology of Carbon Nanotubes and their Composites: A Review." *Composites Science and Technology* 61.13 (2001): 1899-912. Web.
- [17] Ma, Peng-Cheng. "Dispersion and Functionalization of Carbon Nanotubes for Polymer-Based Nanocomposites: A Review." *Composites.Part A, Applied science and manufacturing* 41.10 (2010): 1345-67. Web.
- [18] Andrews, Rodney. "Multiwall Carbon Nanotubes: Synthesis and Application." *Accounts of Chemical Research* 35.12 (2002): 1008-17. WOS. Web.
- [19] Tripathi, D. *Practical Guide to Polypropylene*. Shrewsbury, , GBR: Smithers Rapra, 2002. Web.
- [20] Bikiaris, D. "Effect of Acid Treated Multi-Walled Carbon Nanotubes on the Mechanical, Permeability, Thermal Properties and Thermo-Oxidative Stability of Isotactic Polypropylene." *Polymer Degradation and Stability* 93.5 (2008): 952-67. Web.
- [21] Breuer, O., and Uttandaraman Sundararaj. "Big Returns from Small Fibers: A Review of polymer/carbon Nanotube Composites." *Polymer Composites* 25.6 (2004): 630-45. Web.
- [22] Zdenko Spitalsky, Dimitrios Tasis, Konstantinos Papagelis, Costas Galiotis. "Carbon nanotube-polymer composites: Chemistry, processing, mechanical and electrical properties." *Progress in Polymer Science*, 35 (2010): 357-401.
- [23] Shaffer, MSP. "Fabrication and Characterization of Carbon nanotube/poly(Vinyl Alcohol) Composites." *Advanced materials (Weinheim)* 11.11 (1999): 937-. Web.
- [24] Qian, D. "Load Transfer and Deformation Mechanisms in Carbon Nanotube-Polystyrene Composites." *Applied Physics Letters* 76.20 (2000): 2868. Web.
- [25] Safadi, B., R. Andrews, and E. A. Grulke. "Multiwalled Carbon Nanotube Polymer Composites: Synthesis and Characterization of Thin Films." *Journal of Applied Polymer Science* 84.14 (2002): 2660-9. Web.
- [26] Jin, Zhaoxia, et al. "Dynamic Mechanical Behavior of Melt-Processed Multi-Walled Carbon nanotube/poly(Methyl Methacrylate) Composites." *Chemical Physics Letters* 337.1-3 (2001): 43-7. Web.
- [27] Meincke, O. "Mechanical Properties and Electrical Conductivity of Carbon-Nanotube Filled Polyamide-6 and its Blends with acrylonitrile/butadiene/styrene." *Polymer (Guilford)* 45.3 (2004): 739-48. Web.

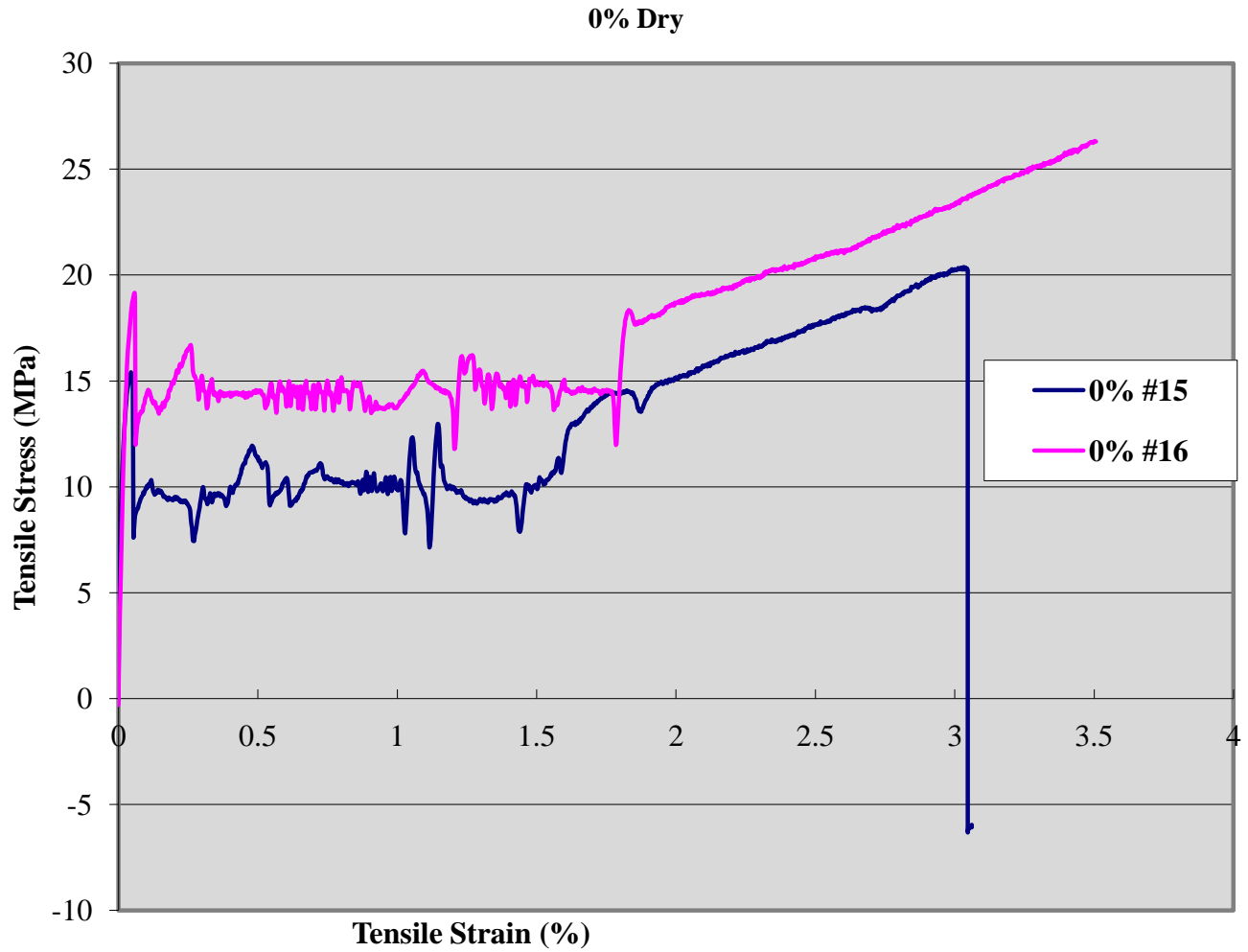


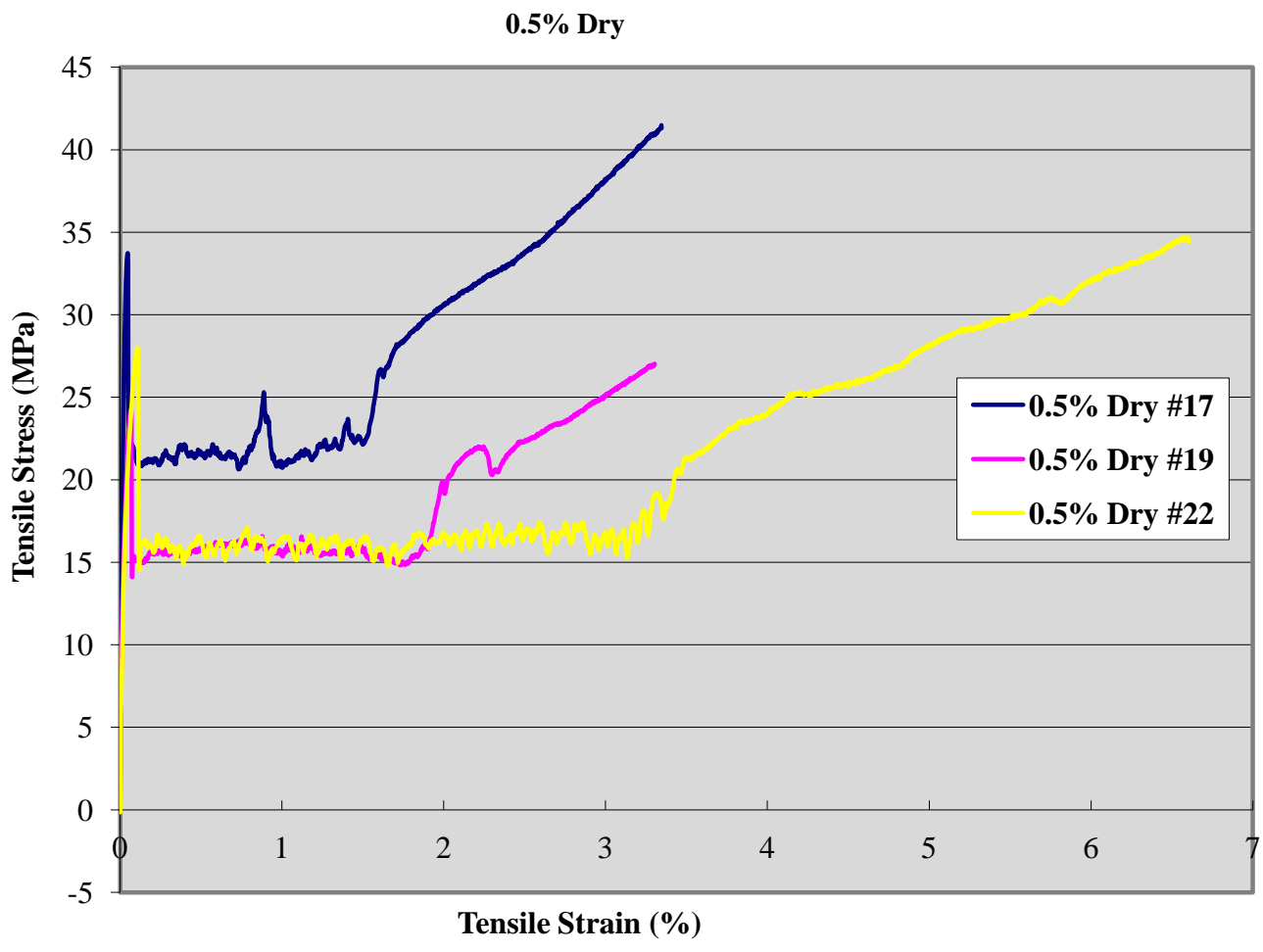
- [28] Bao, S. P. "Mechanical Behaviors of polypropylene/carbon Nanotube Nanocomposites: The Effects of Loading Rate and Temperature." *Materials science & engineering.A, Structural materials : properties, microstructure and processing* 485.1-2 (2007): 508-16. Web.
- [29] Hemmati, M. "Rheological and Mechanical Characterization of Multi-Walled Carbon Nanotubes/Polypropylene Nanocomposites." *Journal of macromolecular science.Physics* 47.6 (2008): 1176-87. Web.
- [30] Chang, T. E. "Microscopic Mechanism of Reinforcement in Single-Wall Carbon nanotube/polypropylene Nanocomposite." *Polymer (Guilford)* 46.2 (2005): 439-44. Web.
- [31] Leelapornpisit, Weawkamol. "Effect of Carbon Nanotubes on the Crystallization and Properties of Polypropylene." *Journal of polymer science.Part B, Polymer physics* 43.18 (2005): 2445-53. Web.
- [32] Grady, Brian. "Nucleation of Polypropylene Crystallization by Single-Walled Carbon Nanotubes." *The journal of physical chemistry.B* 106.23 (2002): 5852-8. Web.
- [33] Shi, Jia-Hua. "Covalent Functionalization of Multiwalled Carbon Nanotubes with Poly(Styrene-Co-Acrylonitrile) by Reactive Melt Blending." *European polymer journal* 45.4 (2009): 1002-8. Web.
- [34] Yang, Bing-Xing. "Enhancement of the Mechanical Properties of Polypropylene using Polypropylene-Grafted Multiwalled Carbon Nanotubes." *Composites Science and Technology* 68.12 (2008): 2490-7. Web.
- [35] Razavi-Nouri, Mohammad. "Effect of Carbon Nanotubes Content on Crystallization Kinetics and Morphology of Polypropylene." *Polymer Testing* 28.1 (2009): 46-52. Web.
- [36] Valentini, L. "Morphological Characterization of Single-Walled Carbon Nanotubes-PP Composites." *Composites Science and Technology* 63.8 (2003): 1149-53. Web.
- [37] Avila-Orta, Carlos A., et al. "Morphological Features and Melting Behavior of Nanocomposites Based on Isotactic Polypropylene and Multiwalled Carbon Nanotubes." *Journal of Applied Polymer Science* 106.4 (2007): 2640-7. Web.
- [38] Esawi, Amal M. K. "Effect of Processing Technique on the Dispersion of Carbon Nanotubes within Polypropylene Carbon Nanotube-Composites and its Effect on their Mechanical Properties." *Polymer composites* 31.5 (2010): 772-80. Web.
- [39] Teng, Chih-Chun. "Effect of MWNT Content on Rheological and Dynamic Mechanical Properties of Multiwalled Carbon nanotube/polypropylene Composites." *Composites.Part A, Applied science and manufacturing* 39.12 (2008): 1869-75. Web.

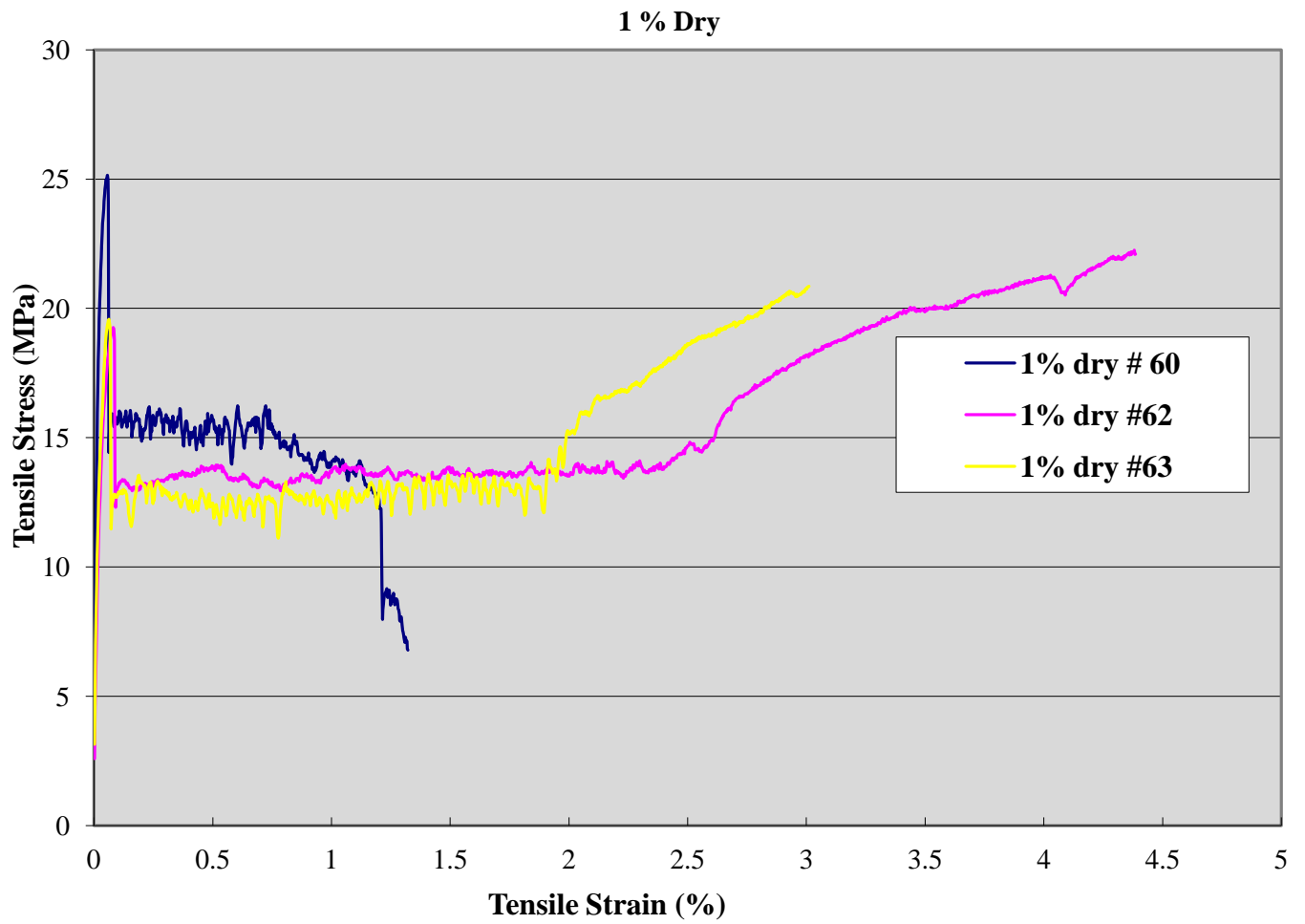
- [40] Fischer-Cripps, Anthony C. "*Nanoindentation*". Secaucus, NJ, USA: Springer-Verlag New York, Incorporated, 2002.
- [41] Lee, Seung Hwan. "Rheological and Electrical Properties of polypropylene/MWNT Composites Prepared with MWNT Masterbatch Chips." *European polymer journal* 44.6 (2008): 1620-30. Web.

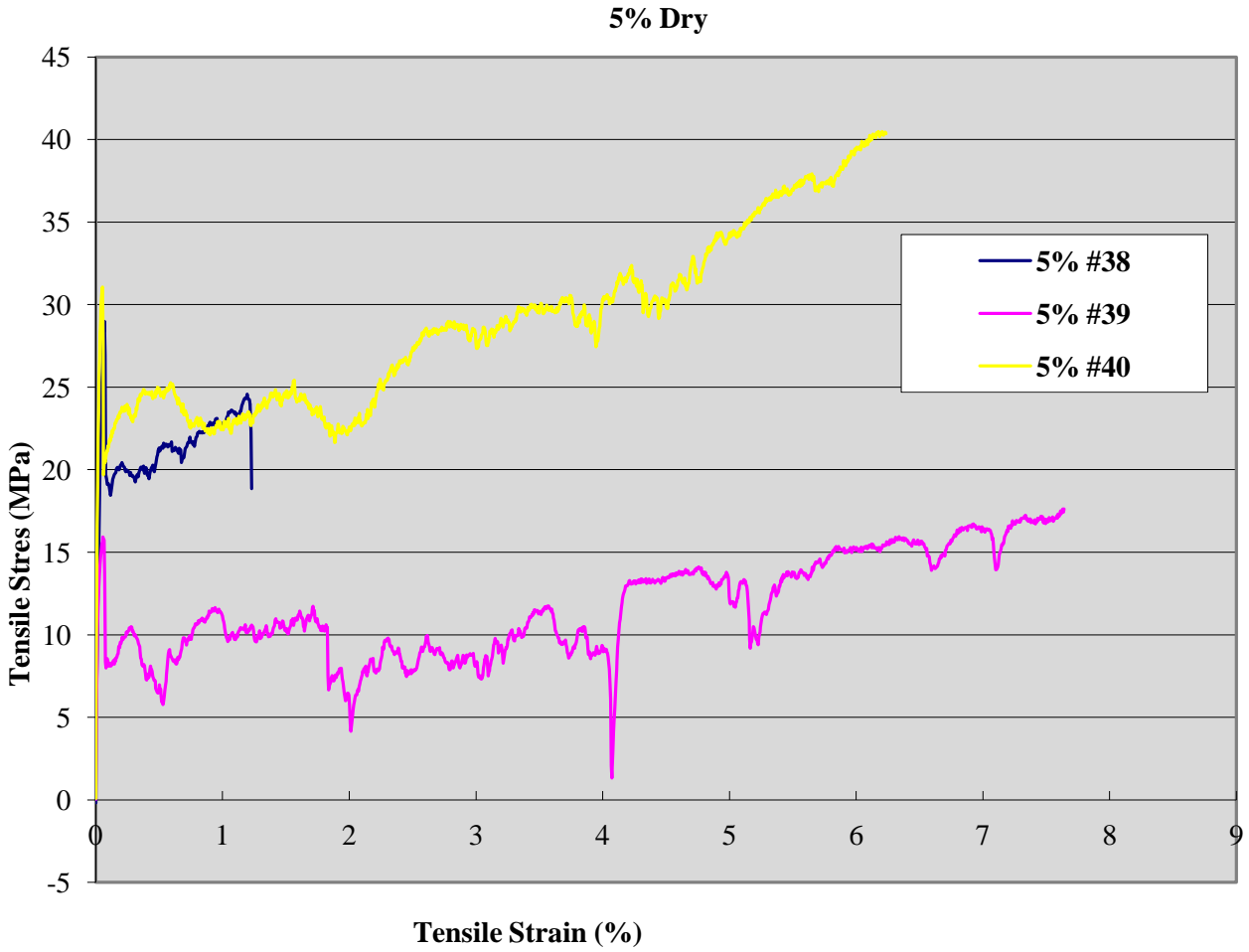
# Appendix I

## Tension Test Results for all dry mixed Samples

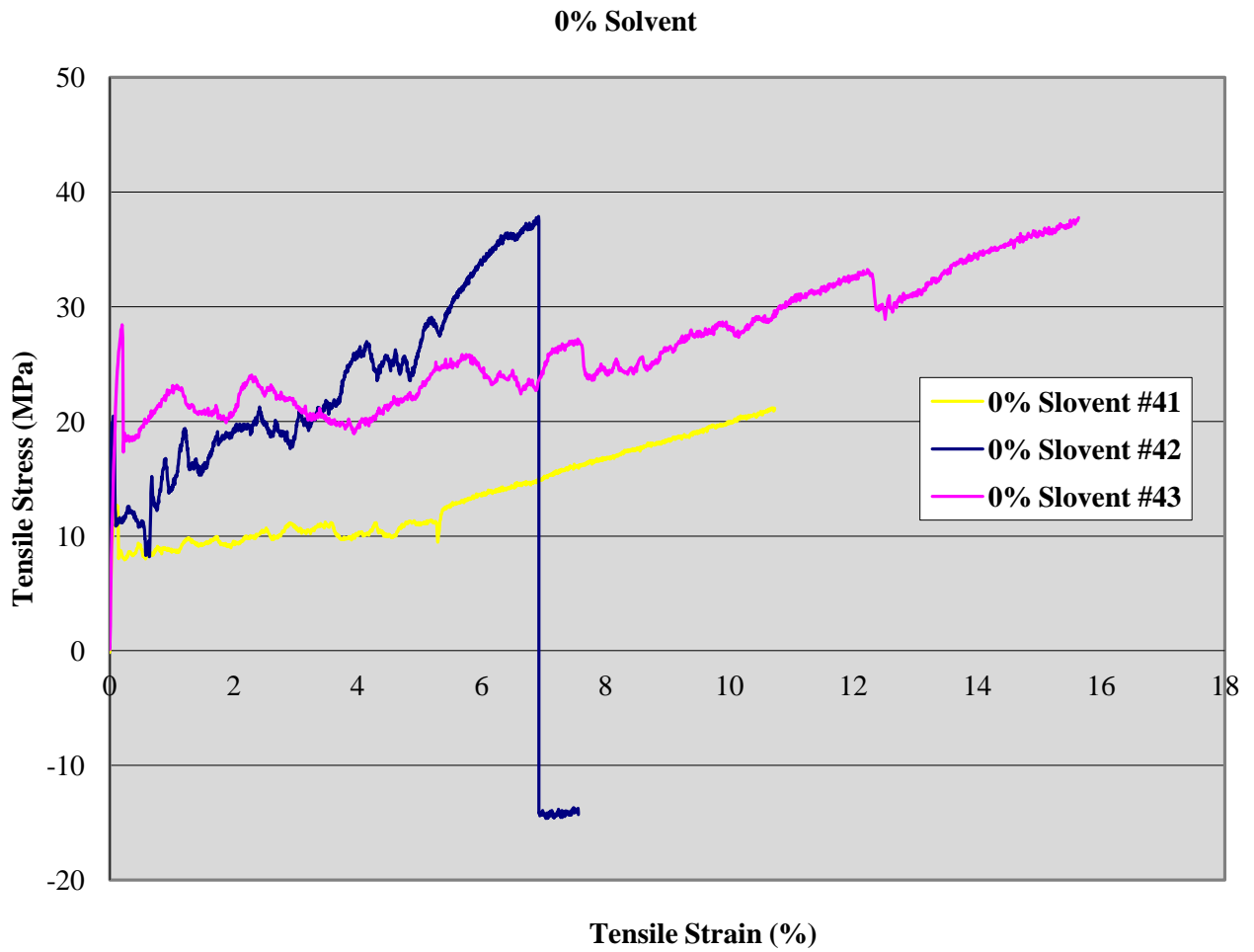


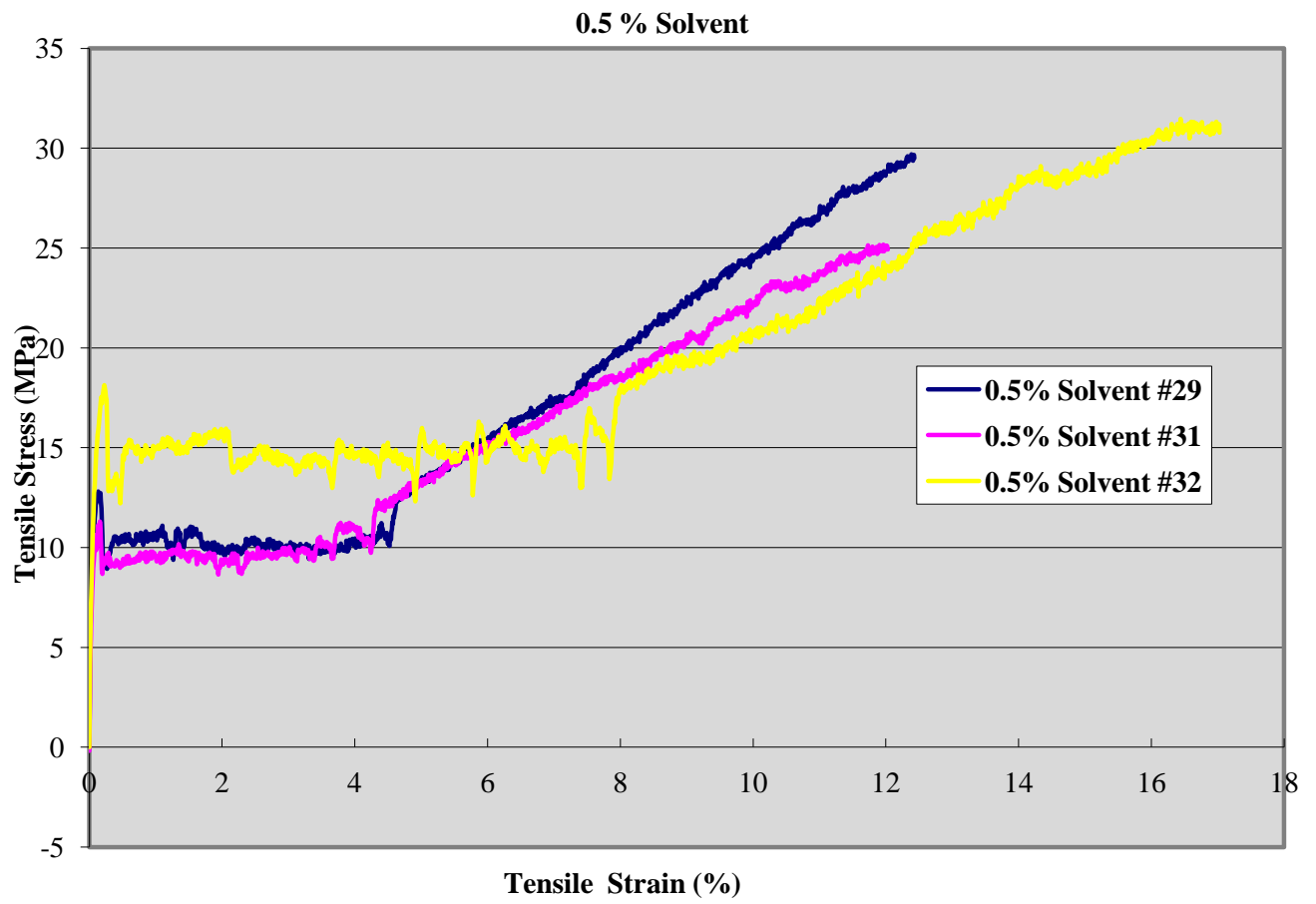






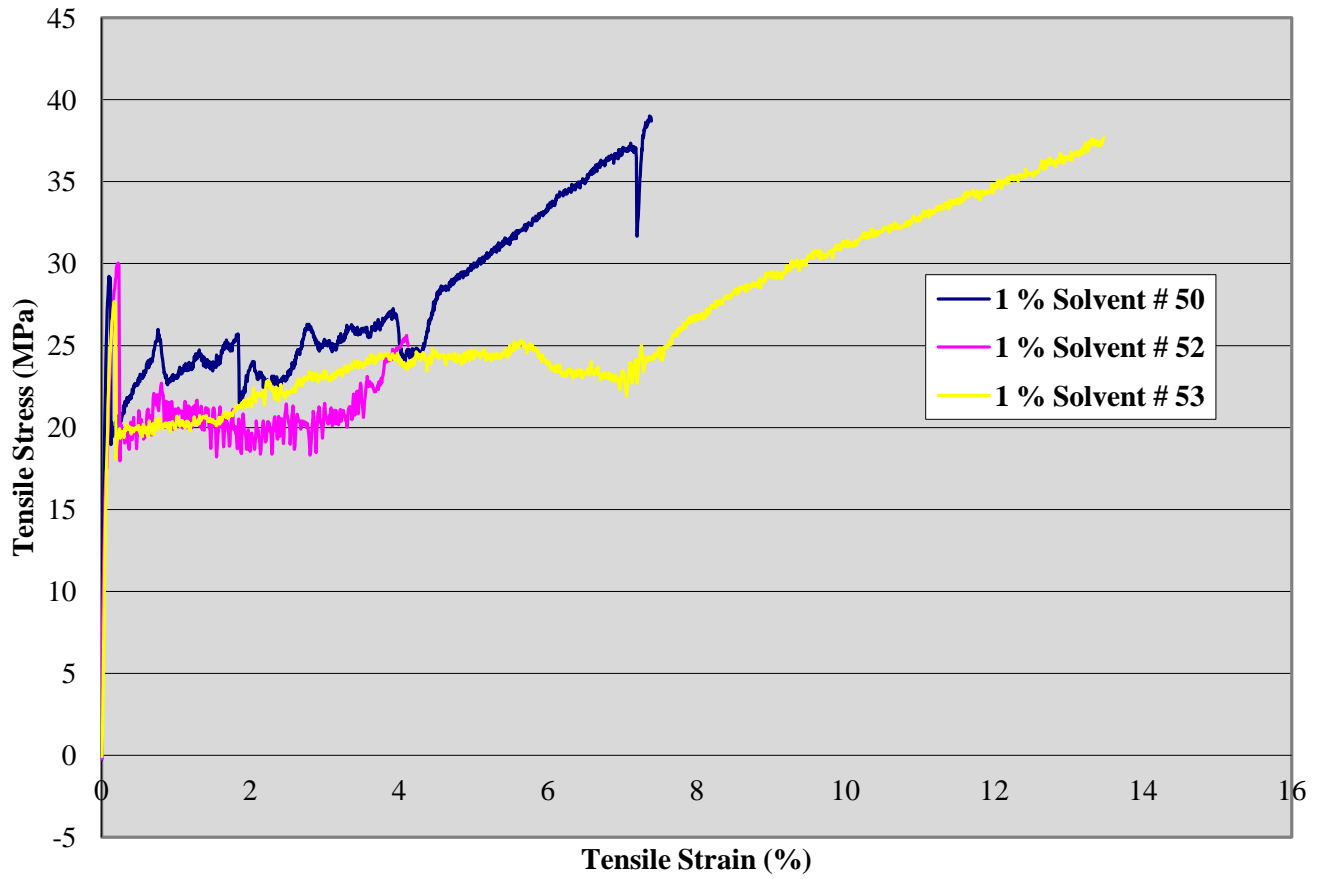
## Tension test results for all solvent mixed samples



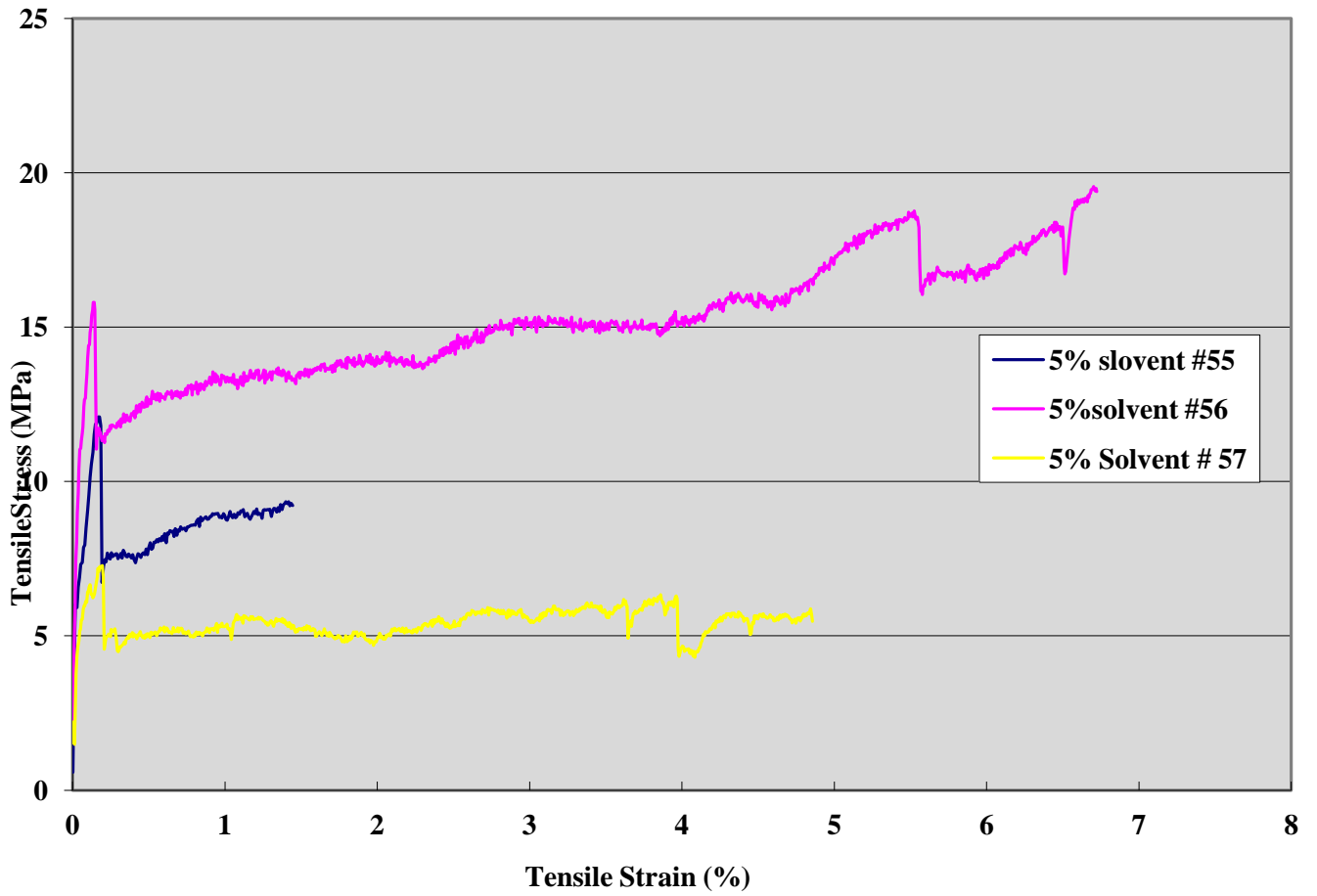




### 1 % Solvent



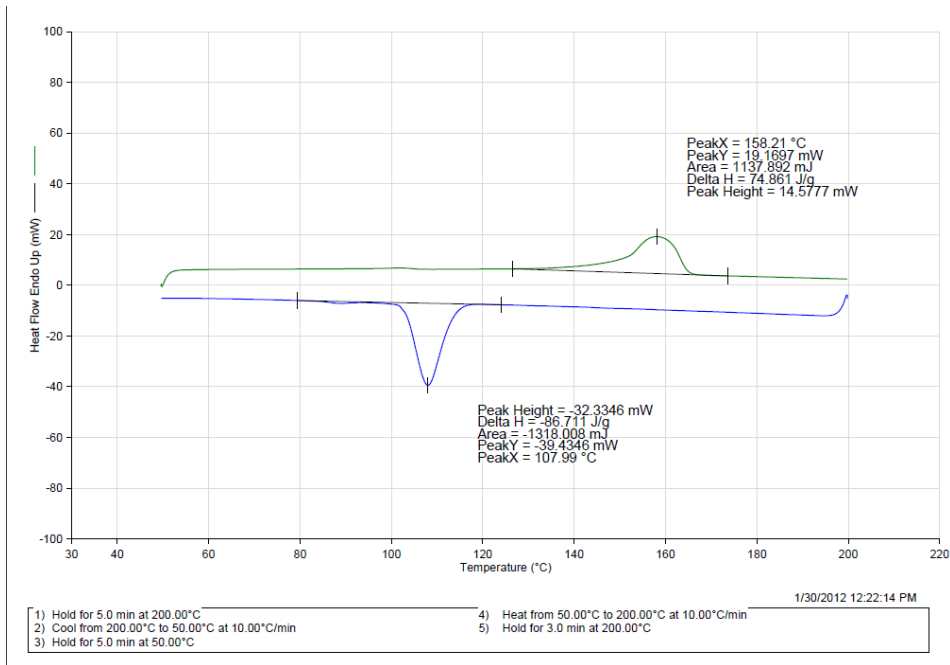
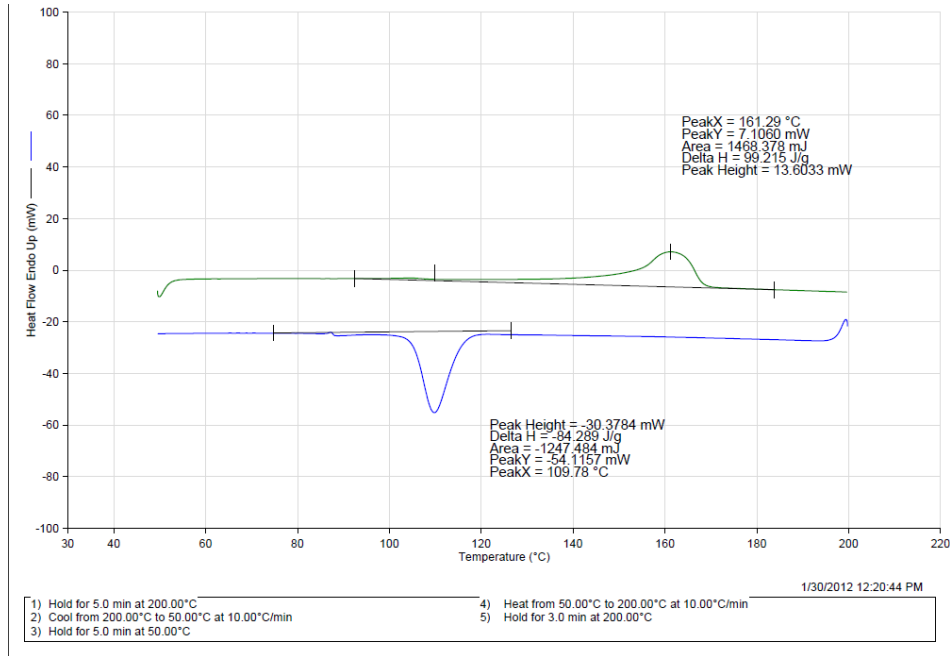
5 % Solvent

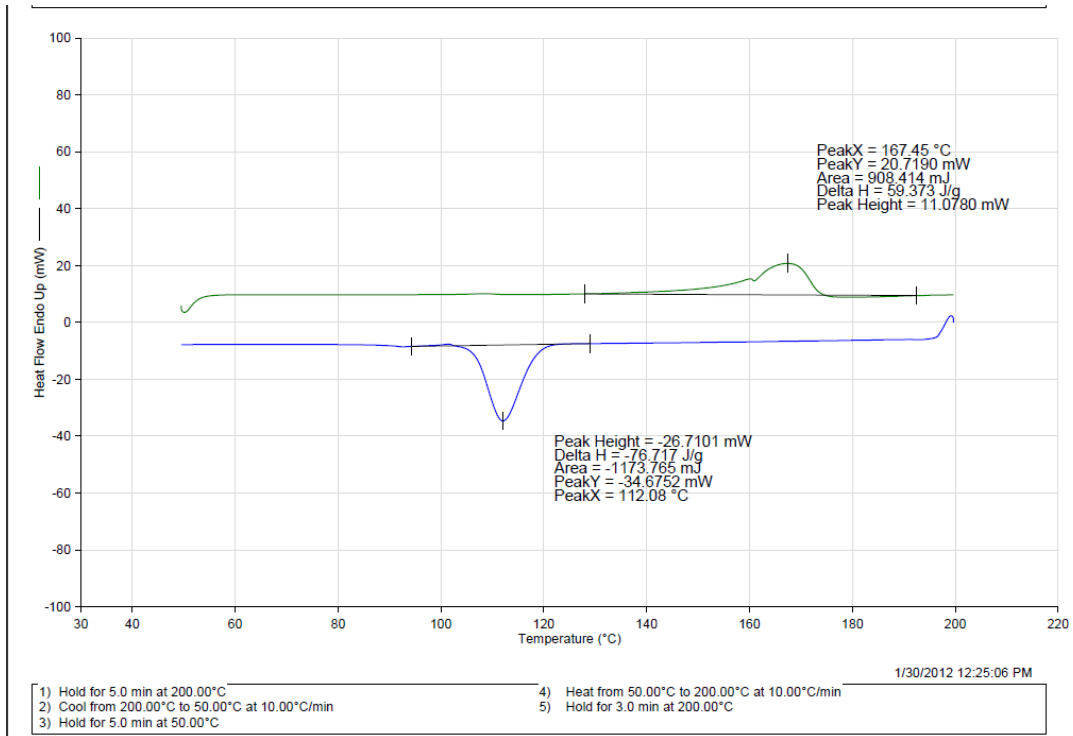


## Appendix II

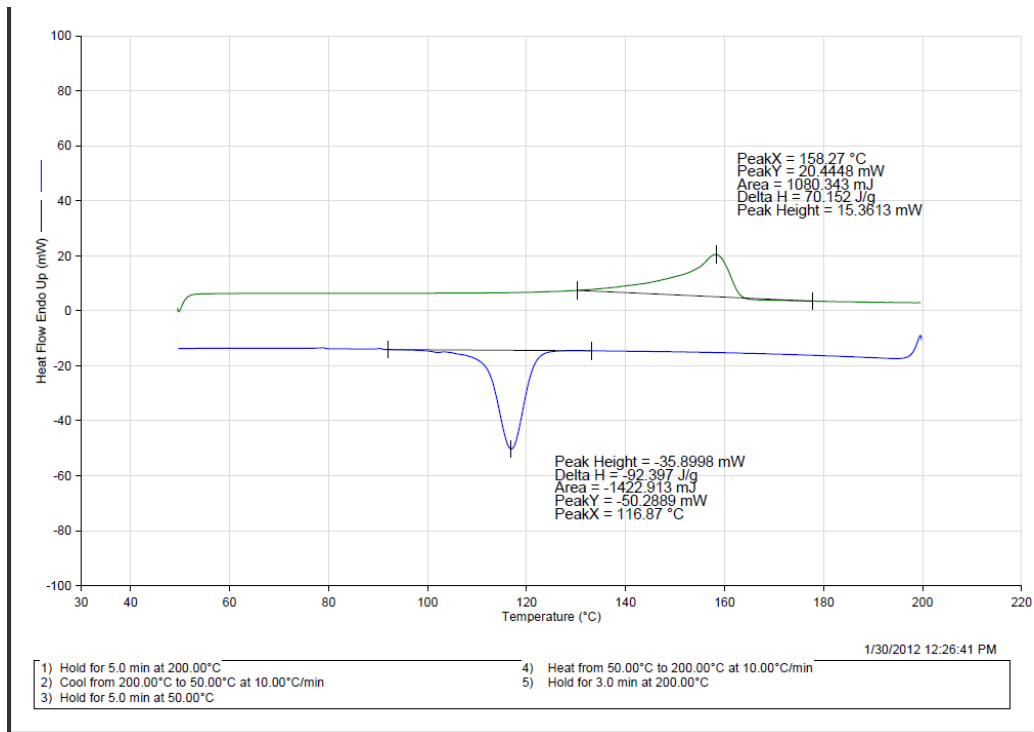
### DSC test results for all dry mixed samples

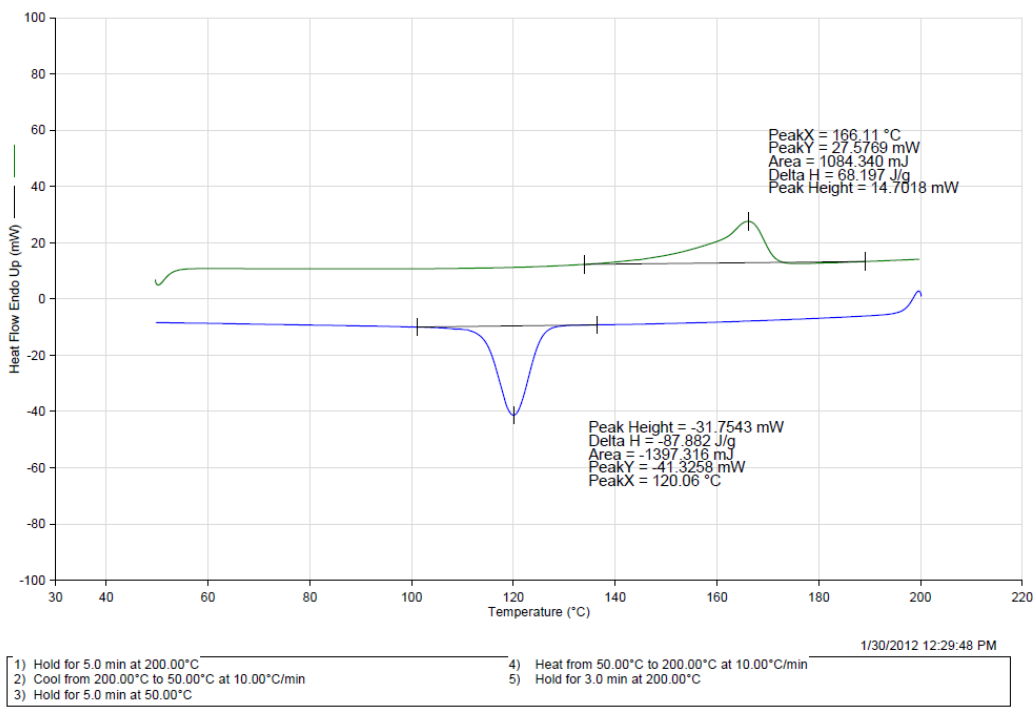
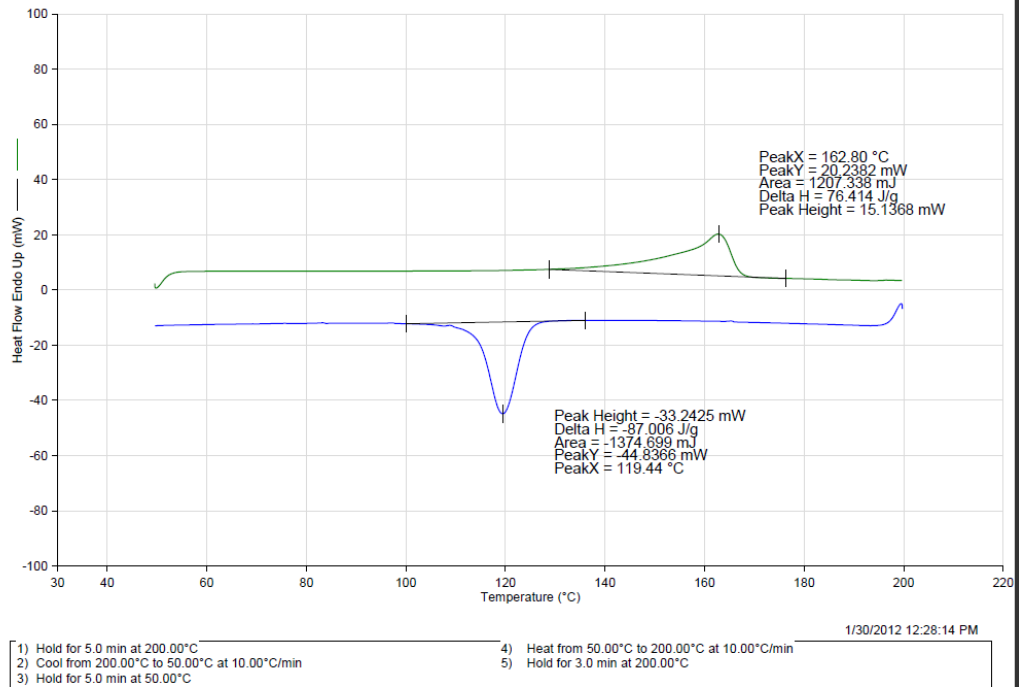
#### 0% dry samples:



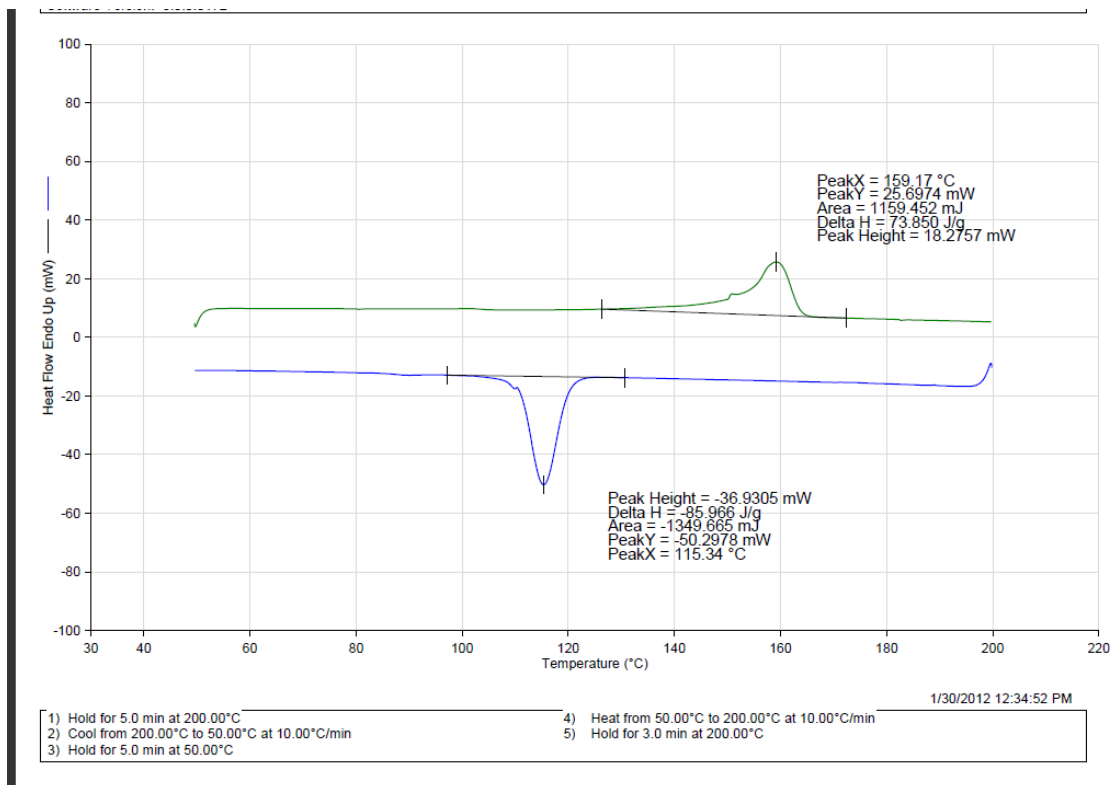
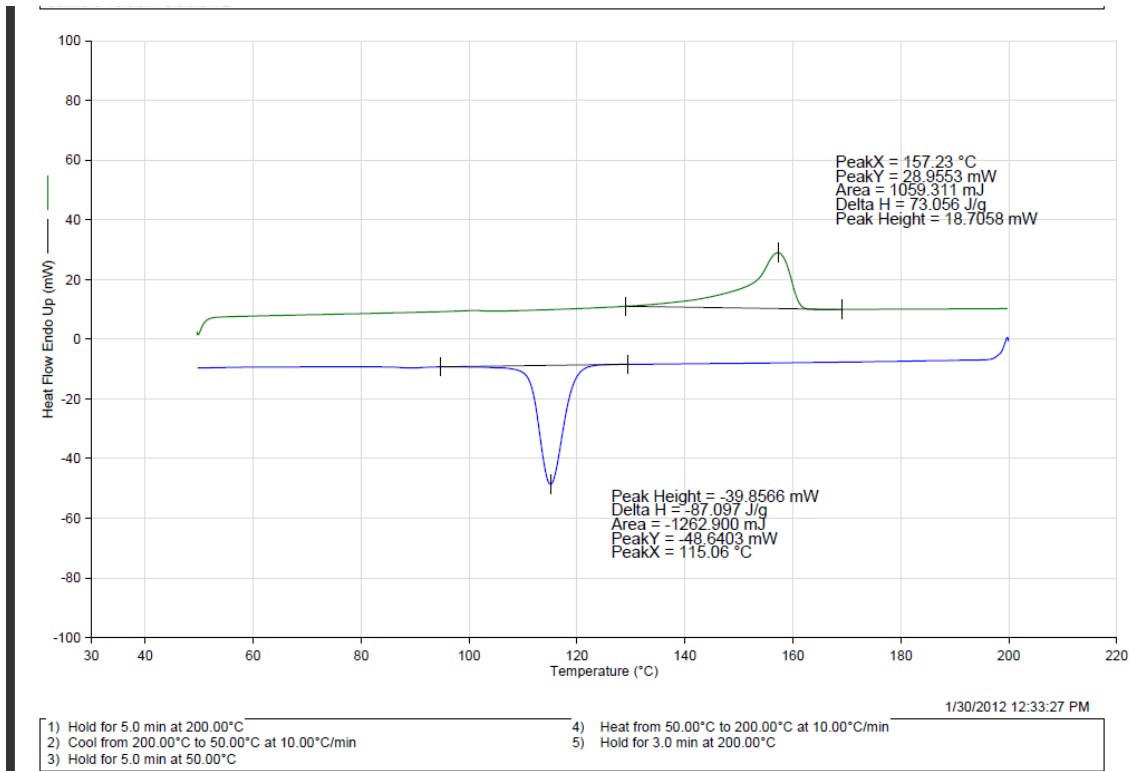


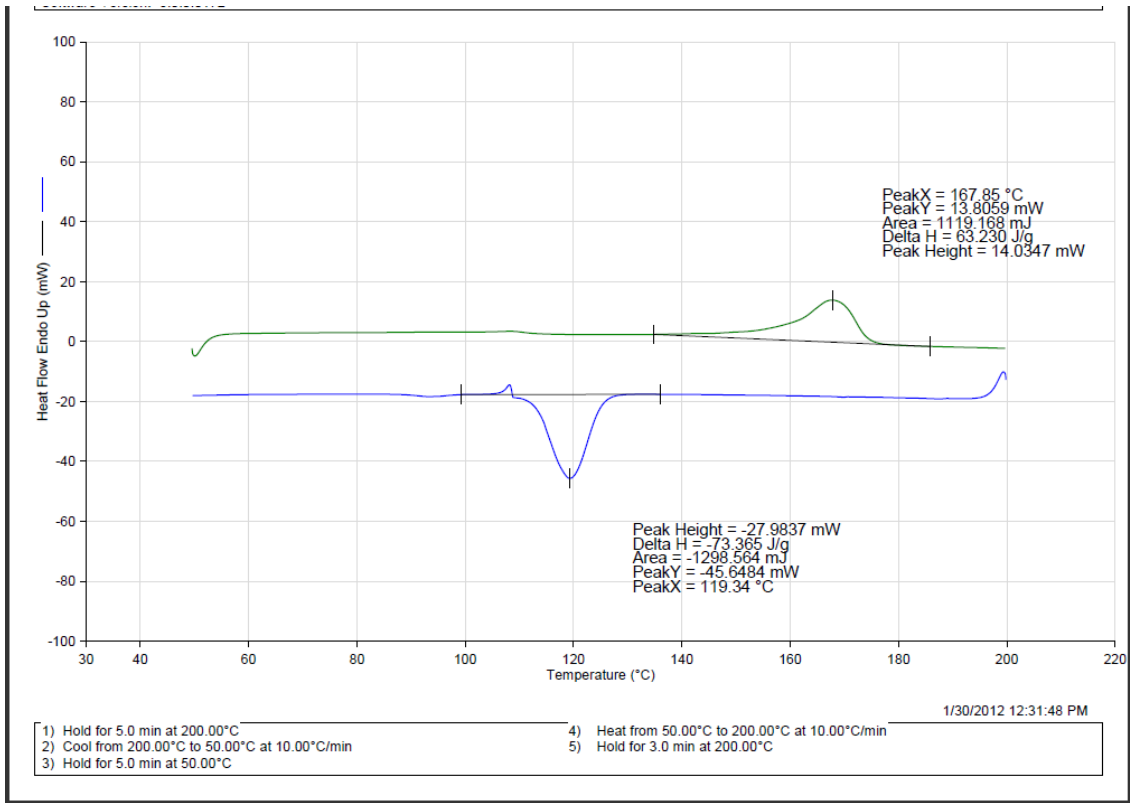
**0.5% dry samples:**



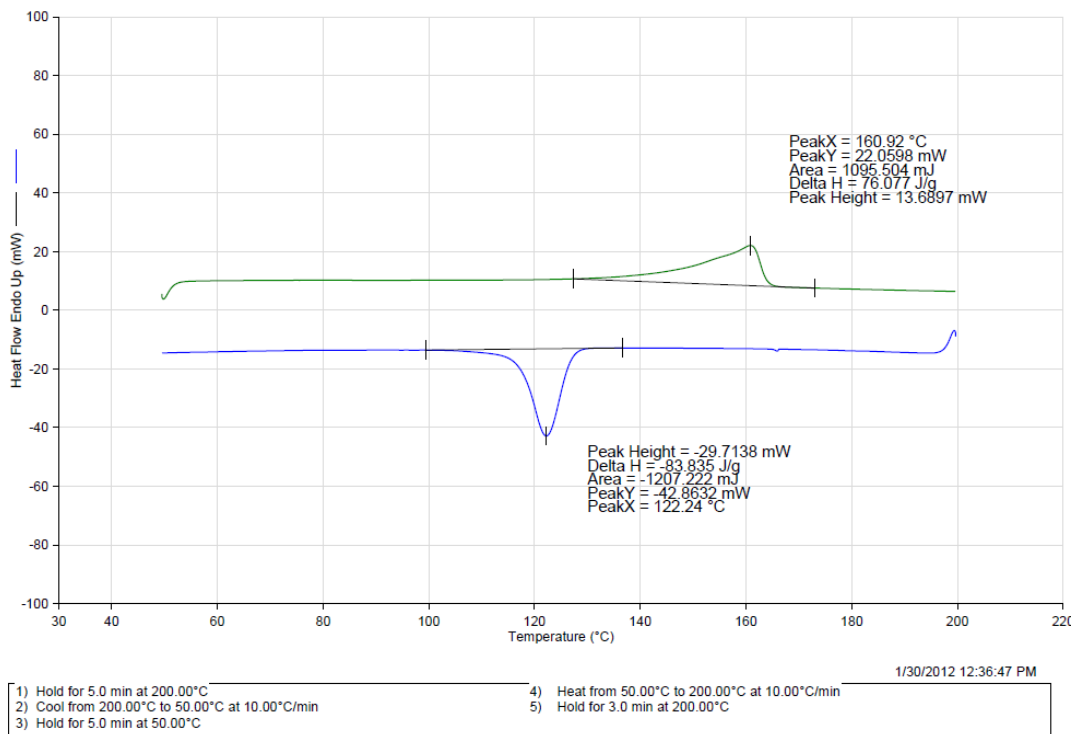


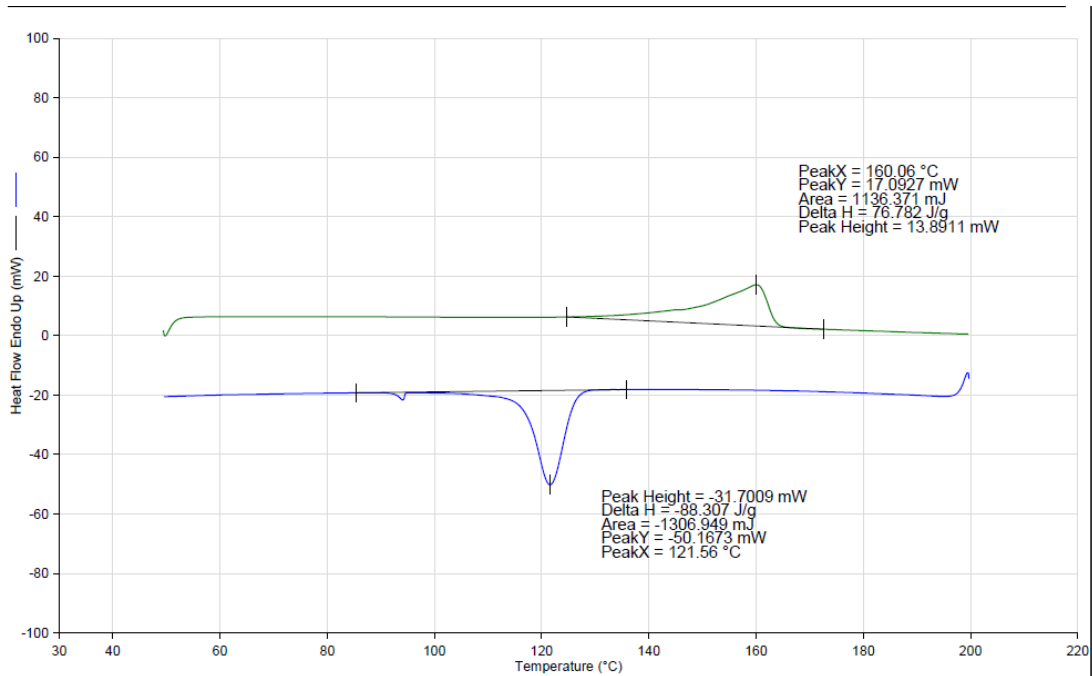
1% dry samples:





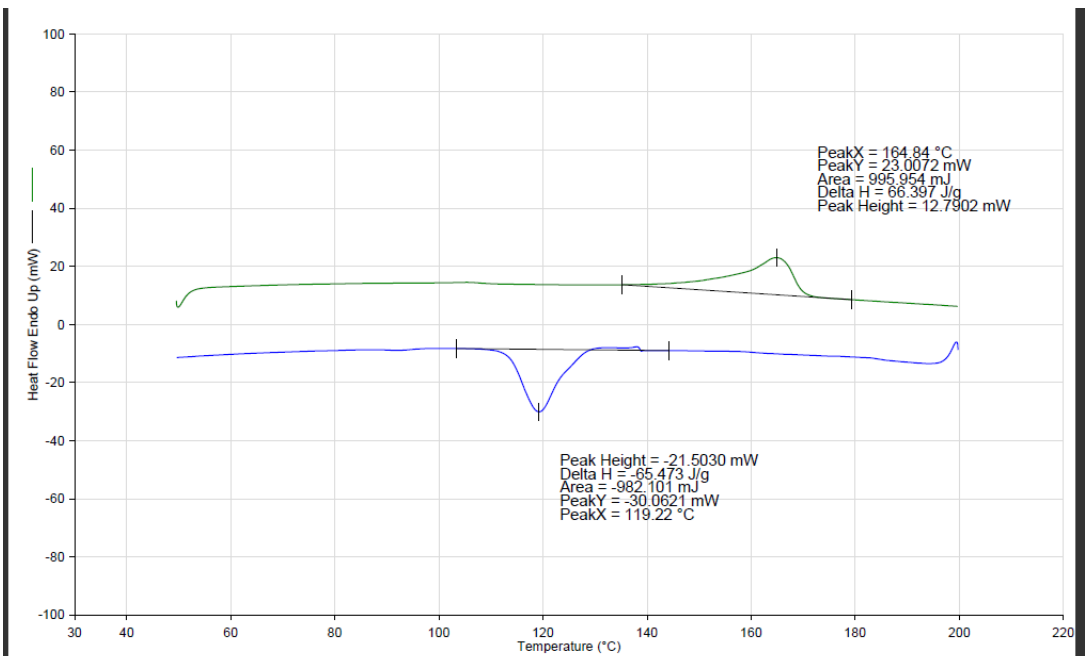
**5% dry samples:**





1/30/2012 12:38:10 PM

- |                                                 |                                                 |
|-------------------------------------------------|-------------------------------------------------|
| 1) Hold for 5.0 min at 200.00°C                 | 4) Heat from 50.00°C to 200.00°C at 10.00°C/min |
| 2) Cool from 200.00°C to 50.00°C at 10.00°C/min | 5) Hold for 3.0 min at 200.00°C                 |
| 3) Hold for 5.0 min at 50.00°C                  |                                                 |



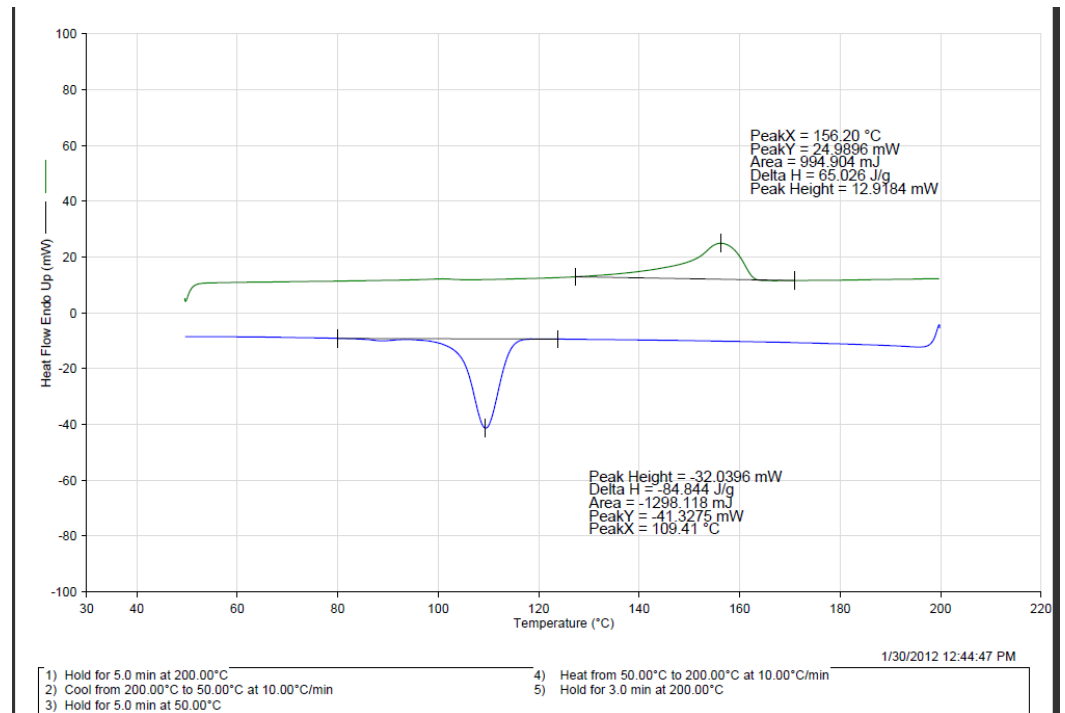
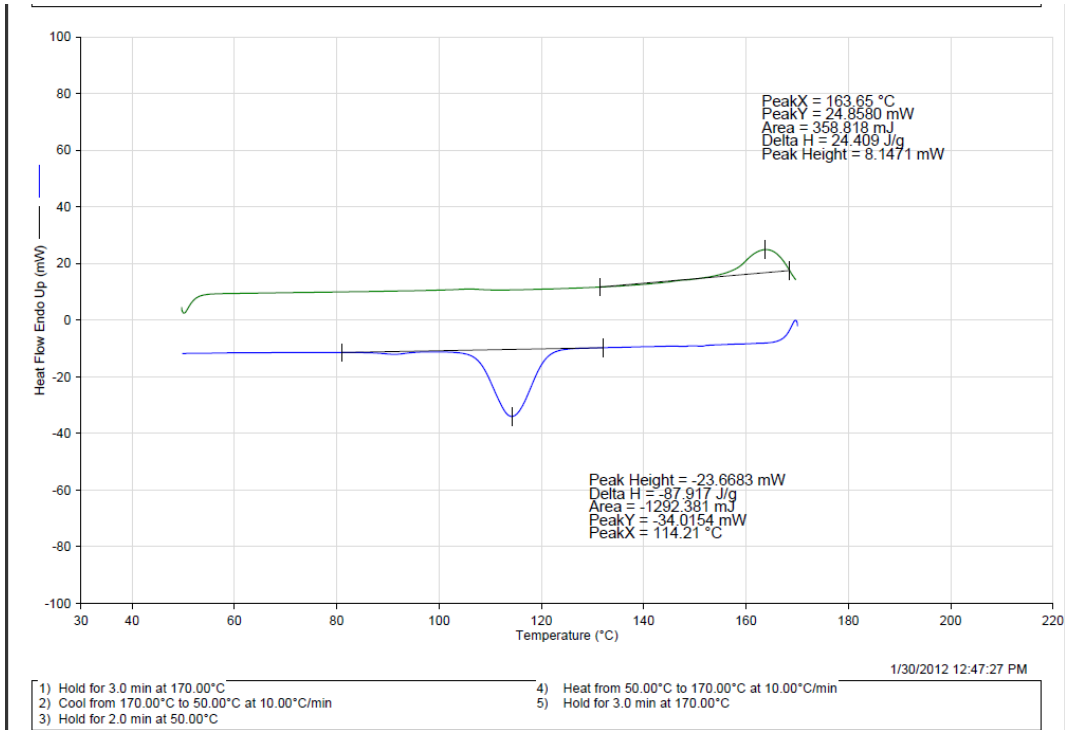
1/30/2012 12:43:27 PM

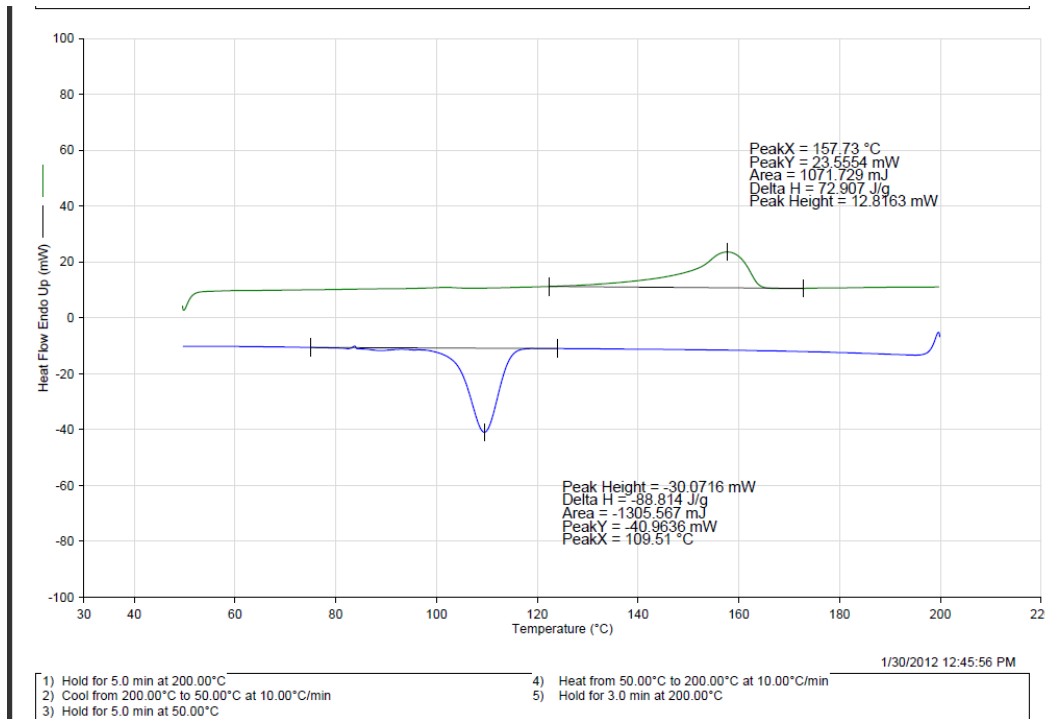
- |                                                 |                                                 |
|-------------------------------------------------|-------------------------------------------------|
| 1) Hold for 5.0 min at 200.00°C                 | 4) Heat from 50.00°C to 200.00°C at 10.00°C/min |
| 2) Cool from 200.00°C to 50.00°C at 10.00°C/min | 5) Hold for 3.0 min at 200.00°C                 |
| 3) Hold for 5.0 min at 50.00°C                  |                                                 |



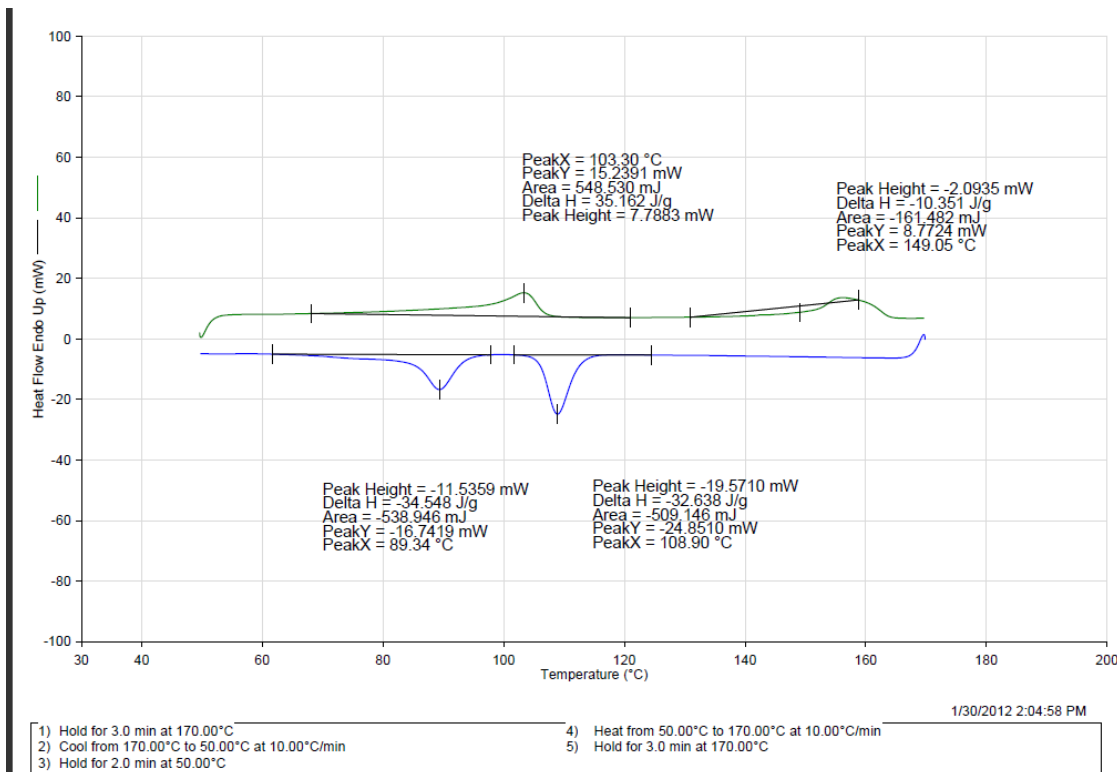
## DSC test results for all solvent mixed samples

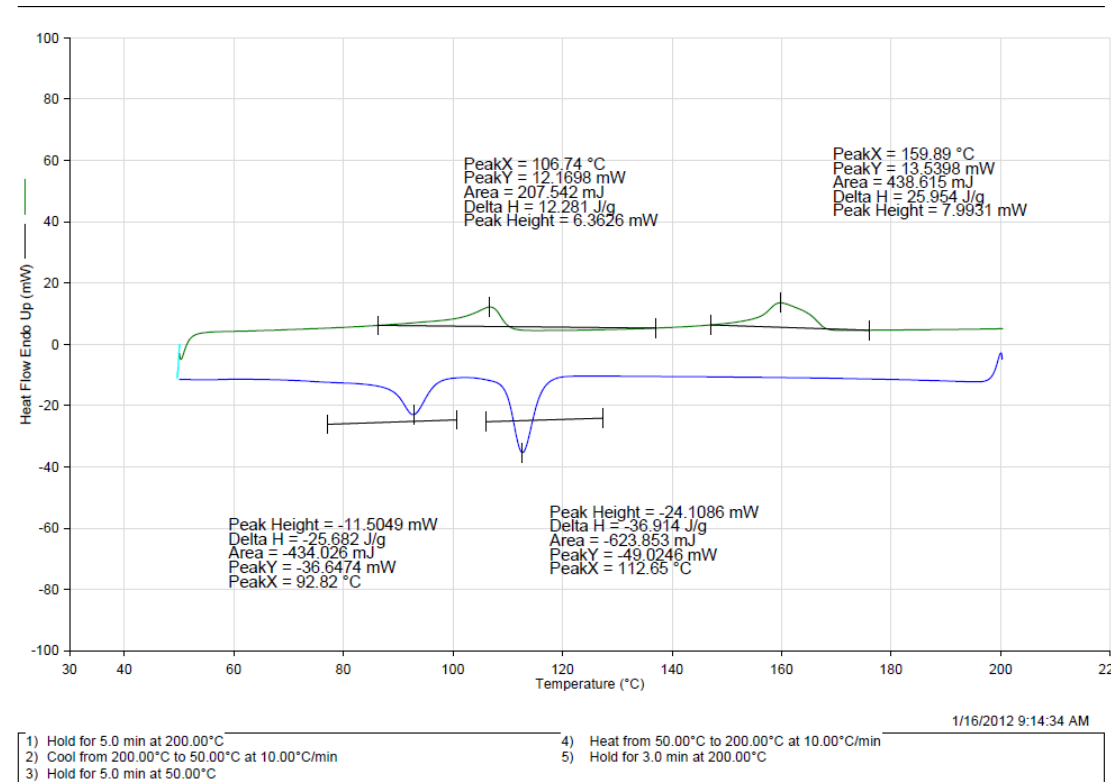
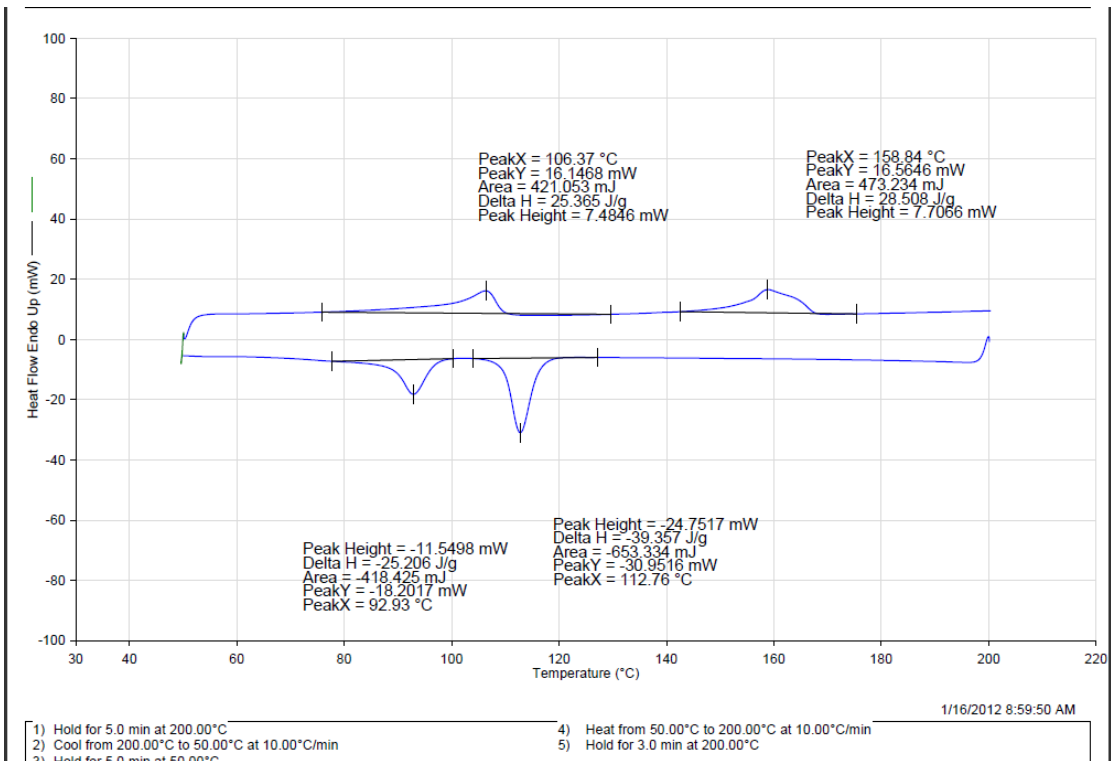
### 0% solvent samples:



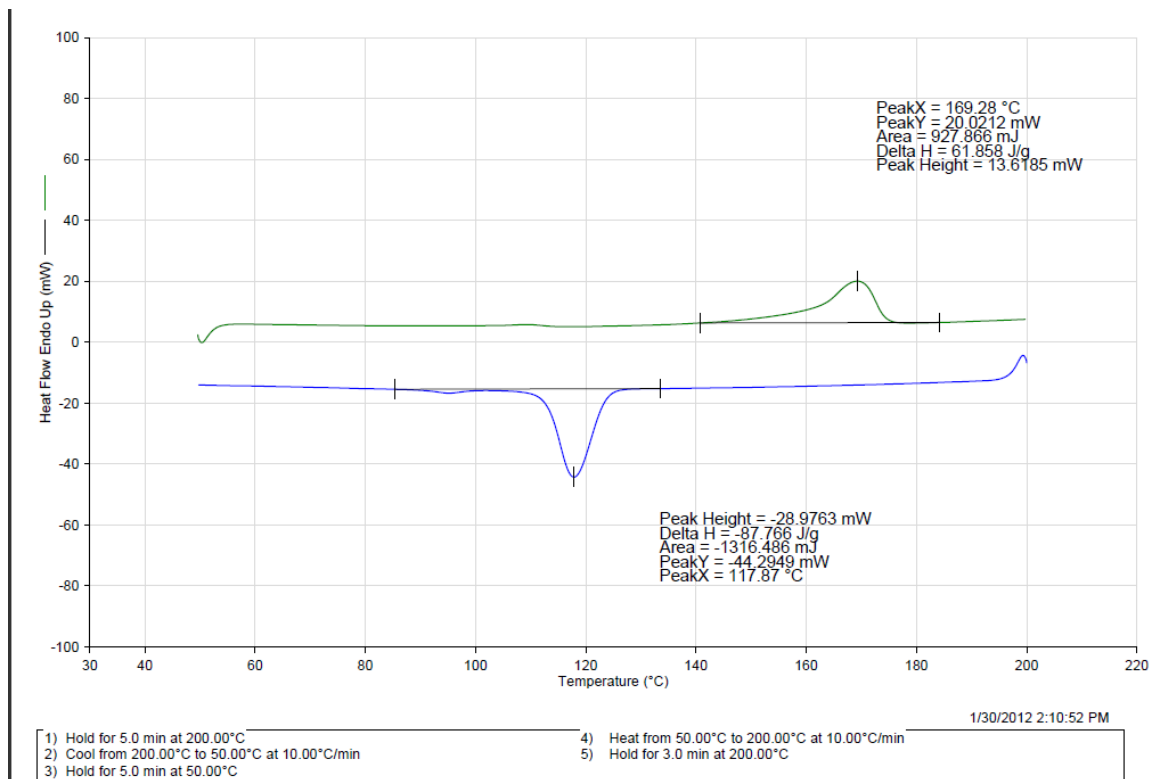
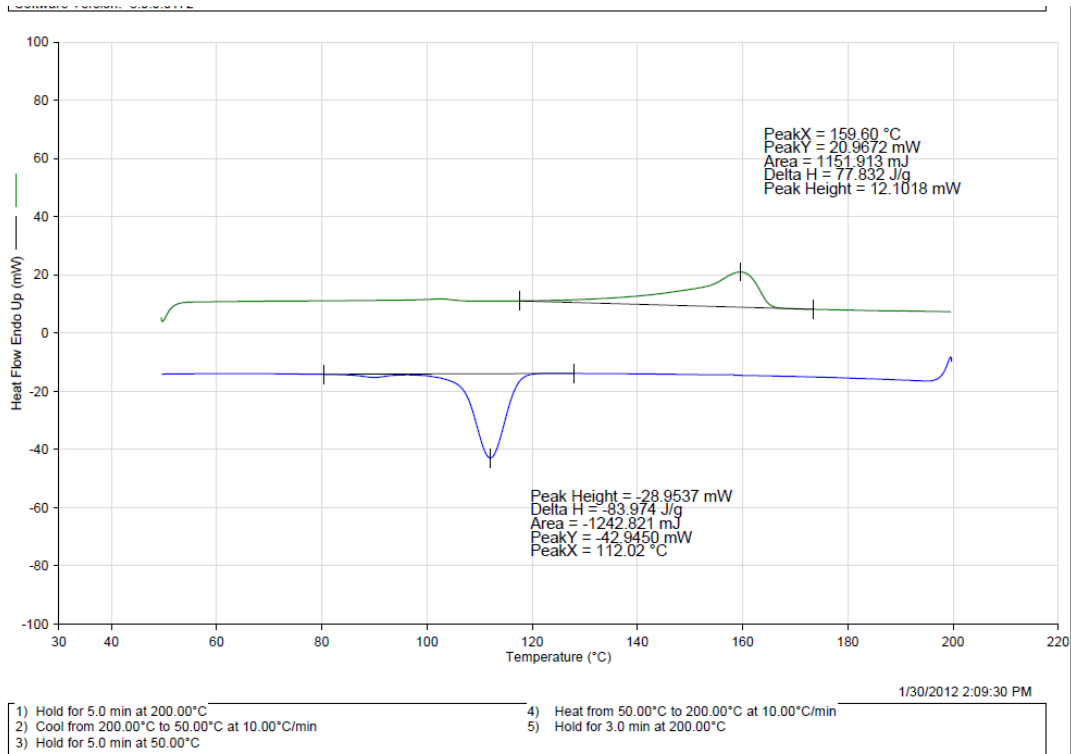


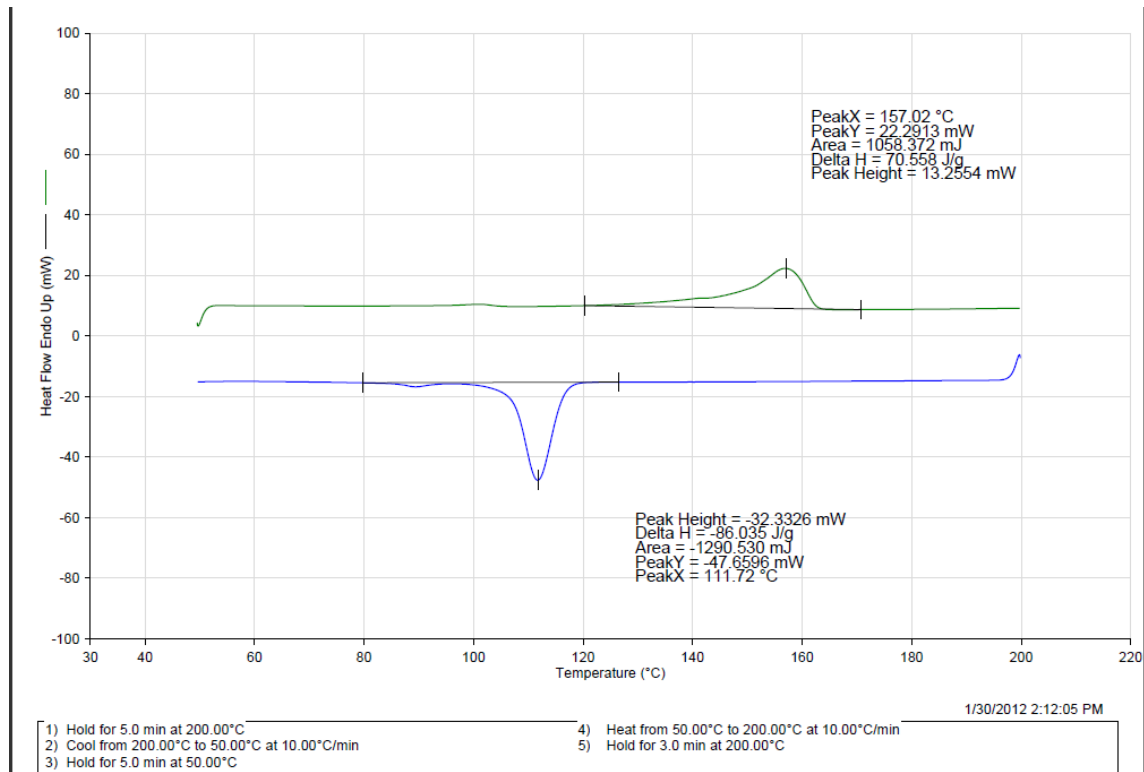
**0.5% solvent samples:**



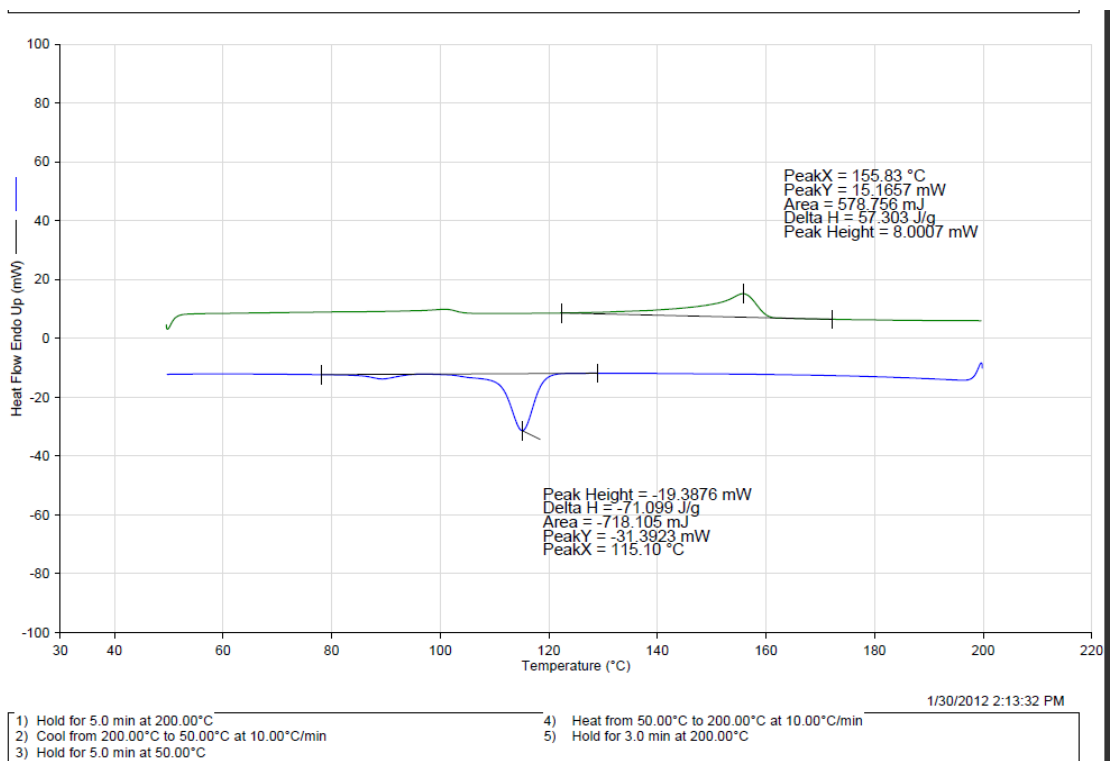


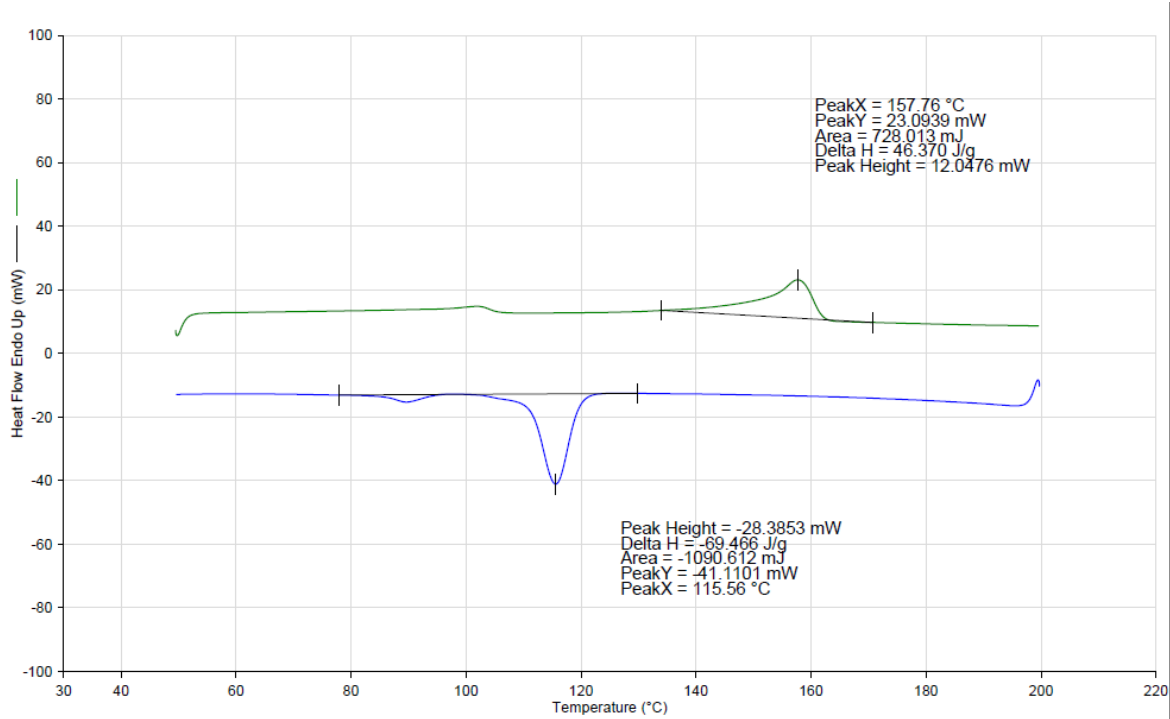
### 1% solvent samples:





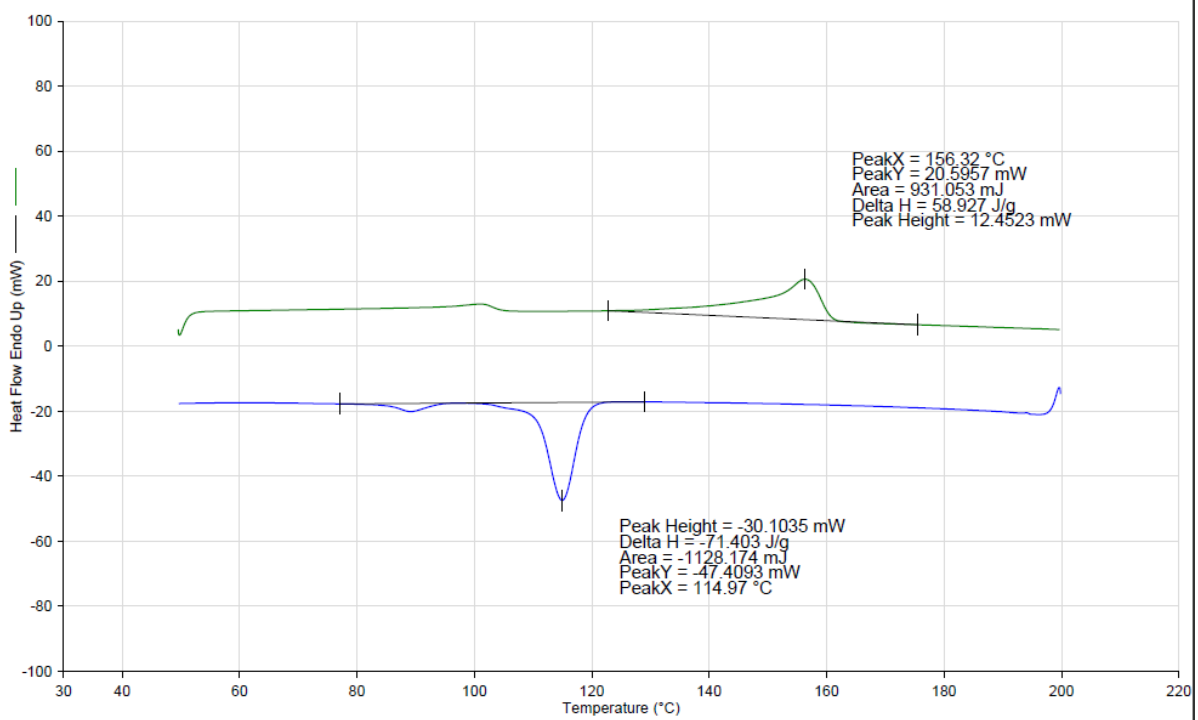
### 5% solvent samples:





1/30/2012 2:15:06 PM

- |                                                 |                                                 |
|-------------------------------------------------|-------------------------------------------------|
| 1) Hold for 5.0 min at 200.00°C                 | 4) Heat from 50.00°C to 200.00°C at 10.00°C/min |
| 2) Cool from 200.00°C to 50.00°C at 10.00°C/min | 5) Hold for 3.0 min at 200.00°C                 |
| 3) Hold for 5.0 min at 50.00°C                  |                                                 |



1/30/2012 2:16:44 PM

- |                                                 |                                                 |
|-------------------------------------------------|-------------------------------------------------|
| 1) Hold for 5.0 min at 200.00°C                 | 4) Heat from 50.00°C to 200.00°C at 10.00°C/min |
| 2) Cool from 200.00°C to 50.00°C at 10.00°C/min | 5) Hold for 3.0 min at 200.00°C                 |
| 3) Hold for 5.0 min at 50.00°C                  |                                                 |